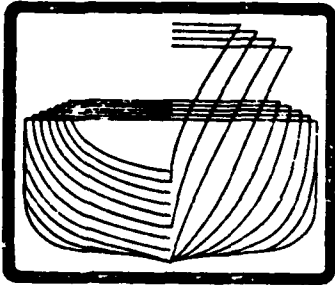


LEVEL II

2

AD A 071 891



**NAVAL SHIP
ENGINEERING CENTER**

Naval Sea Systems Command
Public Affairs Office
Classification Office
Distribution Statement A
R. Besett # 77-153

18 JUL 1976

**TECHNICAL PRACTICES MANUAL
FOR
SURFACE SHIP STACK DESIGN
NAVSEC REPORT 6136-76-18
JULY 1976**

**DDC
RECEIVED
JUL 27 1979
RESULTED
D**

DDC FILE COPY

**HULL FORM AND FLUID DYNAMICS BRANCH (SEC 6136)
NAVAL SHIP ENGINEERING CENTER
HYATTSVILLE, MARYLAND 20782**

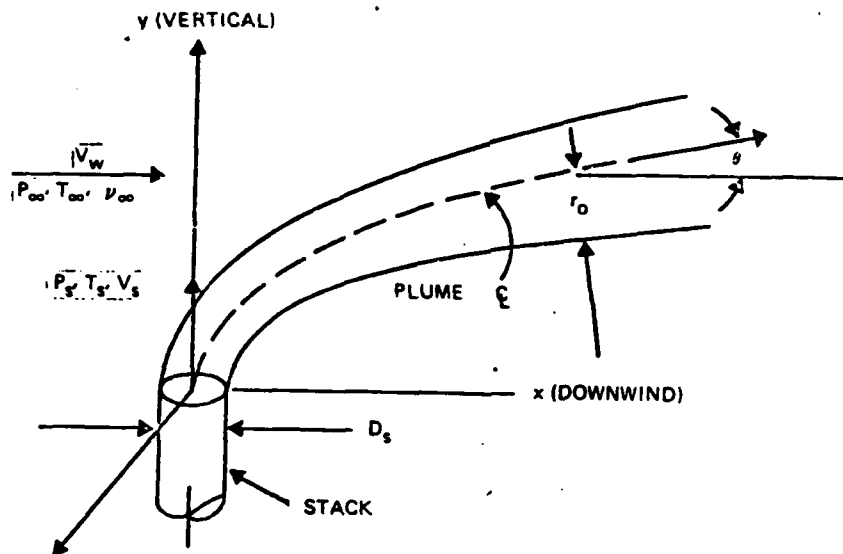
Approved for public release, Distribution unlimited.

79 07-24-001

ABSTRACT

↙ This manual contains a procedure for the design of stacks on U.S. Naval ships based upon the experience already gained by the Navy as well as commercial ship stack design practices. The techniques described in detail include design guidance for the height and shape of exhaust gas stacks, prediction of plume trajectories, estimation of downwind plume gas temperatures, and model testing techniques. The manual is divided into two parts. The first part contains a step-by-step procedure, with examples, for auxiliary vessels with conventional stacks and combatant vessels with low profile stacks. Design tools are included in the form of tables, graphs, computer programs, etc. The second part of the manual contains the basic rationale, historical and experimental foundation for the design practices as well as a section describing model testing techniques. In addition, problems unique to Naval ships, such as air operations and temperature limitations of topside electronics gear, are discussed. ↗

NOMENCLATURE



A_s	Exhaust pipe area (total for one or several pipes).
D_s	Equivalent exhaust pipe diameter = $(4A_s/\pi)^{1/2}$
R_s	Equivalent exhaust pipe radius = $D_s/2$
V_A	Ship speed
V_s	Velocity of stack gas exhaust averaged over the exhaust area
V_T	True wind speed
V_w	Average horizontal laminar wind velocity (relative)
V_s/V_w	Velocity ratio
T_s	Average stack gas exhaust temperature
T_∞	Ambient wind temperature
T_m	Plume centerline temperature (along the plume)
ϕ	Temperature ratio = $\frac{T_m - T_\infty}{T_s - T_\infty}$
θ	Yaw angle of relative wind
g	Gravitational constant

NOMENCLATURE (Continued)

S	Plume length measured along plume
ν_{∞}	Kinematic viscosity of wind
ρ_{∞}	Density of wind
ρ_s	Density of stack gas at stack exit
r_0	Maximum plume radius at a point, S, along the plume
T, r	Plume temperature, T, at radius, r, at a point, S, along the plume
Re_s	Ship Reynold's number = $V_w L_s / \nu_{\infty}$
L_s	Characteristic length of ship model
Fr	Stack exit Froude number = $v_s / (g R_s (T_s - T_{\infty}) / T_{\infty})^{1/2}$
x	Horizontal distance downwind from stack exit center-line
y	Vertical distance above stack exit
Re_s	Stack Reynold's number = $D_s V_w / \nu_{\infty}$
Re_2	Local flow Reynold's number = $x v_s / \nu_{\infty}$
OF	Temperature in degrees Fahrenheit
OR	Temperature in degrees Rankine (OF + 459.67°)
b	Width of stack casing at base
e	Uptake duct extension/b
H	Height of stack exit above datum/b
h'	Interpenetration/b
h_t	Turbulent zone height above datum/b
ρ	Interpenetration fraction

NOMENCLATURE (Concluded)

L_b	Buoyancy length scale
L_m	Momentum length scale = $R_s V_s/V_w$
M	Mass flow ratio = \dot{m}_w/\dot{m}_s
\dot{m}_w	Mass flow of mixing air
\dot{m}_s	Mass flow of stack gas
ψ	Plume temperature ratio

TABLE OF CONTENTS

ABSTRACT	i
NOMENCLATURE	ii
1.0 DESIGN GUIDANCE	1-1
1.1 DESIGN PROCEDURE	1-1
1.1.1 Conceptual Design	1-1
1.1.1.1 Superstructure Design and Turbulent Zone Height.	1-1
1.1.1.2 Stack Gas Design Data	1-4
1.1.1.3 Velocity Ratio Calculations.	1-4
1.1.1.4 Stack Shape and Height	1-7
1.1.1.5 Plume Trajectory and Iso- therms	1-14
1.1.2 Preliminary Design	1-16
1.1.2.1 General Stack Shape Design Guidelines	1-16
1.1.2.2 Velocity Ratio Probabili- ties	1-17
1.1.2.3 Model Testing	1-19
1.1.2.4 Air Operations	1-20
1.1.3 Contract Design	1-21
1.1.3.1 Final Design Isotherms and Trajectories	1-21
1.1.3.2 Heat Sensitive Components	1-21
1.2 AUXILIARY SHIP DESIGN EXAMPLE	1-24
1.2.1 Superstructure Configuration and Stack Height	1-24
1.2.2 Velocity Ratio	1-26
1.2.3 Stack Configuration	1-28
1.2.4 Plume Trajectories and Isotherms	1-29
1.2.5 Probability Analysis	1-29
1.3 COMBATANT SHIP DESIGN EXAMPLE	1-35
1.3.1 Superstructure Configuration and Stack Height	1-35
1.3.2 Velocity Ratio	1-36
1.3.3 Stack Configuration	1-36
1.3.4 Plume Trajectories and Isotherms	1-36
1.3.5 Probability Analysis	1-36

2.0	BACKGROUND AND THEORY	2-1
2.1	TURBULENT FLOW AND THE STACK GAS PLUME	2-1
2.1.1	Nature of Stack Emissions	2-1
2.1.1.1	Soot	2-1
2.1.1.2	Smoke	2-1
2.1.2	Gas Flow Around Bodies	2-1
2.1.2.1	Two Dimensional Cylinder in an Air Stream	2-1
2.1.2.2	Flow Over Bluff Bodies	2-3
2.1.2.3	Stack Plume Flow	2-3
2.1.2.4	Control of Plume Behavior	2-6
2.1.3	Conventional and Special Stack Shapes	2-7
2.1.3.1	Streamline Stacks	2-7
2.1.3.2	Fins	2-9
2.1.3.3	Vanes Above the Outer Casing	2-9
2.1.3.4	F.C.M./Valensi (Strombos) Funnel	2-9
2.1.3.5	Added Air or Dampers	2-9
2.1.3.6	Athwartships Terminal Exten- sions	2-13
2.1.3.7	Annulus	2-13
2.1.3.8	Eductors	2-13
2.2	PLUME BEHAVIOR THEORY	2-16
2.2.1	Plume Prediction Equations	2-16
2.2.1.1	Trajectory	2-16
2.2.1.2	Plume Temperature	2-16
2.2.1.3	Plume Radius	2-19
2.2.2	Sources of Information	2-19
2.3	MODEL TESTING	2-29
2.3.1	Introduction	2-29
2.3.2	Fluid Flow in a Test Channel	2-29
2.3.3	Model Scaling Factors	2-30
2.3.3.1	Effect of Reynold's Number	2-30
2.3.3.2	Plume Density	2-32
2.3.4	Necessary Conditions for Plume Model Scaling	2-32
2.3.5	Effect of Tunnel Walls	2-33
2.3.6	Methods of Making the Plume Visible and Determining the Height of the Tur- bulent Zone of Models	2-33
2.3.6.1	Plume Visualization	2-33
2.3.6.2	Boundary Layer Determination	2-34

2.4 THEORY BEHIND STACK HEIGHT PREDICTIONS	2-35
REFERENCES	2-43
APPENDIX A SUPERSTRUCTURE DESIGN IN RELATION TO THE DESCENT OF FUNNEL SMOKE, by Ower and Third	
APPENDIX B MILITARY AIR OPERATIONS	
APPENDIX C HEAT SENSITIVITY OF TYPICAL MILITARY ANTENNAE COMPONENTS	
APPENDIX D BIBLIOGRAPHY	

LIST OF FIGURES

<u>Number</u>		<u>Page</u>
1-1	Stack Design Process	1-2
1-2	Plume Turbulence Relationships	1-3
1-3	Casing and Uptake Shapes Tested by Ower and Third	1-8
1-4	Influence of Stack Design on Inter- penetration h' , 0° Yaw	1-9
1-5	Influence of Stack Design on Inter- penetration h' , 20° Yaw	1-10
1-6	Maximum Yaw Angle for Rule 1	1-12
1-7	Typical Speed/Time Probability Data	1-18
1-8	Stack Design Modifications to Avoid Smoke Nuisance	1-22
1-9	AO Deck House	1-25
1-10	Rule 1 for the AO 177	1-27
1-11	Stack Configuration	1-30
1-12	Aft Plume Displacement, AO 177	1-31
1-13	Fwd Plume Displacement (Following wind) AO 177	1-32
1-14	Operational Velocity Ratios	1-33
1-15	Exhaust Plume Temperature Profiles for the FFG 7	1-37
1-16	FFG 7 Velocity Ratios - Probability of Occurrence	1-39
2-1	Ideal Flow Around a Circular Cylinder	2-2
2-2	Real Gas Flow Around a Circular Cylinder	2-2
2-3	Flow Around a Bluff Body	2-3
2-4	Resultant Path of Stack Gases in the Wind	2-4
2-5	Clydebank Funnel	2-8
2-6	Thornycroft Funnel Acker, Ref. [3]	2-10
2-7	Strombos Type Funnel Model	2-11
2-8	Damper Arrangement on the "Independence" Acker, Ref. [3]	1-12
2-9	DE 1052 Stack - Section Looking Aft	2-14
2-10	Eductors on the DD 963	2-15
2-11	Charwat's Equation and the Glamorgan Data	2-17
2-12	Plume Temperature EQ 2.2 and Data From Glamorgan, LM 2500, and Charwat's Model Test	2-18
2-13	Interpenetration of the Plume	2-36
2-14	Probability of Exceeding Wind Speed	2-38
2-15	Vector Diagram of the Velocities	2-39
2-16	Influence of Stack Design on Inter- penetration h' , 0° Yaw	2-40
2-17	Influence of Stack Design on Inter- penetration h' , 20° Yaw	2-41
2-18	Maximum Yaw Angle for Rule 1	2-42

LIST OF TABLES

<u>Number</u>		<u>Page</u>
1-1	Stack Exit Velocity	1-4
1-2	Velocity Ratios for Various Ship Types	1-6
1-3	Interpenetration Fraction	1-7
1-4	Minimum V_s/V_w Values to Comply with Rule 2	1-13
1-5	Operating Limitations for Topside Components ($^{\circ}F$)	1-23
1-6	Exhaust Characteristics at Full Power	1-28
1-7	Power Plant Performance Parameters	1-34
1-8	FFG 7 Exhaust Characteristics at Full Power	1-35
1-9	FFG 7 Performance Data	1-36
2-1	Plume Behavior Theories	2-20
2-2	Plume Interpenetration	2-35
C-1	Temperature Characteristics	C-11
C-2	Recommended Ambient Temperature ($^{\circ}C$)	C-12

1.0 DESIGN GUIDANCE

1.1 Design Procedure

This section of the Stack Design Manual contains a specific stack design procedure that is geared to coordinate with the complete ship design. The design process has been divided into three steps which are:

1. Conceptual Design
2. Preliminary Design
3. Contract Design

The contents of this procedure and its relationship to the complete design process is illustrated in Figure 1-1. This manual also includes two worked examples. The ships are the AO 177 and the Patrol Frigate (FFG 7). The former is typical of an auxiliary vessel and the latter is an example of a small combatant ship. The type of naval ship being considered will have a large effect on the design procedure to be followed.

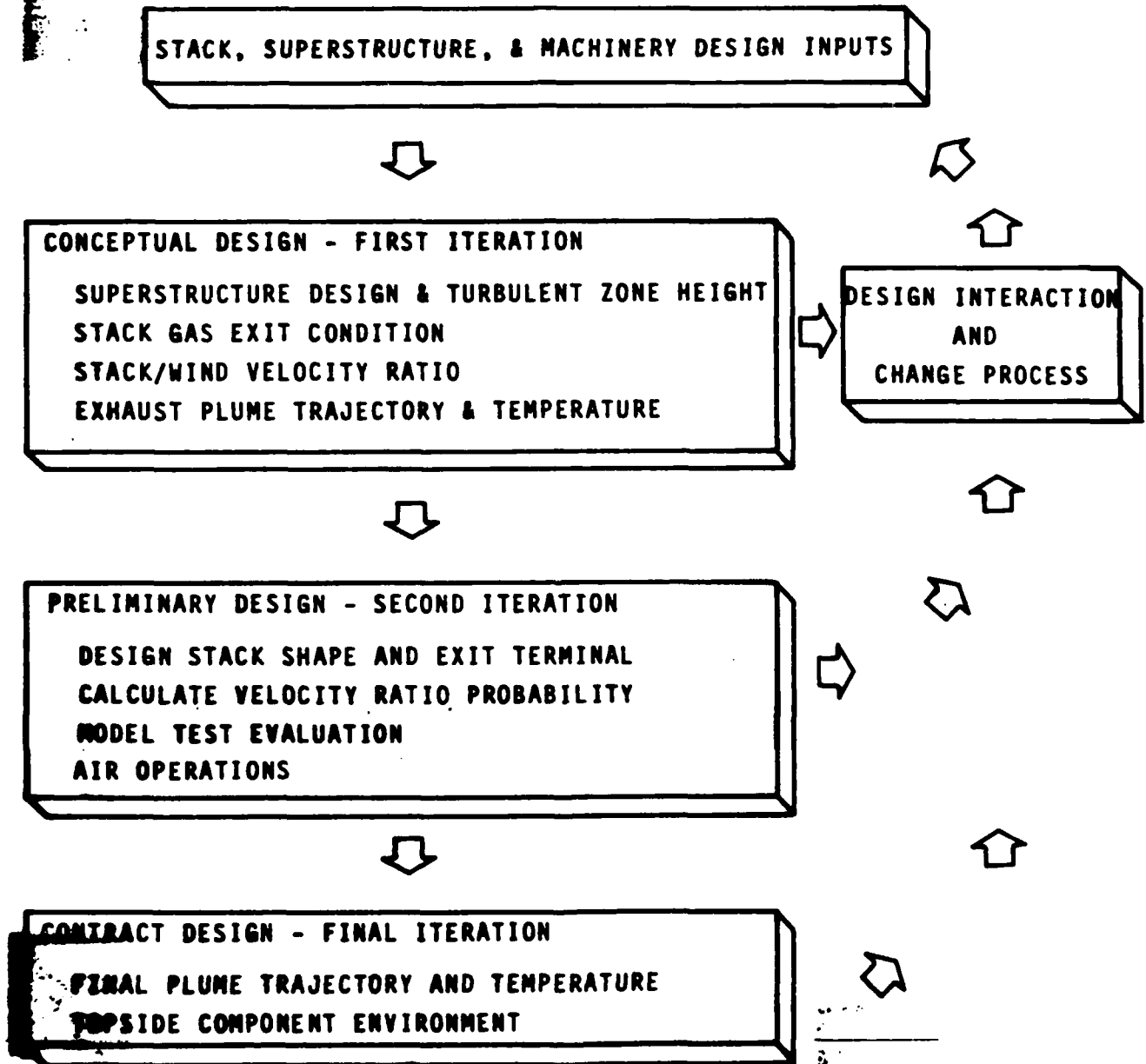
1.1.1 Conceptual Design

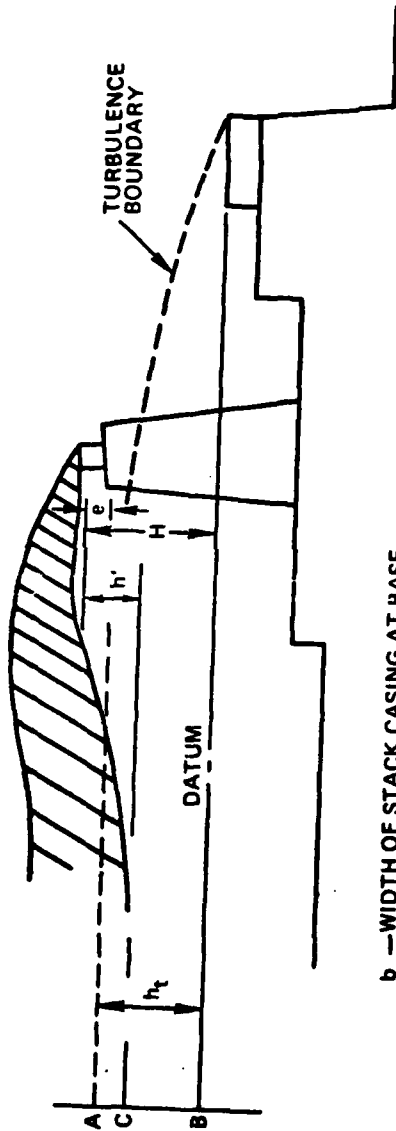
The conceptual stage of stack design is a first cut study that can be executed quickly and which will roughly indicate any major problems with the design. Two elements are involved, the turbulent zone of air flow over the ship and the design of the stack. The object is to design the stack so that the exhaust gas plume is projected far enough above the turbulent zone boundary that little mixing takes place, see Figure 1-2.

1.1.1.1 Superstructure Design and Turbulent Zone Height - The height of the turbulent zone is a function of the superstructure geometry. The first data reviewed should be the topside arrangements, deck plans, and outboard profile. Examination of the arrangement drawing can reveal potential ways of lowering the turbulent zone height. Ower and Third [4]¹ have systematically organized formulae and diagrams to predict turbulent zone height for various superstructure shapes of interest. Appendix A contains extracts from the paper by Ower and Third. The height (h) of the boundary above the highest deck can be considerably reduced by suitable rounding of the edges of the superstructure, particularly in elevation. Structures with less length than breadth generate higher turbulence boundaries than longer structures, and the benefits derived from rounding edges are lost.

¹Brackets [] denote references.

FIGURE 1-1: STACK DESIGN PROCESS





- b — WIDTH OF STACK CASING AT BASE
- e — UPTAKE DUCT EXTENSION.²
- H — HEIGHT OF STACK EXIT ABOVE DATUM.²
- h' — INTERPENETRATION²
- h_t — TURBULENT ZONE HEIGHT ABOVE DATUM.²
- P — INTERPENETRATION FRACTION OF PLUME AND TURBULENT ZONE $\left(\frac{AC}{AB}\right)$

NOTES: (1) h' IS A NEGATIVE VALUE IN THE EXAMPLE ABOVE.
 (2) EXPRESSED IN TERMS OF STACK WIDTH b.
 (3) SOURCE; REFERENCE 5.

FIGURE 1-2 PLUME-TURBULENCE RELATIONSHIPS

1.1.1.2 Stack Gas Design Data - In the design of a stack certain input data are required. One item is the ship operating profile, which is usually presented in the form of a nomogram with velocity range vs. percent time the ship will be operating within that range, also called the speed/time profile.

Engine exhaust characteristics are also needed. The characteristics include volume flow vs. ship speed and exhaust temperature vs. ship speed. For example of how these data are applied, see page 1-29 and page 1-33.

1.1.1.3 Velocity Ratio Calculation - The first step in stack design is to estimate the exit velocity of the stack gas (V_s). With that velocity, the velocity ratio (ratio of stack to wind velocity) can be formed.

Stack area is calculated using the minimum acceptable backpressure at maximum power. Backpressure is specified by the engine manufacturer, or in the case of steam plants, taken from boiler backpressure criteria. If no other data are available the following procedure can be used to approximate exhaust velocity at full power.

Calculate the exhaust stack exit flow area (A_s) and equivalent diameter ($D_s = \sqrt{4A_s/\pi}$) with the following data, assuming no major obstructions in the duct flow path; use the exhaust volume flow (ft^3/sec) from engine characteristics, and the maximum exhaust velocities (ft/sec) from table 1-1.

Table 1-1 Stack Exit Velocity

Ship Class	Stack Height	Stack Exit Velocity (ft/sec)	
		Steam	Gas Turbine
All - Stack Height Abv. Turbulent Zone		130	180
All - Low Profile Stack		180-200	250

For the purpose of this manual, 40 kts is taken as the worst absolute wind speed. This velocity corresponds to the wind velocity in the North Atlantic that is annually exceeded about 2 percent of the time. Higher wind speeds will cool the plume faster and can be expected to contain more turbulence.

With V_s and V_w the velocity ratio (V_s/V_w) can be calculated. The acceptability of the velocity ratio in terms of effectiveness in ejecting the exhaust gas plume clear of the ship is determined through comparison with previous designs. A table is then assembled in the form of Table 1-2 which contains the velocity ratios for the ship speeds being considered and a head wind and tail wind of 40 kts each. The resulting velocity ratios are compared to the values of Table 1-2 and adjustments of stack area are made if the values fall far below these limits. A check should be made so that at some fairly low power setting, such as cruise, the V_s/V_w should not fall below 1.0. This checks well with AO 177 in Table 102 and also with the experience of Nolan [1, p. 22].

Table 1-2 Velocity Ratios for Various Ship Types
40 Knot True Wind Speed (V_T)

Ship Type	Power Level	Ship Speed kts	$T_{S/OR}$	V_S Ft/Sec	V_S/V_W Headwind	V_S/V_W Tailwind
Combatant Destroyer (DG/AEGIS) (a)	Max	30	1257	236	2.00	14.60
	Cruise	20	1090	152	1.50	4.45
	Idle	10	953	54	.64	1.06
Combatant Frigate (a) (FFG 7)	Max	28	1240	264	2.30	13.20
	Cruise	20	1110	186	1.85	5.46
	Idle	5	1060	56	.56	.95
Auxiliary Tanker (AO 177) (b)	Max	21-23	1320	130	1.24	4.28
	Cruise	20	1275	105	1.04	3.11
	15 kts Ahead	15	1250	63	.68	1.47
	10 kts Astern	-10	1260	88	1.70	1.04
Helo- carrier (Sea Control Ship) (a)	Max	25	1310	234	2.13	9.24
	Sustained	22	1317	251	2.40	8.26
	Half Throttle	17	1182	161	1.70	3.97
	Slow Ahead	9	1127	131	1.58	2.50

(a) Low profile stack design

(b) Stack height penetrates boundary layer

1.1.1.4 Stack Shape and Height - Background and rationale for this technique is presented in Section 2.4. See Figure 1-2 for a definition of terms. The design procedure follows:

(a) Determine the height of the turbulent zone (h_t) with procedure described in Appendix A. Refer to Section 1.1.1.1.

(b) Determine the casing shape and the projection of the exhaust smoke pipe above the top of the casing. Figure 1-3 presents offsets for various stack shapes. Figures 1-4 and 1-5 from Reference [5] gives the interpenetration (h') of the plume as a function of velocity ratio for a number of model stacks. The largest (absolute) value of interpenetration (h') possible is most desirable. These stacks were tested individually in a region of laminar flow. Referring to Figures 1-4 and 1-5, the streamlined uptake (No. 2) consistently shows good performance. Special tops were included in the model series to preserve the benefits of a projecting uptake and improve overall appearance of the stack. All the stacks in these plots have projecting uptakes that extend above the casing top 0.475 times the casing width at the base. Successful designs with projections as small as 1/4 to 1/2 of this extension have been achieved. Extension values of 2 to 4 feet or about 1/4 to 1/3 of the base width have consistently given good results in more recent model tests conducted by the U.S. Navy and may be used. The plots can be used for stack designs that can be approximated by the stacks included in the model series. The choice of casing shape depends on the selected critical yaw angles that are likely to present problems, see section 1.1.2.2. A $\pm 30^\circ$ yaw angle (wind angle off-the-bow) is standard for air operations on U.S. Naval vessels.

(c) Two basic rules were formulated by Ower and Third [5] for stack casing design: Rule 1 - the lower boundary of the smoke plume may be allowed to penetrate the zone of turbulence created by the ship's structure to a vertical depth in accordance with the following table.

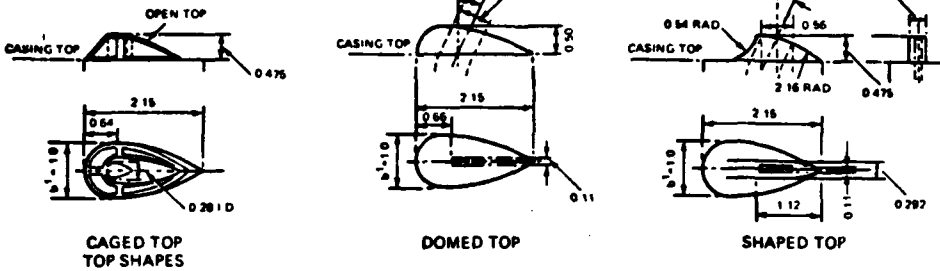
TABLE 1-3

Interpenetration Fraction

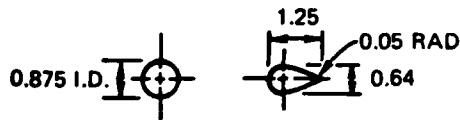
Interpenetration (h')	Interpenetration Fraction
	Allowed (p)
Above -0.5	.35
-0.5 to -1.5	.50
Below -1.5	.70

WIND DIRECTION (HEADWIND)

TOP SHAPES



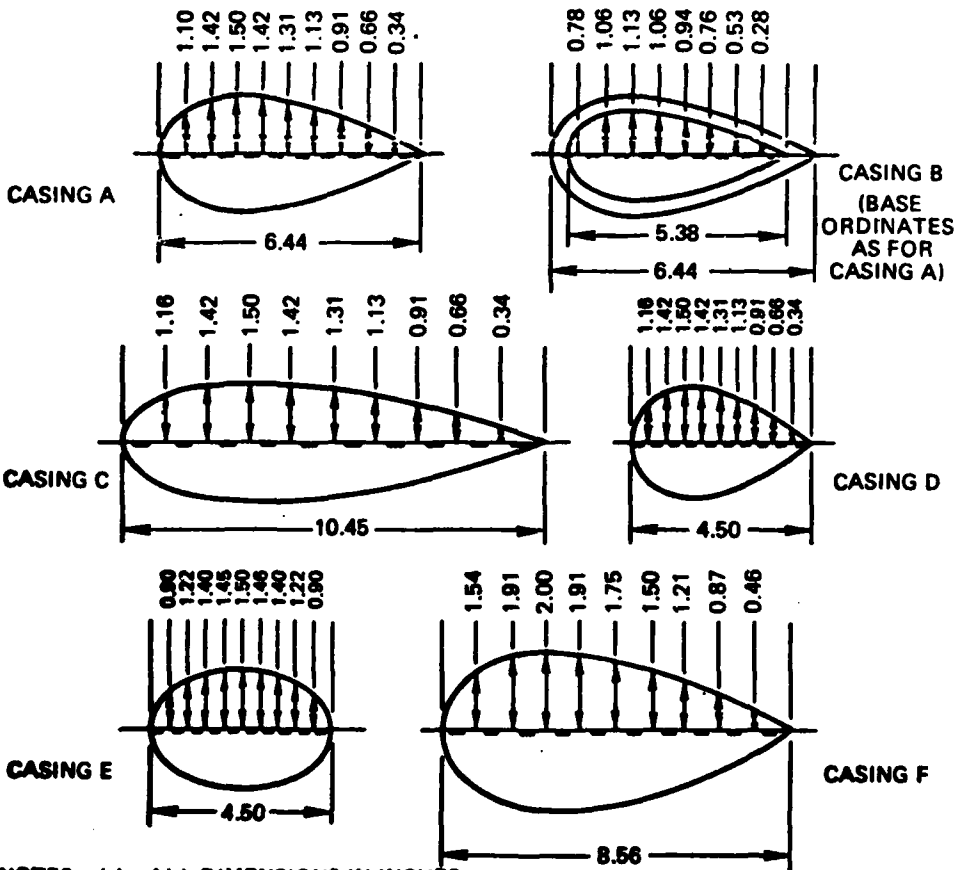
UPTAKE SHAPES



CASING SHAPES

CIRCULAR

STREAMLINED



(a) ALL DIMENSIONS IN INCHES.
 (b) SOURCE; REFERENCE [5]

FIGURE 1-3 CASING AND UPTAKE SHAPES TESTED BY OWER AND THIRD

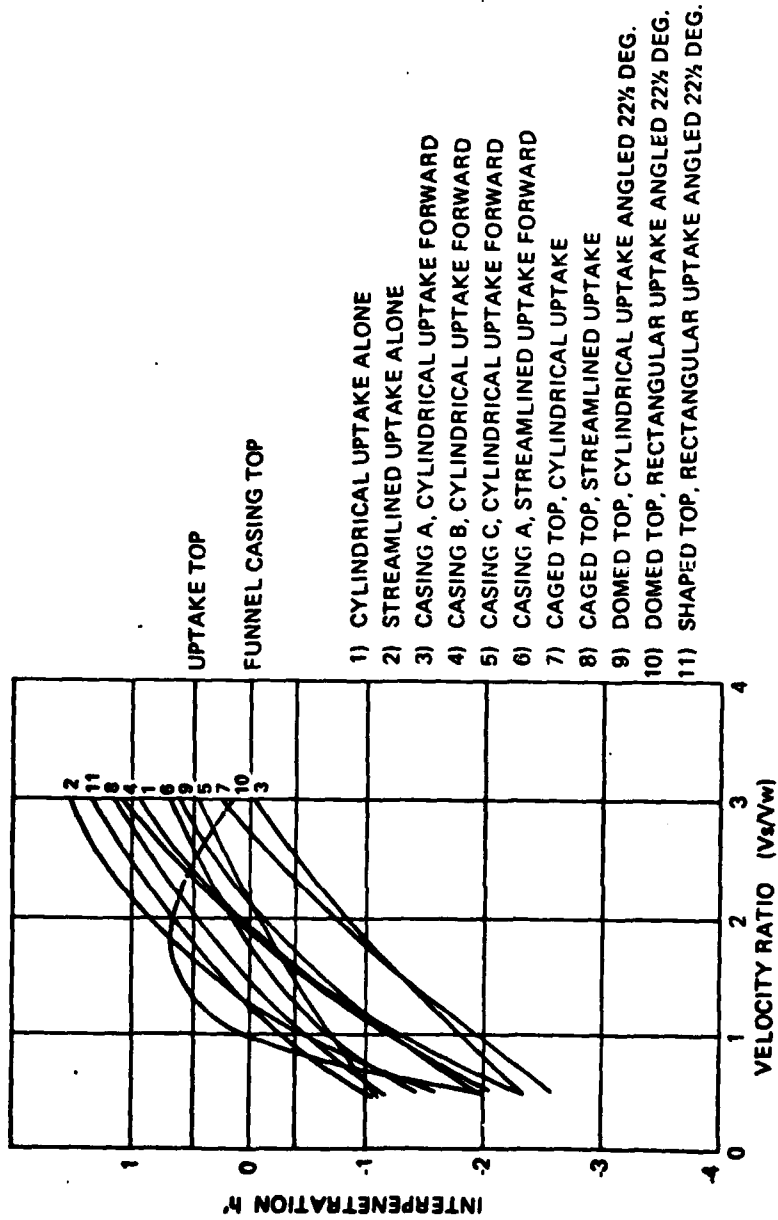


FIGURE 1-4 INFLUENCE OF STACK DESIGN ON INTERPENETRATION N'
 $\theta = 0.475$ (APPROX.), 0 DEG. YAW (FOR DEFINITIONS OF
 SYMBOLS SEE FIGURE 1-2)

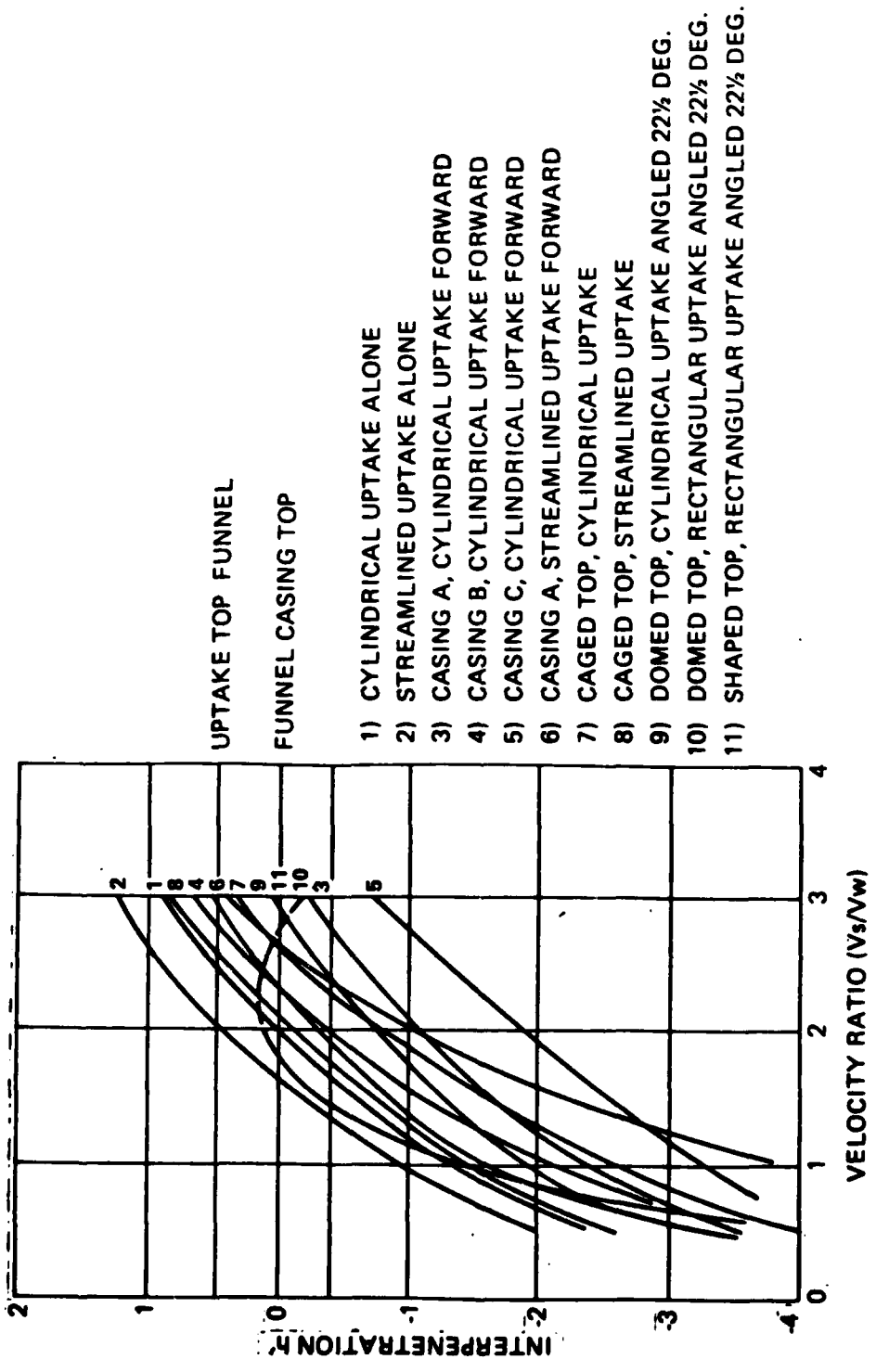


FIGURE 1-5 INFLUENCE OF STACK DESIGN ON INTERPENETRATION h'
 ○ = 0.475 (APPROX.), 20 DEG. YAW

Rule 2 - The lower boundary of the smoke plume must not descend below the stack top by an interpenetration distance (h') greater than two stack widths ($2b$). For stack heights of less than $2b$, the allowable interpenetration distance is reduced accordingly. This rule is applicable to all angles of yaw between $\pm 30^\circ$.

(d) If no criteria exists for determining the maximum yaw angle for design, determine the value as illustrated on Figure 1-6. Construct a line aft of the stack centerline with a downlook angle of 20° . Extend the intersection radially to the beam of the ship. This angle may be between 10 and 20 degrees. At yaw angles greater than 20 degrees, the smoke plume passes off most ships' decks before penetrating the turbulent zone. Rule 1 can be ignored if the 20° downlook angle does not intersect the centerline of the ship. If the maximum yaw angle is greater than 20° , use 20° in the next calculation.

(e) Calculate velocity ratios at full power for a true wind of 40 knots and the maximum yaw angle for rule 1 by using the following:

$$V_w = \frac{\sin [180 - (\theta + \arcsin ((\sin \theta)(V_A/V_T)))]}{\sin(\theta)/V_T} \quad [1.1]$$

where

V_w = Relative wind speed,

V_T = True wind speed,

V_A = Ship speed, and

θ = Yaw angle of relative wind.

The velocity ratio is then, V_s/V_w

(f) Pick values of h' from Figures 1-4 and 1-5 for the velocity ratio and type of stack selected. Then pick appropriate values of p from Table 1-3.

(g) Use Equation 1.2 to determine the minimum stack height based on Rule 1 for zero yaw and maximum yaw.

$$H = h_t (1 - P) - h' \quad [1.2]$$

(h) Use equation (1.1) to determine the V_w for 30° yaw and a true wind of 30 knots. Check compliance of the velocity ratio under these conditions with Table 1-4 to satisfy Rule 2.

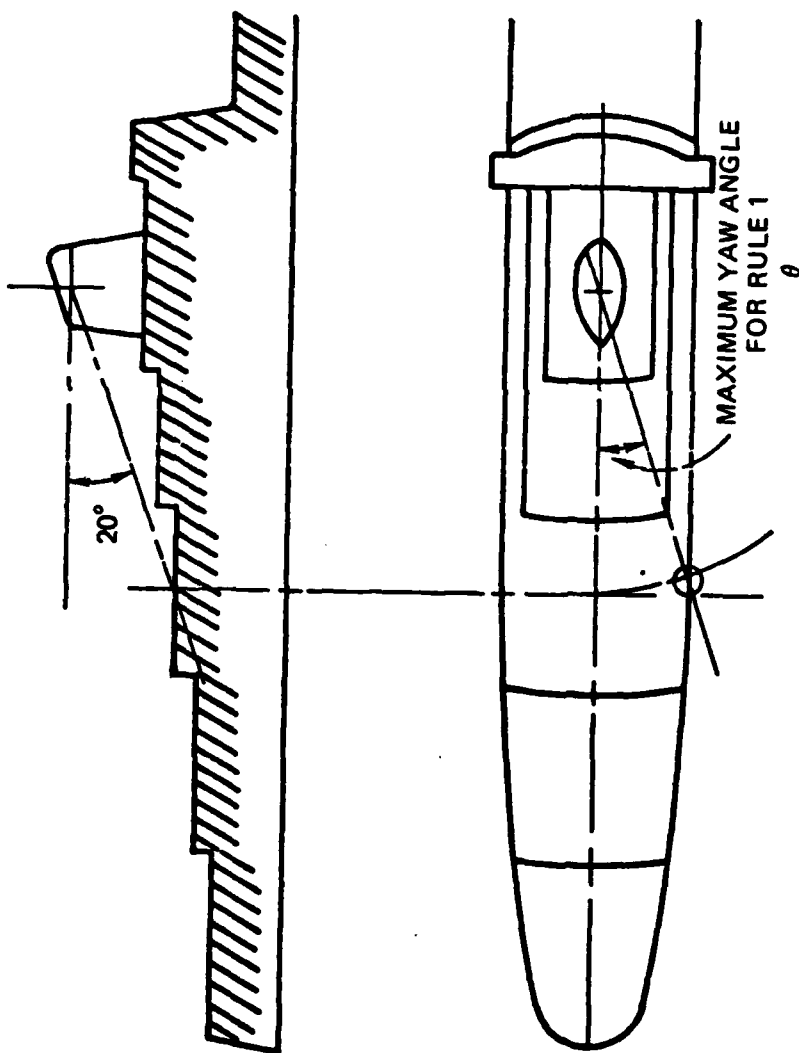


FIGURE 1-6 MAXIMUM YAW ANGLE FOR RULE 1

TABLE 1-4
 MINIMUM V_S/V_W VALUES TO COMPLY WITH RULE 2

h'	Casing A (parallel) cylindrical uptake forward	Casing A, streamlined uptake	Casing B (tapered) cylindrical uptake forward	Streamlined uptake	Rectangular uptake (22 deg.)	Shaped top rectangular uptake (22 deg.)
-2.0	$e=0$ 2.42 $e=0.25$ 1.86 $e=0.475$ 1.48	$e=0.475$ 0.86	$e=0$ 1.59 $e=0.25$ 1.41 $e=0.476$ 1.02	$e=0.475$ 1.06	$e=0.5$ 1.39	$e=0.475$ 1.13

For definitions of e and h' see Figure 1-2.

(i) If Rule 2 is not satisfied, increase the V_s and calculate a new H by going back to (b) and reiterating.

1.1.1.5 Plume Trajectories and Isotherms - Plume trajectories and isotherms are to be drawn directly on the ship's profile. To predict plume trajectory and temperature, the following equations should be applied. (The derivation of which is found in Section 2.2). A step-by-step method for determining the expected peak temperature at a given topside location due to gas turbine exhaust gases is illustrated below.

(a) **Plume Trajectory** - Determine the velocity ratio (V_s/V_w) which has a trajectory through the X and Y coordinates of the selected topside location from equation 1.3. Criteria for critical velocity ratio and operating conditions was presented in Sections 1.1.1 and 1.1.2.

$$\frac{Y}{D_s} = \frac{N(V_s/V_w)(X/R_s)^{0.25}}{(2.4 + 0.3 V_s/V_w)^{0.50}} \quad [1.3]$$

Where:

N = 1.15 for one exhaust pipe
 N = 0.86 for more than one exhaust pipe
 X = Horizontal distance from stack centerline, ft.
 Y = Vertical height above stack exhaust, ft.
 D_s = Equivalent diameter of stack exit area, ft., $=\sqrt{4A_s/\pi}$

(b) **Temperature at the Centerline** - Calculate the non-dimensional plume temperature ratio (ϕ). Calculate the maximum plume temperature (dual engine operation) from the relationship given in Equation 1.4.

$$\phi = \frac{T_m - T_\infty}{T_s - T_\infty} = \frac{(V_s/V_w)^{0.25}}{(s/D_s)} \quad [1.4]$$

where

T_m = Plume centerline temperature, °F, = $\phi (T_s - T_\infty) + T_\infty$

T_s = Average stack gas exhaust temperature, °F

T_∞ = Ambient temperature, °F

s = Plume length measured along the plume

Using equation 1.4, s/D_s is easily plotted along the plume trajectory by using a tick strip to measure distance along the trajectory.

(c) Plume Radius - Finally the radius of the lowest trajectory should be plotted to show the lowest extent of the plume boundary by using the following equation.

$$r_o = R_s + [2 (0.15 + 1.2/(V_s/V_w)) - \frac{1}{2F_R^2}] Y \quad [1.5]$$

where

$$F_R = \frac{V_s}{(gR_s / (\frac{\rho_\infty - \rho_s}{\rho_\infty})^{0.5})} = \frac{V_s}{(gR_s / \frac{T_s - T_\infty}{T_\infty})^{0.5}}$$

and

R_s = Equivalent radius of stack exit = $D_s/2$

g = gravitational constant

ρ_∞ = Density of wind (at standard conditions)

ρ = Density of Stack gas at exit.

The profile drawing with plume trajectories, isotherms and radii allows the designer to estimate the typical temperatures in heat sensitive antennae, weapon systems and other components. (See Appendix C for information about the heat sensitivity of mast mounted equipment.) It also allows him to check for reingestion of exhaust gases, exhaust gas in crew areas and the possibility of plume interference in air operations (See Appendix B for information on air operations.) At this point, adjustments can be made in topside arrangements. This would necessitate an interaction with other design groups. A re-evaluation of Section 1.1 may be necessary after this interaction.

1.1.2 Preliminary Design

Assuming the general design parameters have not changed sufficiently to warrant a reiteration of part 1.1, the next step in the design process, stack design and model testing is usually coincident with Preliminary Design. The general flow problem is not well enough understood to predict the effect of yaw and local obstructions without model testing. Hence the present design technique consists of first studying headwind and tailwind conditions (Section 1.1.1), and then making empirical judgements concerning performance at all yaw angles. When an acceptable design has been derived in this manner, it is normally then model tested.

1.1.2.1 General Stack Shape Design Guidelines - Ower and Third [5] have written an exhaustive paper on stack shape which includes design guidelines for standard designs. For unconventional stack design, special studies to determine the required characteristics are necessary. General guidelines are as follows:

(a) Since the main cause of downwash is the bulk of the funnel casing, this should be reduced as much as possible.

(b) Within the range of normal practice in design, the shape and length/breadth ratio of the casing profile in plan have no great influence on the performance of the funnel. An increase in fineness of the profile gives good results in headwind conditions, but can cause severe eddying at critical yaw angles.

(c) Some improvement can be effected in yaw only by placing the uptake discharge as far aft as possible in the casing.

(d) A tapering casing is beneficial under most circumstances, particularly if it results in an appreciable reduction in breadth at the top.

(e) A substantial improvement results from a simple extension to the uptake beyond the stack top. A streamlined section rather than cylindrical gives improved results.

(f) Specially shaped tops can be designed to take full advantage of the benefits of a projecting uptake. All have as their main object the reduction of the disturbing effect of the casing. Even at the higher angles of yaw, their performance is much better than that of a casing with only a projecting cylindrical uptake. Minor modifications to the shape of these tops do not seem to have a vital bearing on the performance, but with domed shaped tops it is recommended that the uptake discharge be angled at 20-25 deg. to the vertical. Rounding the stack top eliminates tendency for smoke to creep forward over the top [3].

(g) Slope of the stack top. The horizontal top is best but a downward rake aft of 1" per foot does not affect performance. Greater rake deflects the flow downward into the stagnated region. It also forms a large eddy at the forward edge which will cause the smoke to drift forward [3].

These results were based on a study of a typical variety of stack shapes. The authors noted that the stack casing is more detrimental to stack flow than any other individual characteristic. This is due to the downwash caused by the casing. But, casings are now generally used to house machinery and are necessary despite their detrimental effect on gas flow. Typical stack elevations and section shapes are presented in sections 1.2 and 1.3. Also typical examples of well designed casings are described in Section 2.1.3.

1.1.2.2 Velocity Ratio Probabilities - The probabilities of velocity ratios when the relative wind comes from various directions can be calculated by the NAVSEC computer program entitled, "Mean Stack Gas Velocity Ratios and Probabilities of Relative Wind Direction for Known Ship Speed and Exhaust Speed Characteristics" [20].

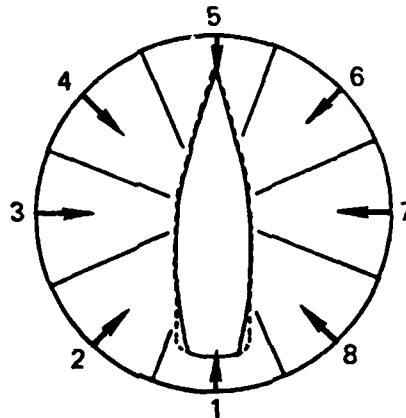
This program computes mean stack gas to relative wind velocity ratios and the probabilities that the relative wind-over-the-deck, \bar{V}_{wod} , will be from each of n equal sectors. Only the solutions for sectors on one side of the ship are calculated because their mirror sectors have equal solutions. The tailwind sector is always analyzed first.

The weighted mean velocity ratio, $(R = V_g/V_w)$, is calculated for each sector. Also calculated for each sector are ten values of the probability that the velocity ratio will be less than R , where R varies from 1.0 to 5.5. A plot of these ten points yields the cumulative probability curve as a function of R throughout the range.

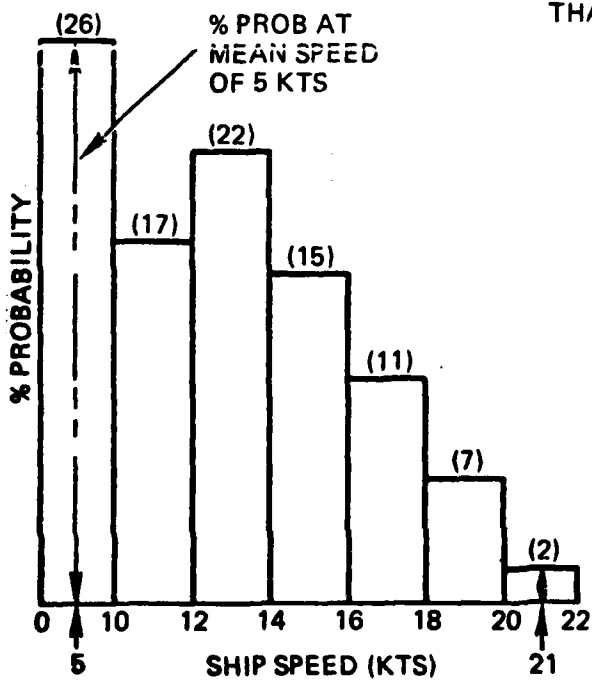
The data required to operate the program are:

(a) The number of sectors to be analyzed. See Figure 1-7(A).

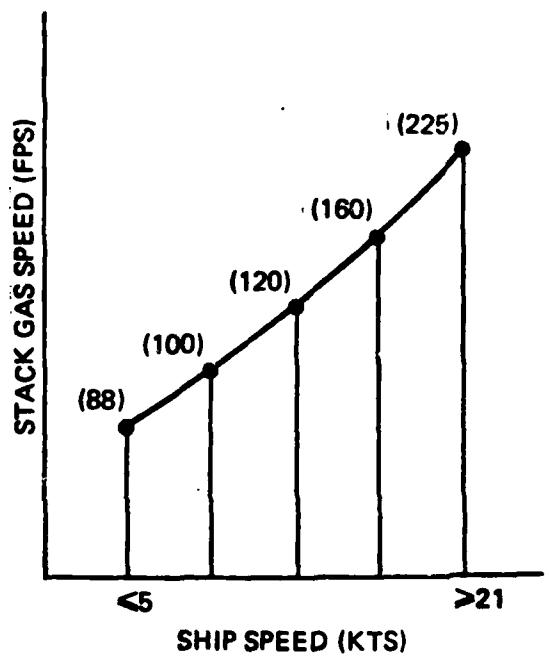
(b) A ship speed profile with 15 or fewer discrete ship speeds and their associated probabilities of occurrence. See Figure 1-7(B).



(A)
 NUMBER OF SECTORS
 (8 SHOWN)
 (ANY INTEGER GREATER
 THAN 1)



(B)
 SHIP SPEED PROFILE
 (UP TO 15 SPEEDS)



(C)
 V_{STACK} AS FUNCTION OF V_{SHIP}
 (EXACTLY 5 DATA POINTS)

FIGURE 1-7 TYPICAL SPEED/TIME PROBABILITY DATA

(c) Five values of ship speed with the corresponding stack exhaust speed. The range of these ship speeds must span the range of the ship speed profile. See Figure 1-7(C).

The program is based on solutions to a number of special case problems utilizing discrete values of ship speed and wind speed. A typical problem involving eight sectors and seven ship speeds requires just under two hours to solve.

Ten discrete wind velocities and their probabilities of occurrence have been assumed by the program. These winds are based on meteorological data from the North Atlantic, and they represent a reasonable worst case.

1.1.2.3 Model Testing - The scope of a model test program will vary greatly depending on the nature of the design. It is now possible to design an auxiliary vessel with a high stack and few heat sensitive antennae without resorting to model tests. On the other hand a very unusual configuration, such as the eductors on the DD 963, would require extensive testing of the stack alone as well as waterline ship model tests. During the design of the Sea Control Ship, three versions of a modified streamline stack, which would be inexpensive to build, although not as aerodynamically desirable as a streamlined stack, were tested and a design selected.

For typical design, there are two kinds of model tests:

- (a) Individual stack
- (b) Ship waterline model with or without the stack

Individual stack tests are conducted when studying different stack shapes. Traditionally these tests developed because it was felt that the small stacks on ship models would present scaling problems. However, test results by Ower and Third [5] suggest the critical Reynold's number does not affect the downwash by any appreciable amount. For details on model testing techniques and practices, see Section 2.3.

1.1.2.4 Air Operations - Aircraft operations are affected in two ways by topside arrangements and stack design. First, airflow patterns downwind of the deckhouse, helo hanger, or stack must be investigated during the model study. The landing area may be exposed to reverse or erratic flow conditions in the depression or "burble" region which exists downwind of these structures. It is this depression region that is formed by the downwash which tends to suck down or disperse the plume. The complex effects and interaction of locally generated boundary layers cannot be adequately predicted. It has been the traditional role of smoke model testing of new ship designs to isolate these problems. Ower and Third [4] have defined superstructure design techniques which can minimize the effects.

The second consideration is the effect of the hot gas plume crossing the flight path during air operations. The exhaust gas affects the aircraft by (1) power loss in the gas turbine engines, and (2) loss of lift due to a reduction in air density. Thus it is necessary to define an envelope of exhaust gas temperature for various wind velocities and relative headings. The normal approach pattern is from downwind flying into the relative wind heading. This provides maximum lift at any given engine power level. However, NAVAIR insists that there be clear approach paths from any angle between 90° and 270° relative to the bow. To allow consideration of various approach angles by the aircraft, the exhaust gas trajectory and temperature should be evaluated at several relative wind angles (0° , 30° , and 45°).

Appendix B contains further criteria for air operations on naval vessels.

1.1.3 Contract Design

Model testing is usually completed during the early phase of contract design. Hopefully any major changes to topside arrangements and the stack design can be resolved at this time. Based on the previous studies conducted, it is now appropriate to choose a final design configuration.

1.1.3.1 Final Design Isotherms and Trajectories - Resolution of design conflicts or deficiencies at this stage requires design changes which affect other equipment systems. Actions which can be taken are illustrated on Figure 1-8. In increasing order of complexity, they include the following:

1. Change stack shape.
2. Increase the velocity ratio through the use of exit nozzles, dampers, or added air.
3. Raise the stack.
4. Consider special stack designs.

1.1.3.2 Heat Sensitive Components - The equipment items listed in Table 1-5 are required by procurement specifications not to exceed the limitations of MIL-E-16400 (149°F operating and 167°F non-operating). Increasing the ambient temperatures beyond these values, although non-fatal from the standpoint of immediate failure, will have a negative effect upon component service life and result in shorter maintenance intervals.

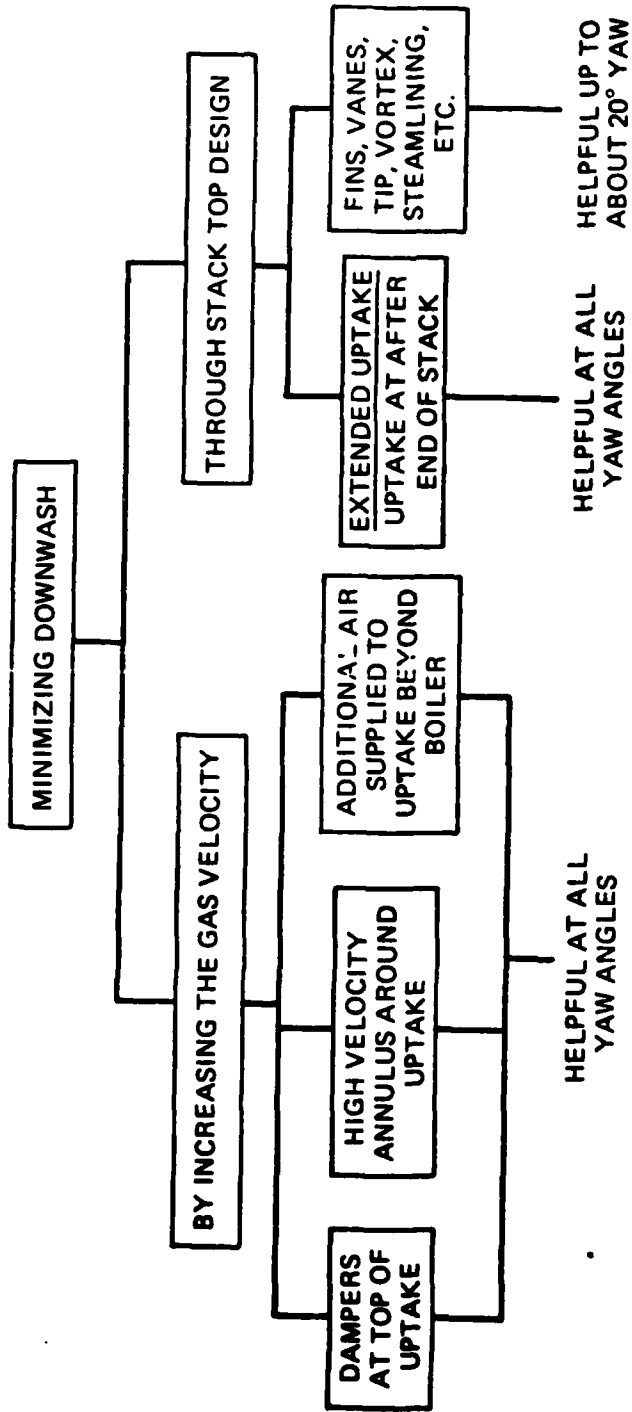


FIGURE 1-8 STACK DESIGN MODIFICATIONS TO AVOID SMOKE NUISANCE

TABLE 1-5

OPERATING LIMITATIONS FOR TOPSIDE COMPONENTS (°F)

<u>Item</u>	<u>Long Term</u>	<u>Short-Term (less than 10 min/hr.)</u>
A. <u>Coaxial Cable:</u> (RG-214, RG-218, RG-333, and 1-5/8" Foam Filled)		
Applied RF Pwr/Rating		
100%	104	104
50%	140	140
20%	162	162
10%	169	169
0%	176	176
B. <u>Wave Guides:</u> (Rigid & Flexible)	185	212
C. <u>Misc. Line of Sight Items:</u> (Radar, TACSATCOM, AS-899, AS-1174, AN/URD-4, AN/URN-3)	176	185
D. <u>Antenna-Couplers:</u>		
AN/SRA-17	185	212
AN/SRA-43	172	185
E. <u>Antenna Insulators</u>		
Fiberglass	185	212
Ceramic Bowl	185	212
Ceramic Strain Relief	185	221
F. <u>Wire Rope</u>		
Vinyl Covered	176	176
Unjacketed	185	221
G. <u>Weapons:</u>		
CIWS (Phalanx)	150	150

1.2 Auxiliary Ship Design Example

The FY75 Auxiliary Oiler AO-177 stack configuration was selected as a design sample. Reference 21 summarizes the design efforts of SEC 6136 during Preliminary and Contract Design of the AO-177.

1.2.1 Superstructure Configuration and Stack Height

The reference drawing used was the General Arrangements (Inboard Profile) dated 16 April 1974. Critical areas identified during the drawing review were possible impingement of the exhaust plume on:

(a) The ship's superstructure adjacent (forward) of the stack exit terminal.

(b) The ship's antenna mast and mast-mounted electronics components forty (40) feet forward of the stack.

(c) The helicopter operations (hovering) area above VERTREP, forty (40) feet aft of the stack discharge.

Boundary Layer Height

The AO-177 deck house is shown in Figure 1-9. The boundary layer height (H) can be calculated from:

$$H = B \times h_t \quad [1.6]$$

where

B = deck house beam (unity) (Note that in Appendix A, the deck house beam is designated as b.)

h_t = boundary layer max. height expressed in terms of deck house beam (B). This term should not be confused with interpenetration (h').

Sample calculations for two representative deckhouse beam widths were made, 80 and 38 feet. The boundary layer height for each of these cases then lies between:

$$H_1 = 0.42(80) = 33.6 \text{ ft (above the deckhouse)}$$

$$h_t = 0.42 \text{ from test number 74, Appendix A}$$

or adding the 4 ft. bulwark

$$H_1 = 33.6 + 4 = 37.6 \text{ ft. (above the 07 level)}$$

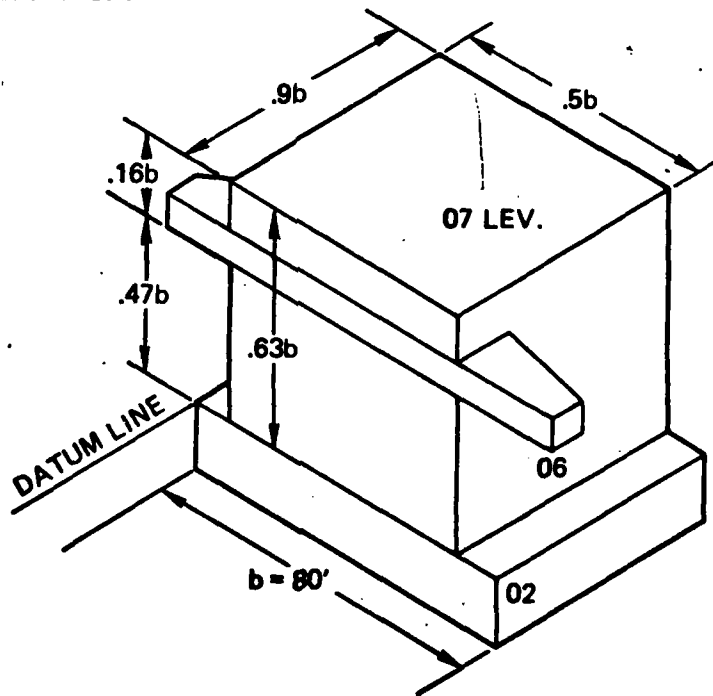
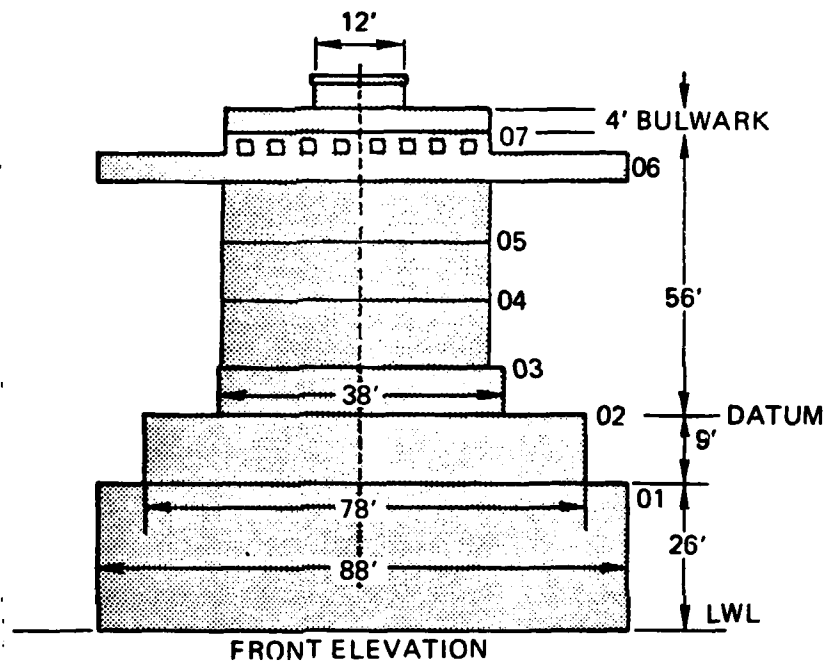


FIG. 1-9 AO DECK HOUSE

or alternatively

$$H_2 = 0.68(38) + 4 = 29.8 \text{ ft (above the 07 level)}$$

$$h_t = 0.68 \text{ from test number 9, Appendix A.}$$

In this case the mean value for boundary layer height (H) was chosen:

$$H = (H_1 + H_2)/2 = 33.7 \text{ ft (above the 07 level).}$$

1.2.2 Velocity Ratio

The design velocity ratio is determined using the method of Ower and Third. The ship profile is illustrated in Figure 1-10. The procedure for applying Rule 1 is as follows [5]:

(a) Find the maximum yaw angle for which Rule 1 should be applied. This will vary between 10 and 20 degrees. At yaw angles greater than 20 degrees, the smoke plume passes off most ships' deck before penetrating the turbulent zone.

(b) Draw a line from the stack casing top at a down angle of 20 degrees below the horizontal. The downward sloping line should be rotated to form a cone whose apex is at the stack terminal. The maximum yaw angle in plan view is where the cone intersects the beam of the ship.

(c) Since the cone clears the ship' decks, see Figure 1-10, Rule 1 does not apply.

Therefore, the next step is to apply Rule 2. Assuming a maximum ship speed of 23 knots (V_A), and true wind speed of 30 knots (V_T), and a yaw (θ) of 30 degrees, determine the relative wind speed (V_w) from equation 1.1:

$$V_w = \frac{\sin[180^\circ - (30^\circ + \arcsin((\sin 30^\circ)(23/30)))]}{\sin 30^\circ/30}$$
$$= 47.6 \text{ knots or } 80.4 \text{ ft/sec.}$$

Selecting a 130 ft/sec stack exit velocity (V_s) from Table 1-1, the design velocity ratio becomes:

$$V_s/V_w = \frac{130}{80.4} = 1.62 \quad [1.9]$$

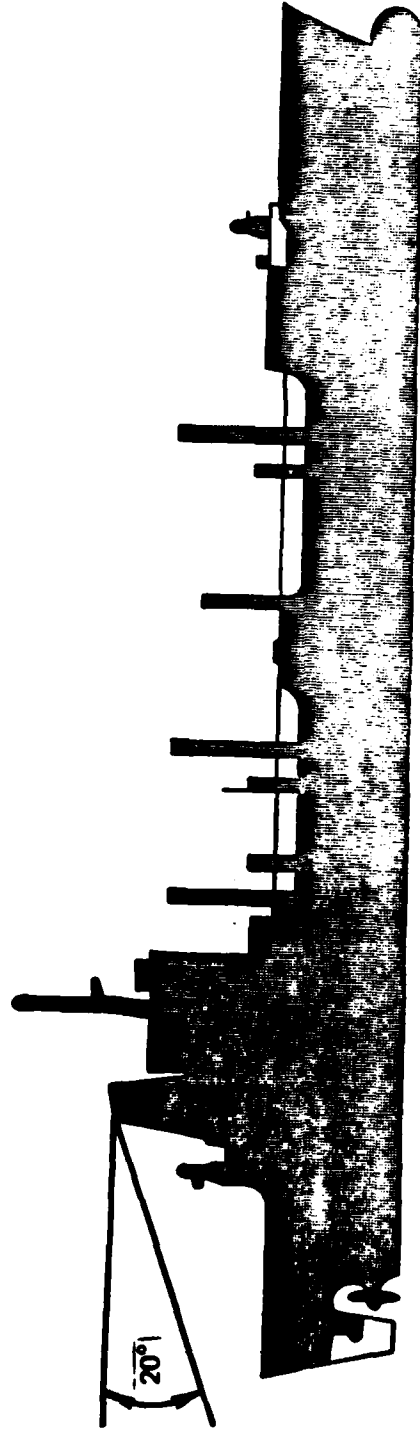


FIG. 1-10 RULE 1 FOR THE AO177

This value of V_s/V_w is well above most of velocity ratios presented in Table 1-2 for Auxiliary Tankers. The reason is that a 30 knot true wind speed was used rather than the worst case condition of 40 knots. Either raising the true wind speed (V_T) or lowering the maximum yaw angle (θ) will lower the design velocity ratio. Changing the true wind speed to 40 knots and redoing the calculation using equation 1.8 yields:

$$V_w = \frac{\sin [180^\circ - (30^\circ + \arcsin(30^\circ)(23/40))]}{\sin(30^\circ)/40} \quad [1.10]$$

$$V_w = 58.2 \text{ knots} = 80.8 \text{ ft/sec}$$

$$V_s/V_w = \frac{130}{80.8} = 1.32 \quad [1.11]$$

A nominal design velocity ratio of 1.3 was selected. The exhaust characteristics at the full power sustained speed condition are shown in Table 1-6.

TABLE 1-6

AO-177 EXHAUST CHARACTERISTICS AT FULL POWER

Ship Type	Ship Class	Stack Exhaust Velocity at Sustained Full Power	Stack Area	Stack Diameter	Exhaust Temperature at Sustained Full Power
Auxiliary	AO177	130 ft/sec	9.62ft ²	3.5 ft	400°F

1.2.3 Stack Configuration

The final AO 177 stack configuration is shown in Figure 1-11. The configuration must closely approximate Ower and Thirds case (9) (see Figure 1-5), a domed top cylindrical uptake with 22-1/2 degree slope. From figure 1-5 at a velocity ratio of 1.6, the interpenetration (h') distance allowed is:

$$h' = -1.2$$

Taking the interpenetration fraction (p) from Table 1-3, p = 0.5. From Figure 1-2

$$p = 1 - \frac{H + h'}{h_t}$$

Solving for h':

$$h' = h_t(1 - p) - H$$

$$h' = 34(0.5) - 33 = -16'$$

and

$$b = \frac{16}{h'} = \frac{16}{1.2} = 13.3 \text{ ft.}$$

A nominal value of 14 feet base width was chosen at the center line of the stack as shown in Figure 1-11. The domed top was simplified to a 45 degree slope to simplify construction. Theory would call for a pipe extension (e) of $0.475 \times 14 \text{ ft} \approx 6 \text{ ft}$. However, previous model test experience (reference 7) had shown a 3 ft pipe extension with this shape to be sufficient.

1.2.4 Plume Trajectories and Isotherms

Predictions of plume trajectory and centerline temperature in headwind and tailwind conditions using equations 1.3 and 1.4 are shown on Figures 1-12 and 1-13 respectively. Table 1-7 presents the respective ship operating conditions and power plant parameters used to calculate the plume conditions.

1.2.5 Probability Analysis

The combined cumulative probabilities of ship speed, exhaust velocity, and true wind speed as a function of time were used in the computer program described in section 1.1.2.2. The program calculates a mean stack-to-relative wind velocity ratio (V_s/V_w), and the percent of time that relative winds will occur in each identified sector. To select a design velocity ratio (V_s/V_w) and condition, a factor of 10% of the total time in each segment was used. The 10% value was considered a reasonable percentage of time which some form of adverse gas entrainment could be accepted. The mean and design velocity ratios and their respective probability of occurrence are shown on Figure 1-14.

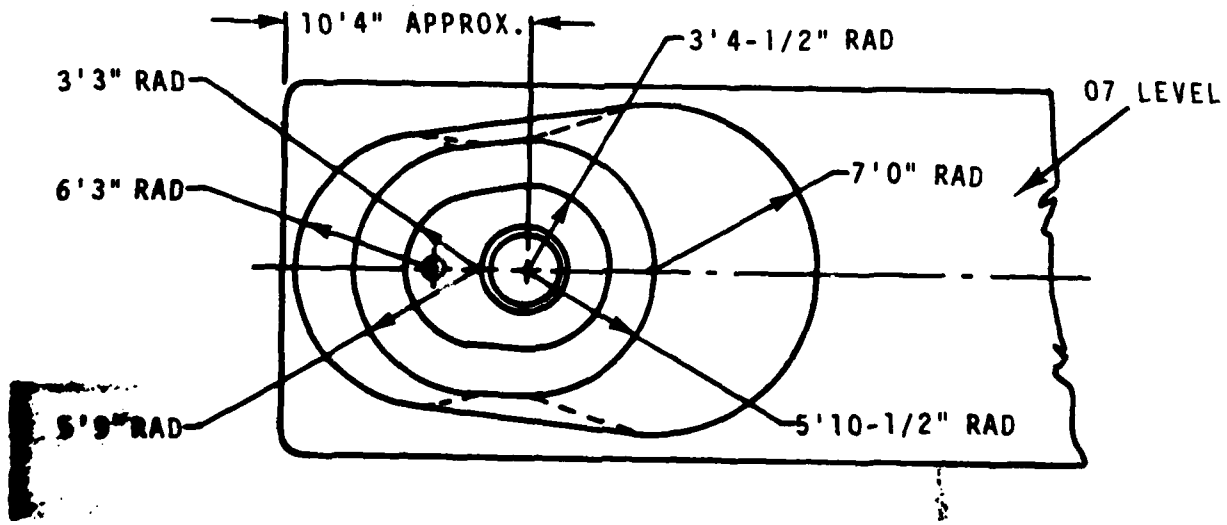
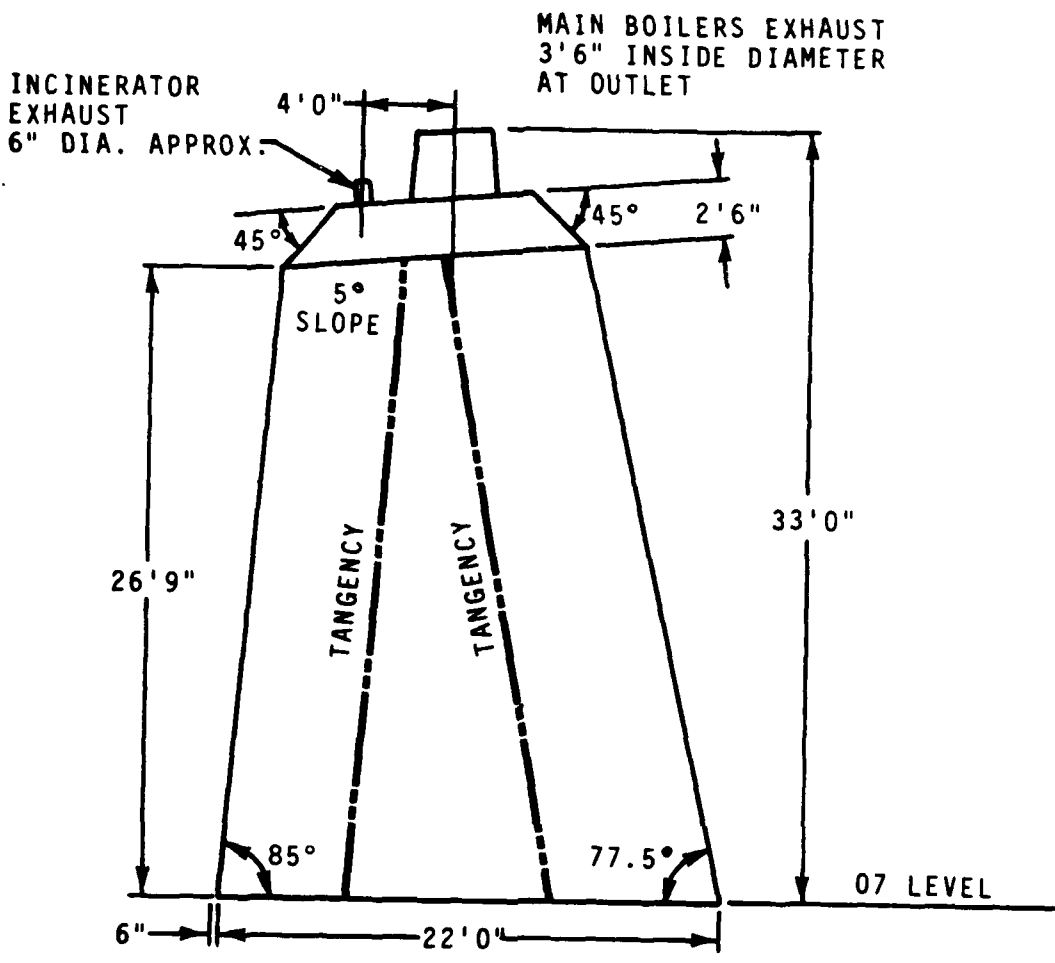


FIGURE 1-11 STACK CONFIGURATION

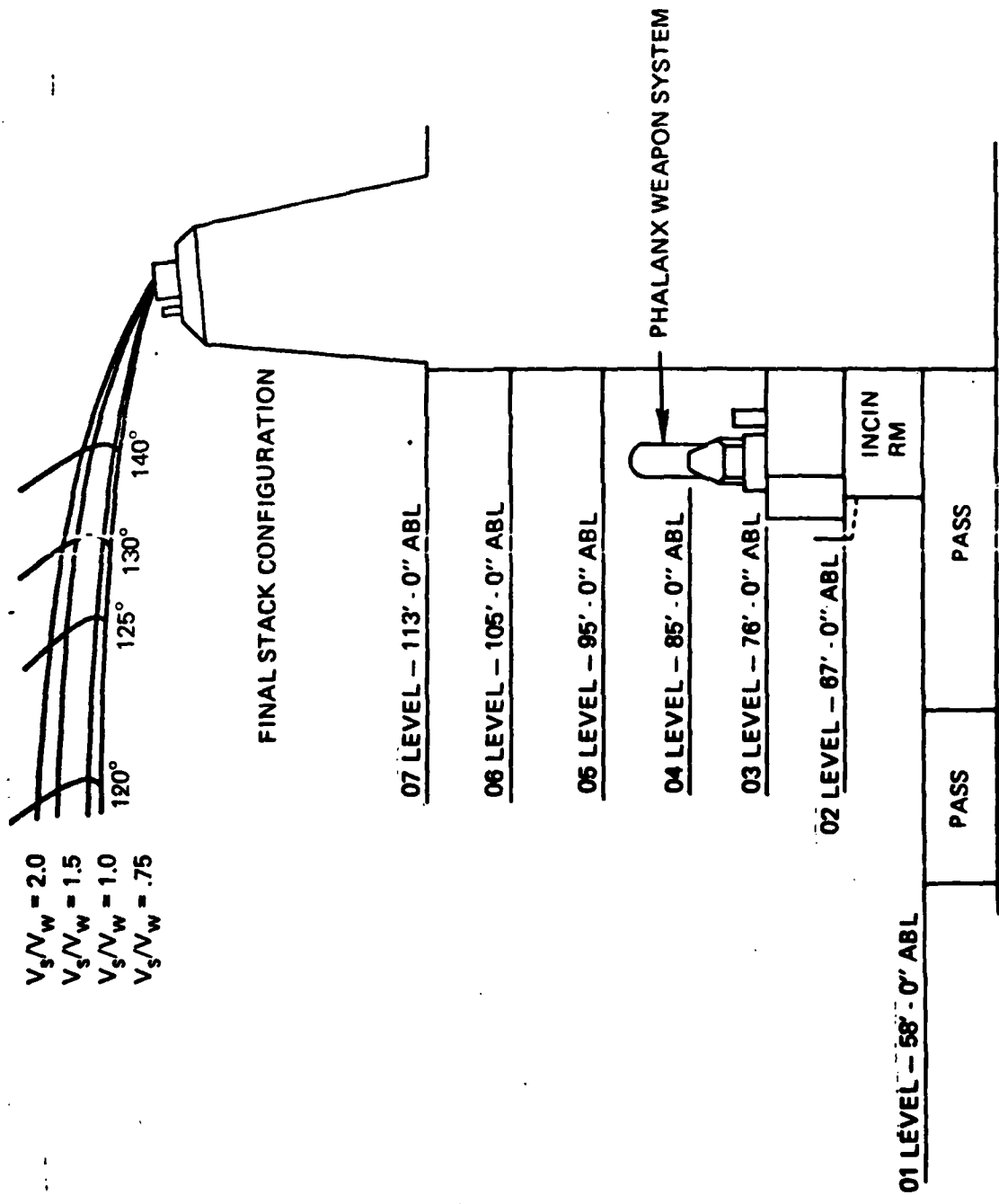
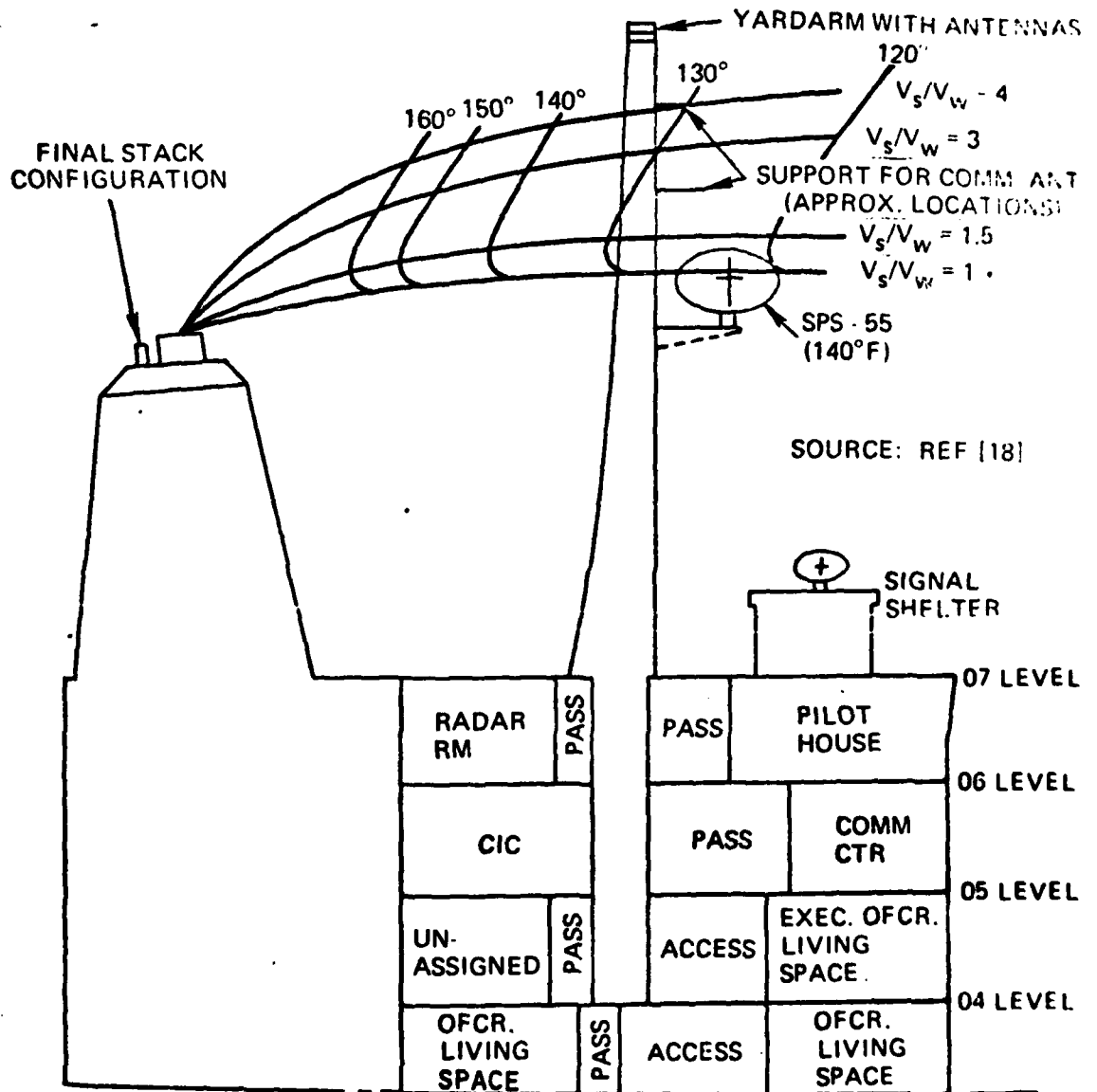


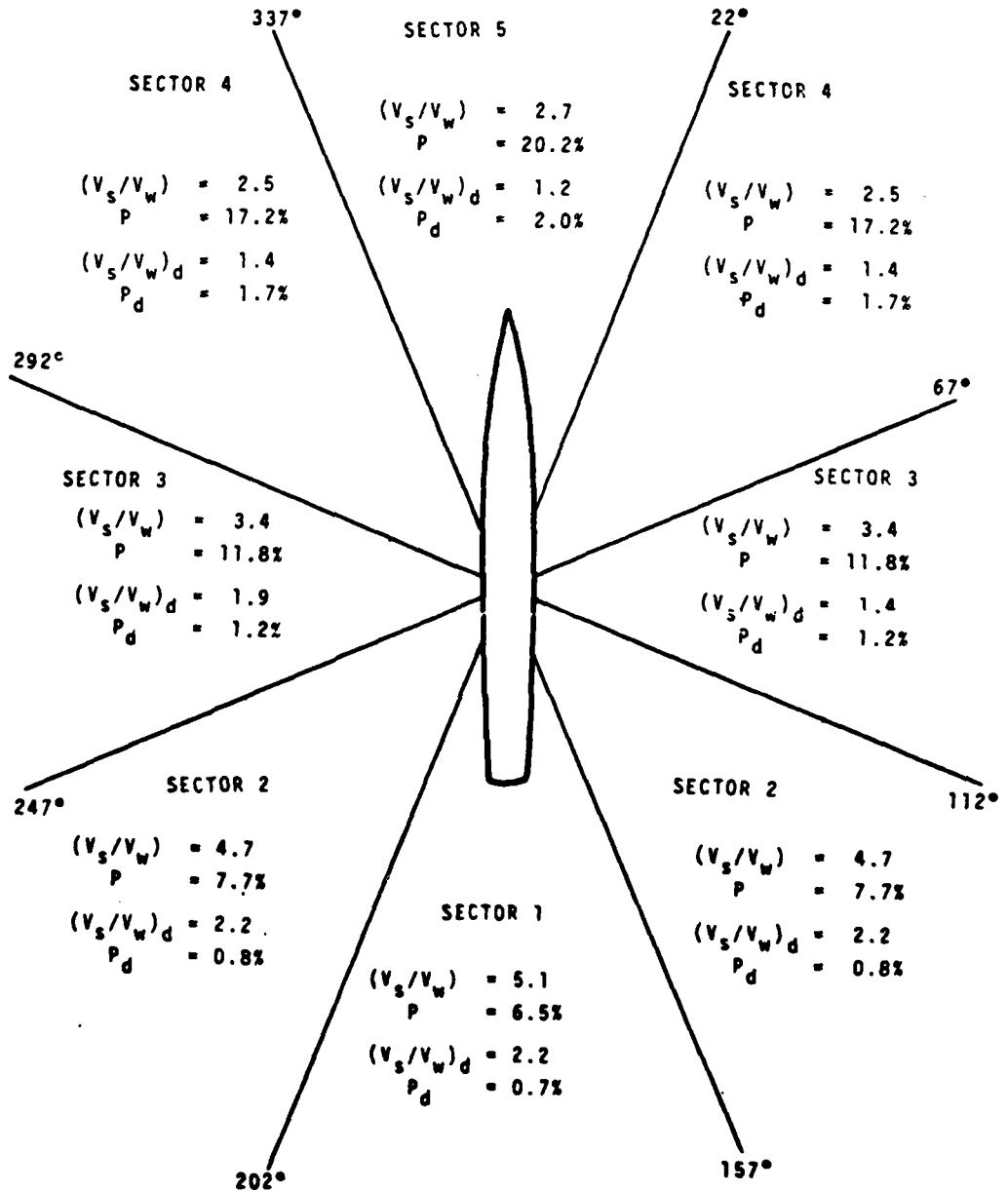
FIG. 1-12 AFT PLUME DISPLACEMENT AO177



[FIG. 1-13 FWD PLUME DISPLACEMENT (FOLLOWING WIND) AO177

FIGURE 1-14

OPERATIONAL VELOCITY RATIOS



(V_s/V_w) = MEAN STACK-TO-RELATIVE WIND VELOCITY RATIO
 P = PROBABILITY OF ENCOUNTERING THIS WIND VELOCITY RATIO IN THAT SECTOR
 $(V_s/V_w)_d$ = DESIGN STACK-TO-RELATIVE WIND VELOCITY RATIO WHICH WILL OCCUR LESS THAN 10% THE TOTAL TIME
 P_d = PROBABILITY OF ENCOUNTERING $(V_s/V_w)_d$ IN THAT SECTOR

TABLE 1-7

POWER PLANT PERFORMANCE PARAMETERS (1), (2)

<u>Full Power</u>	<u>Combined Propulsion Boiler Exhaust Airflow</u>
Gas Temperature, stack	400°F
Velocity @ stack exit	130 ft/sec
Exhaust weight flow	61 lb/sec
Ship speed	21-23 knots
 <u>Cruise Power (Max)</u>	
Gas Temperature, stack	355°F
Velocity @ stack exit	105 ft/sec
Exhaust weight flow	49 lb/sec
Ship speed	20 knots
 <u>15 Knots</u>	
Gas Temperature, stack	330°F
Velocity at Stack exit	63 ft/sec
Exhaust weight flow	30 lb/sec
 <u>10 Knots (Astern)</u>	
Gas Temperature, stack	340°F
Velocity at stack exit	88 ft/sec
Exhaust weight flow	42 lb/sec

-
- (1) Ambient Temperature (T_{∞}) = 100°F
(2) Stack Diameter = 3.5 Ft.

1.3 Combatant Ship Design Example

The FFG-7 (Patrol Frigate) stack configuration was selected as the combatant design example. References [14, 16, 22 and 23] summarize the design efforts conducted during Preliminary and Contract Design of the FFG-7.

1.3.1 Superstructure Configuration and Stack Height

The design procedure followed in the auxiliary tanker example is not generally applicable to combatant ship stacks. This is due to the fact that most combatant ship designs utilize low profile stack configurations. This minimizes topside weight, and provides the least obstruction for radar and weapons coverage.

A serious problem existed at the end of the Preliminary Design Phase of FFG-7. The stacks had been configured with only a cowling protruding above the top deck of the superstructure. Clearly then, there is no need to check boundary layer heights, the stack discharge would always be well within the turbulent zone.

To determine the minimum stack height which would be satisfactory, a model test was conducted [22]. The results indicated hot exhaust gas reingested into the inlets. Insufficient vertical clearance of the stack discharge terminal caused the plume to get trapped and attach to the deck at velocity ratios (V_s/V_w) of 2.0 and under. Recommendations resulting from the model study were to:

(a) Raise the stacks to a height of 6 feet above the 03 level (top deck) with the uptake pipes extending an additional 2 feet higher than the terminal top.

(b) Reduce the uptake exit area to increase the uptake velocity and momentum.

The resulting sustained full power design conditions are given in Table 1-8.

Table 1-8: FFG-7 Exhaust Characteristics at Full Power

Ship Type	Ship Class	Stack Exit Velocity	Stack Area	Stack Diameter	Exhaust Temperature
Combatant	FFG-7	264 ft/sec	17.05 ft ²	4.7 ft	780°F

1.3.2 Velocity Ratio

Velocity ratios were tabulated for a number of operating conditions. Table 1-9 presents these data.

TABLE 1-9

FFG-7 Performance Data

	OPERATING MODE		
	Full Power	Cruise	Idle
Stack Exit Temperature (°F)	780	650	600
Velocity (ft/sec)(V _s)	264	186	56
Ship Speed, knots	28	20	5
Velocity Ratio			
0 deg Yaw	2.30	1.85	0.56
30 deg Yaw	2.53	1.96	0.75
180 deg Yaw	13.20	5.46	0.95
V _w = 40 kt; T _A = 100°F			

1.3.3 Stack Configuration

The stack configuration selected was similar to Owen and Third's casing A (Figure 1-3) [5] with a forward cylindrical section. The stack casing was not angled. No attempt at altering the stack shape to improve performance was made because of the extremely low height of the stack terminal.

1.3.4 Plume Trajectories

Exhaust plume temperature profiles for the FFG-7 are shown on Figure 1-15 for the sustained full power condition. The method used to calculate these curves is the same as that presented in section 1.1.1.5.

1.3.5 Probability Analysis

The probability of occurrence of a specific plume incidence temperature (T) for a selected topside location (x, y) can be expressed as the conditional probability:

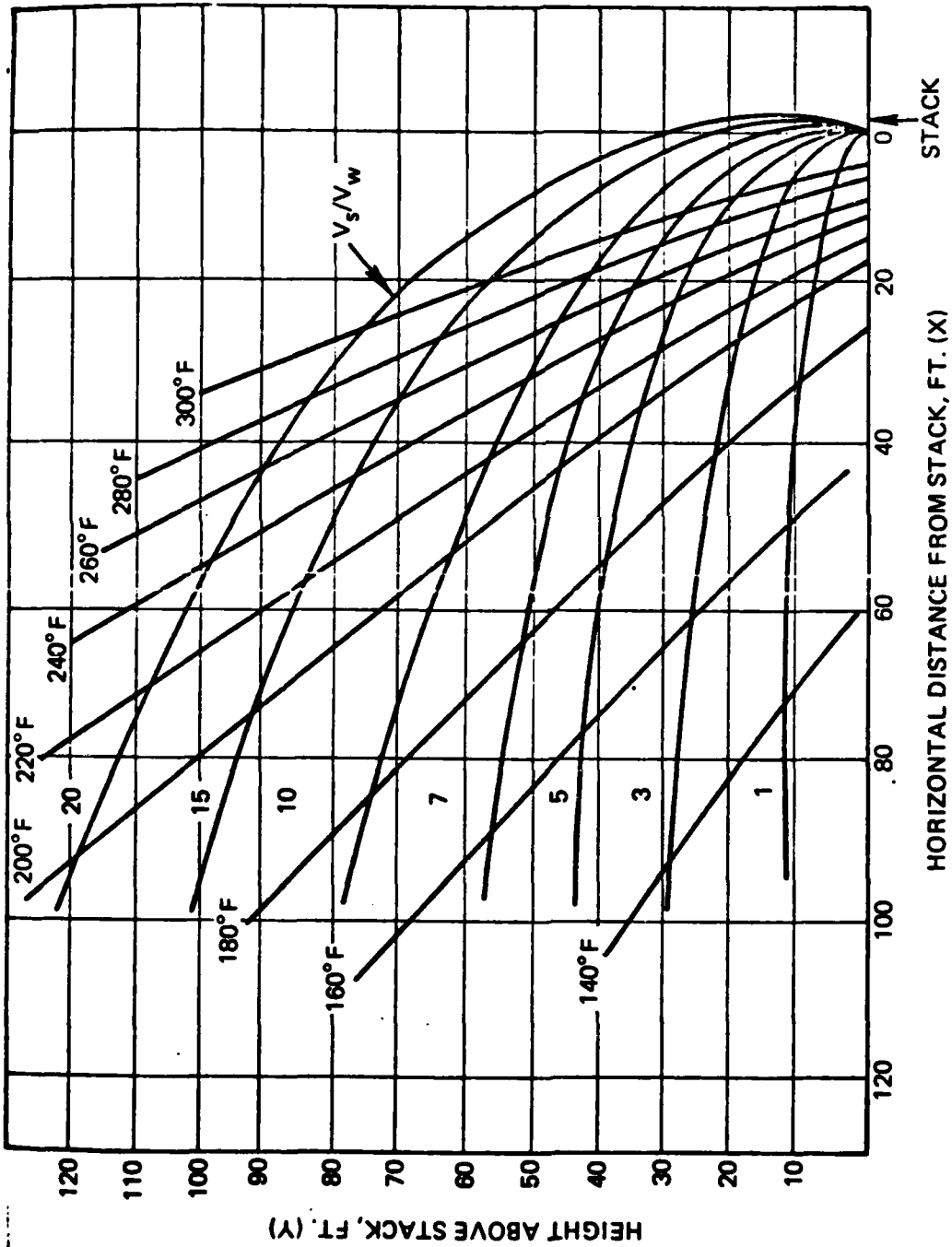


FIG. 1-15 EXHAUST PLUME TEMPERATURE PROFILES FOR THE FFG-7

$$P[V_S/V_W] = P[T_A \times V_W \times V_A \times \theta]$$

where

T_A = ambient air temperature

$P[]$ = probability of variable in parenthesis occurring

θ = yaw angle of wind

V_A = ship speed

V_W = true wind speed

V_S = stack exit velocity

All parameters are assumed to be stochastically independent (i.e., not influenced by one another), the probability can be expressed as:

$$P[V_S/V_W] = P[T_A] \cdot P[V_W] \cdot P[V_A] \cdot P[\theta]$$

Hand calculations were used in this case. Some of the variables used in the analysis, along with the cumulative results, are shown in Figure 1-16. Each set of input parameters was conservatively chosen so that the lowest velocity ratios would result.

FIGURE 1-16 FFG-7 VELOCITY RATIOS - PROBABILITY OF OCCURRENCE

GIVEN EQUALLY PROBABLE HEAD AND TAILWIND RELATIVE DIRECTIONS THEN

<u>WIND SPEED (V_w)</u>	<u>$P(V_w)$</u>	<u>SHIP SPEED (V_A)</u>	<u>$P(V_A)$</u>
< 10 kts	0.29	5 kts (0-10)	0.12
20	0.45	20 (11-22)	0.85
> 40	<u>0.26</u>	30 (23-30)	<u>0.03</u>
	1.00		1.00

VELOCITY RATIO PROBABILITY

<u>V_s/V_w</u>	<u>$P(V_s/V_w)$</u>
< 1.0	0.059
1.0 1.0 - 2.0	0.350
2.0 - 4.0	0.134
4.0 - 6.0	0.022
6.0 - 9.0	0.233
> 9.0	<u>0.202</u>
	1.00

2.0 BACKGROUND AND THEORY

2.1 Turbulent Flow and the Stack Gas Plume

2.1.1 Nature of Stack Emissions

2.1.1.1 Soot - Soot is comprised of relatively large particles that grow on the inner surfaces of the stack which eventually breakoff and are ejected. These particles possess a finite rate of descent [4]. Soot can burn boat covers, discolor paint and corrode steel. It can not be controlled like smoke because soot settles out of the plume while smoke is buoyant and remains in the plume. Soot can be controlled by dust collectors, expansion chambers, insulated stacks or scrubbers [4]. The soot problem is usually worse on a steam operated ship when the engineer blows soot from the boiler surfaces. This often results in a rain of soot on the deck. Although soot is a factor in the design of ship's stack it is a problem that is not addressed in this manual.

2.1.1.2 Smoke - Smoke is a gaseous efflux of very fine particles that will remain suspended indefinitely. These elements make up the bulk of the plume and must be ejected clear of the ship with the plume. Smoke causes many problems when interacting with other systems because it has the following properties:

- Corrosive (contains sulphur)
- Nauseous
- Highly heated (can cause overtemperature damage)
- Not always visible

These properties of smoke mean it must not be ingested into the crew areas, cannot pass uncontrolled through antennae, must be kept clear of helicopter operations, must not be reingested into the engines or other intakes, and must not impinge on any part of the hull or superstructure.

2.1.2 Gas Flow Around Bodies

2.1.2.1 Two Dimensional Cylinder in an Air Stream - Sherlock [8] compared the stack to a long circular cylinder in a cross flow. If the gas in this flow was perfect (i.e., no losses due to viscosity) it would regain its original flow pattern after passing the cylinder as shown in Figure 2-1.

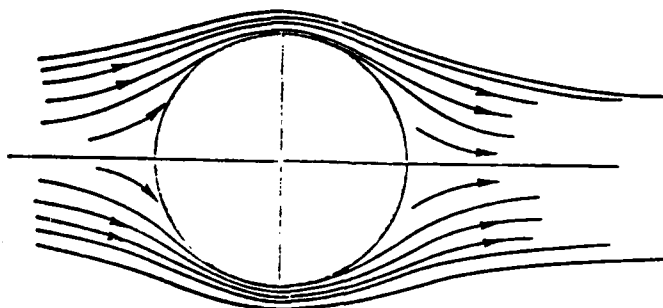


FIGURE 2-1
IDEAL FLOW AROUND A CIRCULAR CYLINDER

As an ideal gas passes the cylinder the velocity of the flow increases. This results in a corresponding increase in kinetic energy with a corresponding decrease in pressure. At the point where the flow passes the maximum width of the cylinder kinetic energy is at a maximum and is sufficient to cause the flow to return to the original streamlines. However, air is not a perfect gas. As a real gas it possesses frictional viscosity which causes kinetic energy losses when traveling past the cylinder. Because of this reduction in kinetic energy the flow cannot return to the original streamlines and is forced to separate as shown in Figure 2-2.

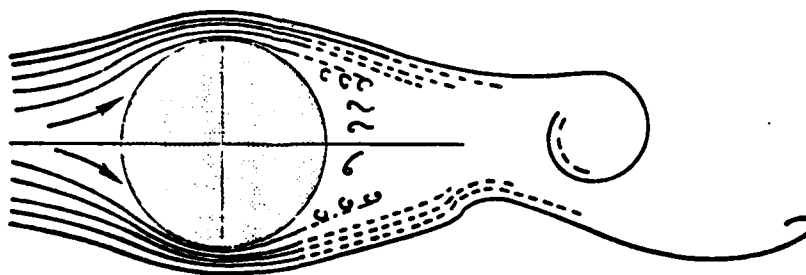


FIGURE 2-2
REAL GAS FLOW AROUND A CIRCULAR CYLINDER

Separation forms a region where the static pressure is lower than free stream but higher than the fast moving layers immediately around it. These fast moving layers support a pressure difference due to their momentum. Eventually they turn in upon themselves and roll up into vortices, with axes parallel to the axis of the cylinder. These vortices flow downstream and slowly disintegrate as the low pressure central region entrains free flowing gases. This causes the vortices to increase in mass and decrease in rotational momentum. Eventually rotation breaks down completely and flow no longer follows any particular pattern. It has been shown that vortices must be staggered to be dynamically stable and form what is known as a "Karman Trail" [5].

2.1.2.2 Flow Over Bluff Bodies [2] - As can be seen in Figure 2-3 the flow over a bluff body separates from the boundary ahead of the body to form an eddy region on the windward surface. A second separation occurs on the leading edge of the upper surface and spreads to fill the area behind the body. Regions above the separation are smooth. The flow has generated a streamline flow over an abrupt obstacle and a turbulent region immediately in contact with the obstacle.

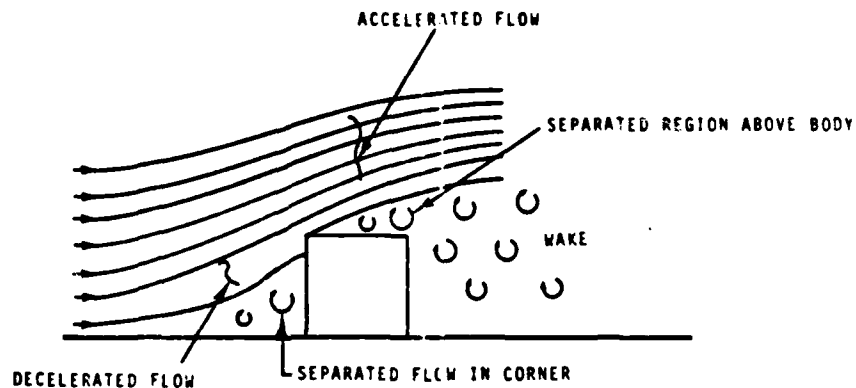


FIGURE 2-3
FLOW AROUND A BLUFF BODY

Mixing of the free stream with the turbulent area occurs at the interface and tends to continue the disturbance downstream. Vortices are generated as shown.

2.1.2.3 Stack Plume Flow - The flow around the ship stack is a combination of the circular cylinder flow and the bluff body flow. To complicate matters this body ejects gases vertically and the entire turbulent flow pattern is subject to abrupt changes as the yaw angle changes.

- o Deformation of the plume as it is bent - Usually, the stack plume is emitted perpendicular to a laminar cross flow. In a region of laminar flow a gas jet has distinct boundaries. At its source the jet has a reasonably uniform velocity profile and relatively low turbulence. As the jet rises it is deflected by the cross flow and the plume bends until its flow is principally horizontal. A pressure field forms around the jet as it is deflected causing it to form a kidney shape [9]. The jet will remain distinct as long as the cross flow is laminar but in a region of turbulent flow the jet will quickly spread out and no longer be distinct. This is what happens if the plume enters the turbulence of the ship's superstructure.

- Local effect - The stack usually can be represented as a short cylinder. Gas flowing around this cylinder experiences an increase in pressure on the windward face and a corresponding decrease of pressure on the sides and back. Air flows over the top and down the back of the stack as is shown in Figure 2-4.

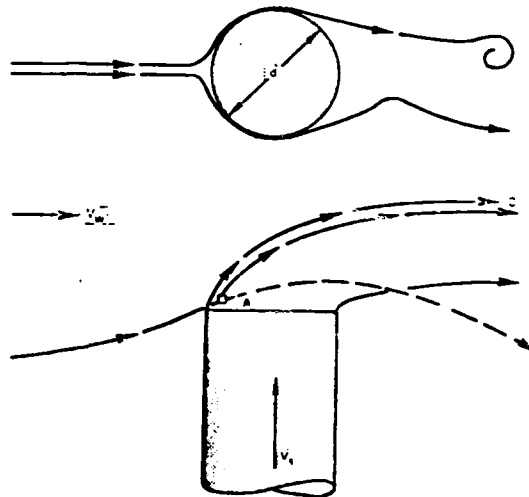


FIGURE 2-4
RESULTANT PATH OF STACK GASES IN THE WIND

If the gas emitted from point A of Figure 2-4 has sufficient velocity, V_g , it will be carried along path C. But, if smoke is emitted at A with a very low V_g then the influence of V_w will cause it to follow a path to B. This second flow is called a "downwash" and if sufficiently strong will cause the smoke to come down to the deck as it mixes in with the vortices behind the stack. For typical merchant ships the "downwash" does not extend more than $1/2$ to 1 stack diameter below the stack outlet [3]. The velocity ratio, V_g/V_w , is the determining factor for "downwash"

being a problem. The amount of "downwash" is also influenced by the shape of the stack and yaw angle. A streamlined stack at small yaw angles will not generate the vortex trail that a circular stack generates. The strength of these trailing vortices is a major contributor to "downwash."

- Ships Turbulent Zone Effect - The superstructure of a ship is composed of a number of bluff bodies each of which contributes its own turbulent wake. Each obstacle acts as a turbulence generator that sheds vortices which gradually mix with the region of laminar flow as they travel downstream. Together these generators combine to form a general turbulent region which encompasses the entire ship superstructure and is known as the turbulent zone. Model tests have confirmed the existence of a turbulent zone that increases in depth aft. These tests have also shown that the turbulent zone is a function of ship superstructure and yaw angle. In the previous section it was noted that when a plume enters a turbulent region it will mix throughout that region. Therefore, if the stack plume enters the turbulent zone via stack "downwash" the smoke will be brought down to the deck. Traditionally the top of the stack was well above the turbulent zone and "downwash" did not cause a problem. But this is not now the case. The transition from laminar to fully turbulent flow is a gradual one that takes place through a region of significant depth. A stack ejecting gas into this transitional region will only perform satisfactorily if "downwash" is properly controlled. The Patrol Frigate is an example of a ship class that ejects the stack gases directly into the turbulent zone. This was possible after increasing the stack gas velocity to 260 ft/sec.
- Yaw Angle - Yaw angle is the angle of the relative wind to the ship's heading. Yaw angle affects both the turbulent zone and the "downwash" around the stack. Usually ship stacks are longer than they are wide and will, therefore, have different flow patterns as the yaw changes. Generally, the performance of an individual stack in a laminar cross wind degenerates as yaw increases beyond 15 to 20 degrees. But a stack model mounted on a

ship structure will exhibit degenerated performance from 15 to 60 degrees and then improved performance from 60 to 90 degrees [3]. This improvement is caused by a change in the direction of flow over the stack. For small yaw angles the flow over the stack is largely horizontal and continues to be horizontal until the flow approaches 60° of yaw. From this point on the vertical sides of the ship become dominant flow directors, the direction of the flow becomes vertical and the vertical flow carries the stack gases higher. The result is improved stack performance.

2.1.2.4 Control of Plume Behavior - The plume can be affected by changing any of the following relationships which in turn affect the height of the turbulent zone, the velocity ratio, plume temperature, and local flow around the stack (i.e., "downwash").

- Type of power plant - Gas turbines usually present the biggest problem with the plume but for small high powered vessels gas turbines have shown themselves to be desirable for other reasons. A gas turbine plant requires four times the air mass flow and will exhaust this large volume of air at 200°C higher than a comparable steam plant [10]. In addition, gas turbines are very sensitive to temperature transients and the increased mass flow makes intake location a critical problem.
- Vessel operating profile - This operating profile is the necessary result of the vessel's mission and is not likely to be changed. The profile contains probabilities of operating velocity ranges and the complimentary mass flow and temperature of the power plant exhaust.
- Stack Area - Stack area directly affects the smoke velocity. The effective outlet area of the stack can be continuously varied with a damper. Multiple stacks can also be employed to keep the stack velocity high while operating at low powers. Both techniques sacrifice efficiency and simplicity for the sake of improved plume performance.

- Location of stack - By merely moving the stack longitudinally it may be possible to exhaust the gases outside the turbulent zone (TZ). Longitudinal stack location can also be used to maximize the distance between stack and antennae and thereby lower the temperature of the gases passing through the antennae.
- Characteristics of the stack - The shape of the stack itself can be used to improve the local flow and reduce the "downwash." There are many variations and a detailed discussion of these can be found in Section 2.1.3.
- Height of the stack or TZ - Both stack height and height of the turbulent zone can be adjusted to decrease the likelihood of plume entrainment in the turbulent zone.

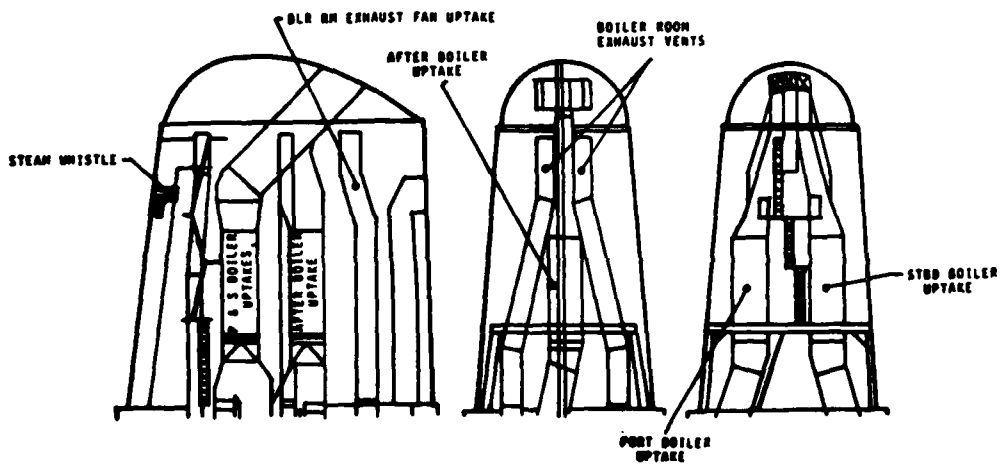
2.1.3 Conventional and Special Stack Shapes

The following stack configurations have one design goal and that is to surround the plume with smooth flowing air at all yaw angles. Most of these shapes work well under some conditions and exhibit little or no improvement for other conditions. They are presented to familiarize the designer with several alternative types of stacks.

2.1.3.1 Streamlined Stacks - Most conventional stack designs have streamlined body sections. Streamlined sections are chosen in preference to cylindrical sections due to architectural and flow considerations (in a headwind). Streamlined stacks with long, slender sections fore and aft cause considerably more suction in a sidewind than an equivalent cylinder. However, aesthetic considerations and fore and aft design conditions dictate selection of streamlined designs.

Acker [3] has shown that a horizontal stack top is better than a raked or sloped top. The horizontal top gives less section aft than a sloping top. If the stack top must be raked for design purposes, 1:12 is a suitable slope. In some special designs, a slope of 1:9 has produced good results.

Although there are numerous variations of streamlined stack types, a good example of this type of stack casing is the Clydebank funnel design. The design was introduced by John Brown & Co., Ltd. in the early 1950's. Figure 2-5 shows some elevation and section views of the casing. The upper one-third has a section similar to Casing A in Figure 1-3. This



ELEVATION AND CROSS-SECTIONS THROUGH THE CLYDEBANK FUNNEL

FIGURE 2-5
CLYDEBANK FUNNEL

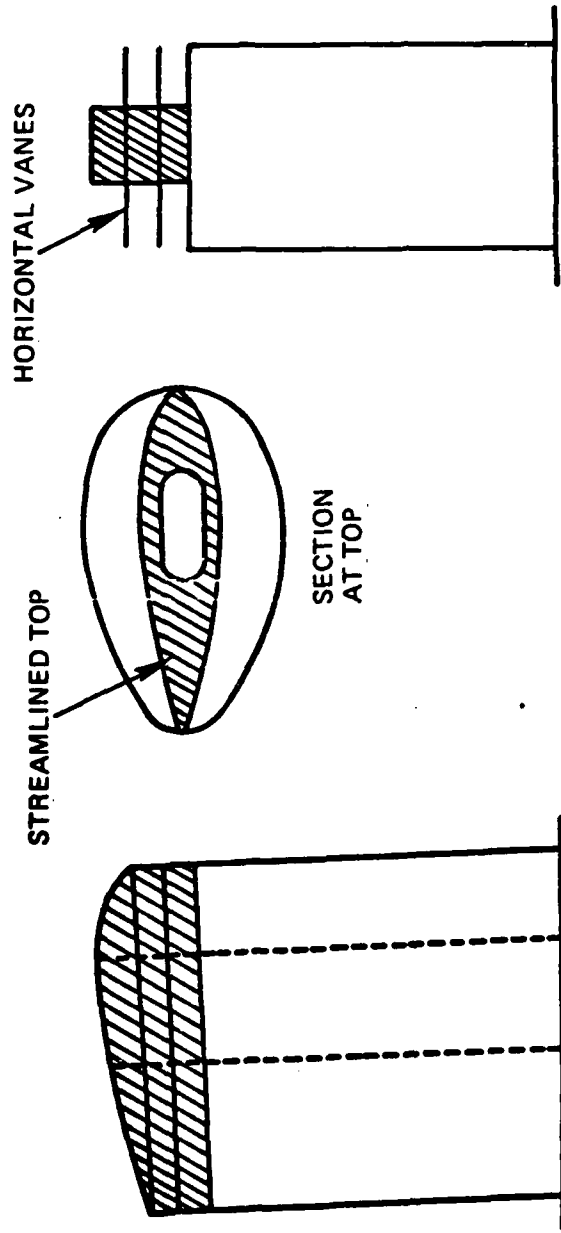


FIG. 2-6 THORNYCROFT FUNNEL ACKER, REF. [3]

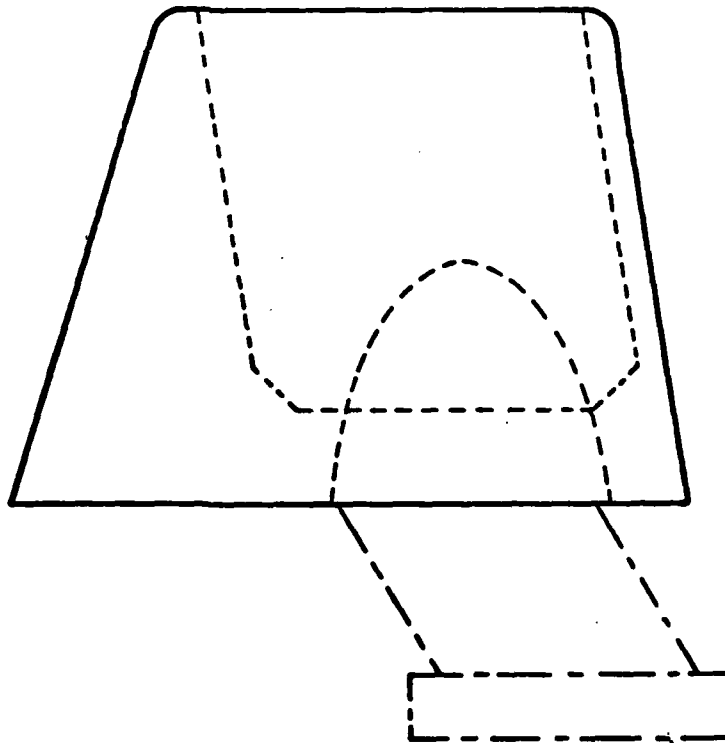
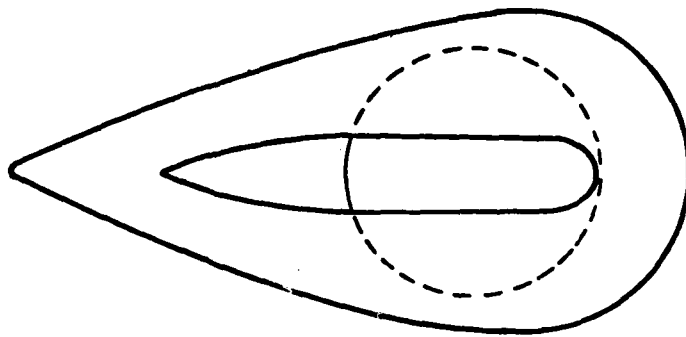


FIGURE 2-7
STROMBOS TYPE FUNNEL MODEL

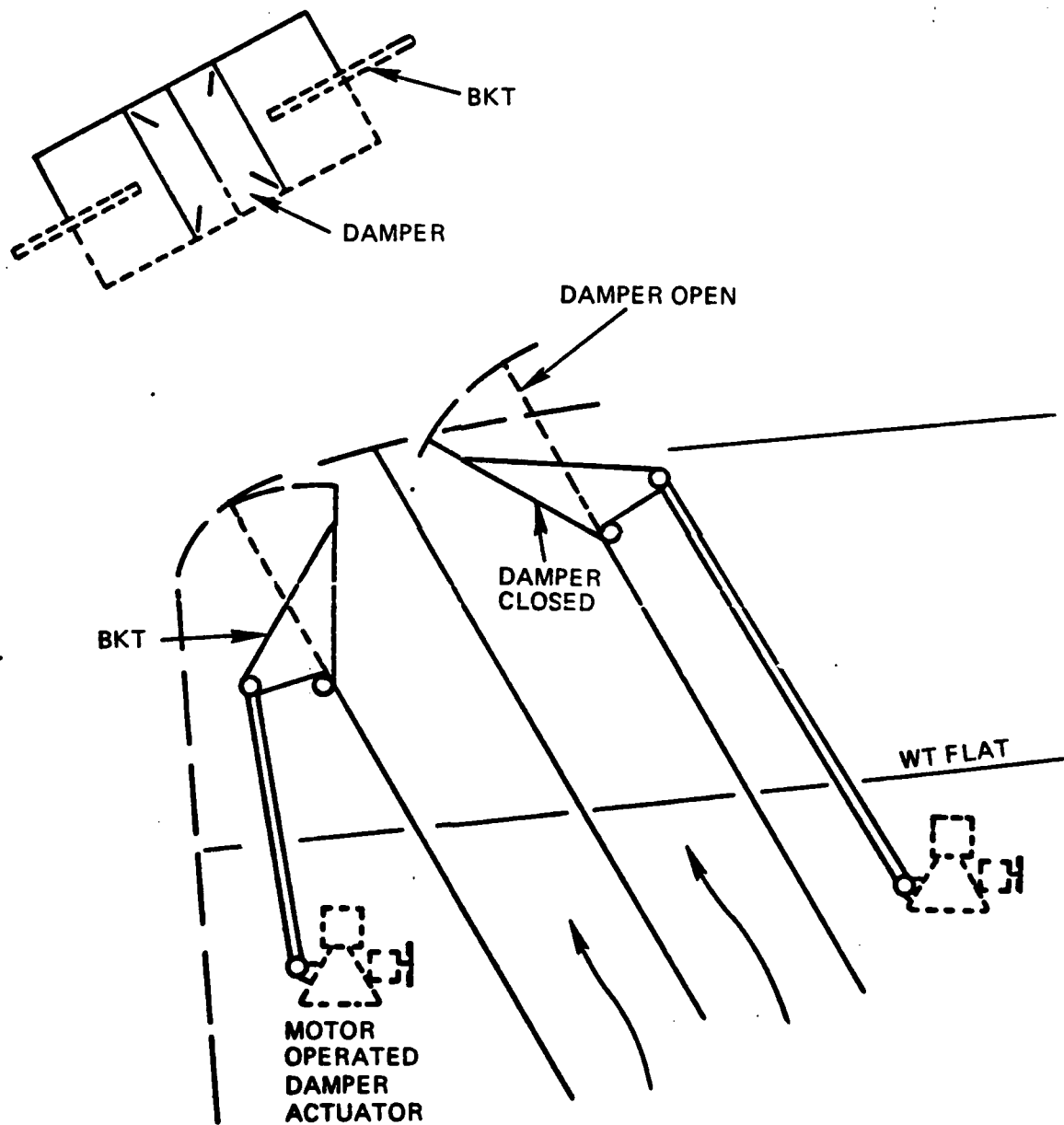


FIG. 2-8 DAMPER ARRANGEMENT ON THE "INDEPENDENCE" ACKER, REF. [3]

2.1.3.6 Athwartships Terminal Extentions - The SS FRANCE stack configuration is a vertical casing with two faired fins extending horizontally athwartships. The smoke is ejected from the ends of these fins and thereby removed from the stagnation region in the lee of the vertical casing. Often in operation the downwind fin is sealed as an extra precaution in keeping stack gas out of the stagnation region. This stack has been successful in eliminating the downwash effect behind the stack even though the stack gases are given no vertical thrust. The DE 1052 stack terminal uses a similar technique to direct exhaust gases clear of the ships superstructure. Exhaust gas is directed into two separate port and starboard terminal pipes angled aft and slightly above horizontal. Figure 2-9 illustrates this design.

2.1.3.7 Annulus - An air annulus surrounding the exhaust flow can improve plume structure and compactness but does not increase the trajectory height. To be effective the annulus should have a velocity not less than one to two times the free stream velocity and at a volume at least equal to the exhaust at full power. Schultz and Matthews [11] tested three annuli with widths 8.8, 16.0 and 24.4 percent of the stack diameter and found the smallest annulus to be best. Acker [3] suggests keeping the annulus width less than 10 percent of the stack diameter.

2.1.3.8 Eductors - Eductors were utilized in the DD 963 to cool the exhaust gases being emitted from the stack. In this design the exhaust temperature into the eductor is 900°F and the temperature out of the eductor is 400-500°F. The cooling eductor air flow is 1.6 to 1.0 times the turbine exhaust flow. Figure 2-10 shows a typical eductor. This design was guided by model tests at UCLA, where many configurations of eductors were tested. At this time any eductor design must be accompanied by detailed model tests.

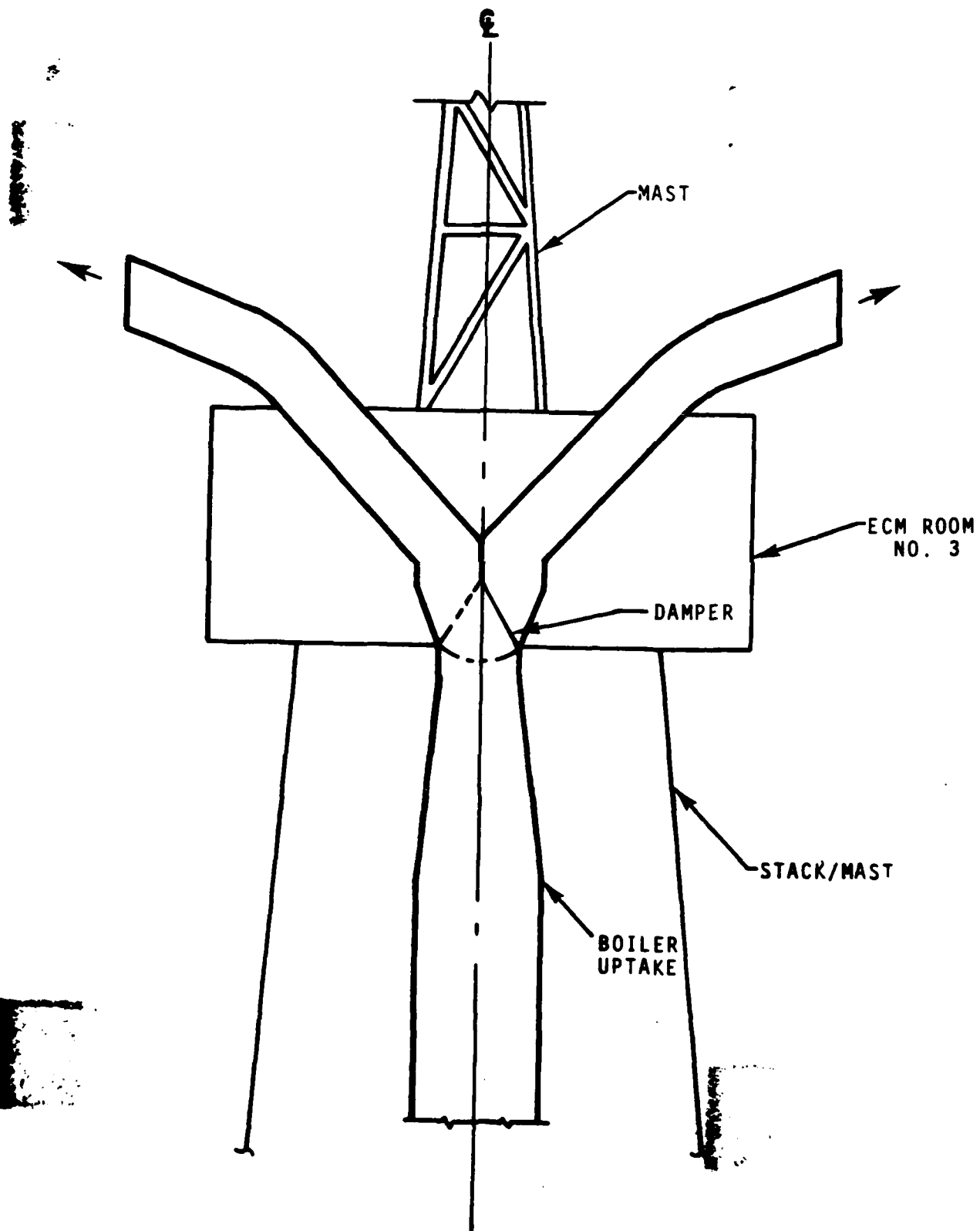


FIGURE 2-9: DE 1052 STACK - SECTION LOOKING AFT

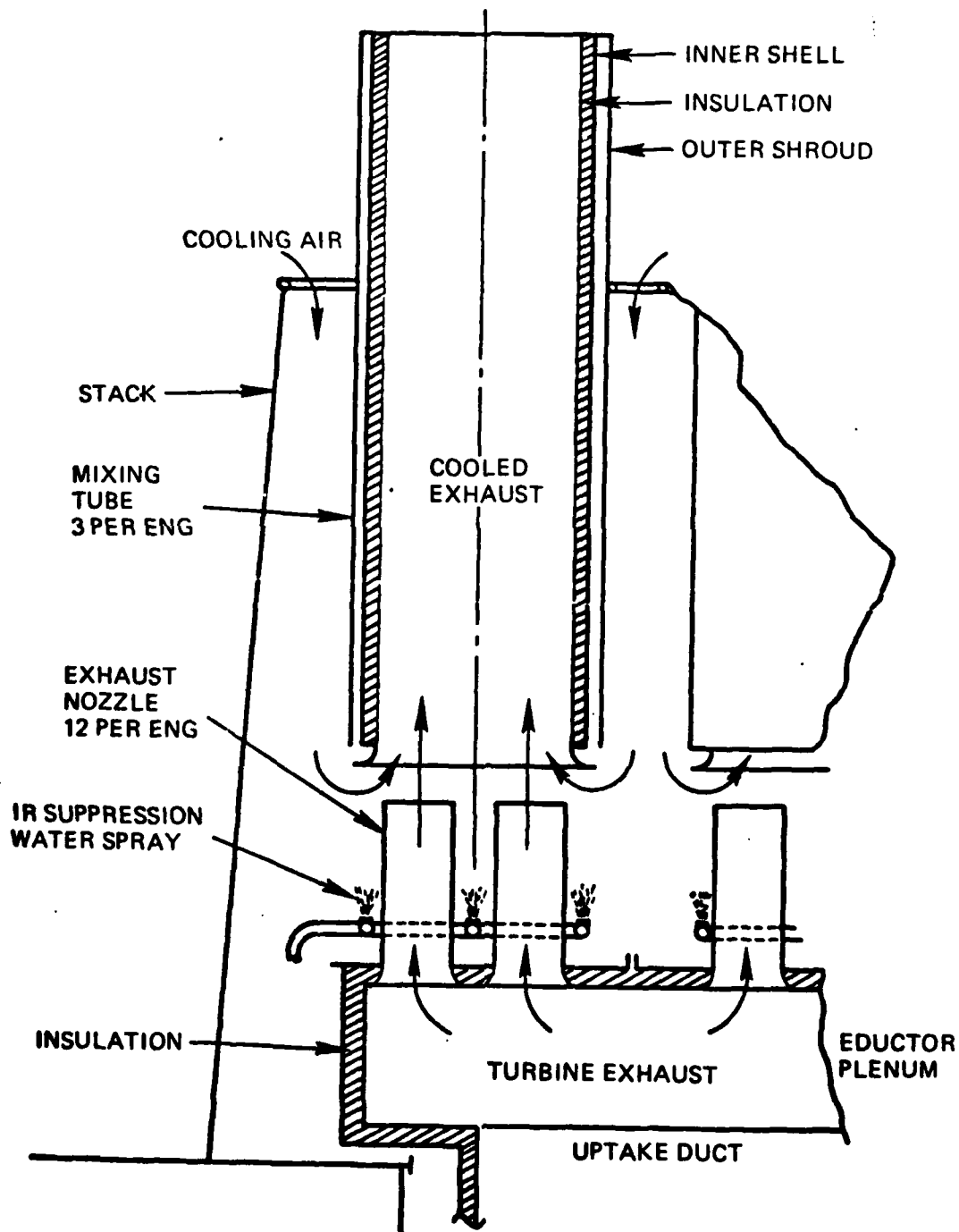


FIG. 2-10 EDUCTORS ON THE DD-963 (MARINE TECHNOLOGY - JAN. 1975) REF. [12]

2.2 Plume Behavior Theory

2.2.1 Plume Prediction Equations - The following equations were found to give the best representation of plume characteristics when compared with full scale and model test data.

2.2.1.1 Trajectory - The form of equation 2.1 was derived by Hoult, Foy and Fourney [13]. Figure 2-11 contains specific results of their theoretical treatment of the gas plume. Charwat conducted model tests during the design of the DD 963 and determined the values of the coefficients of equation 2.1.

$$\frac{y}{D_s} = \frac{(V_s/V_w) [1.7(X/D_s)]^{0.37}}{(1.2 + 0.15 V_s/V_w)^{0.50}} \quad [2.1]$$

Figure 2-11 shows a comparison of equation 2.1 and the data taken during the HMS GLAMORGAN trials [10].

Subsequent review of the GLAMORGAN data, and refinement of the coefficients resulted in the following equation:

$$\frac{y}{D_s} = \frac{N(V_s/V_w) (X/R_s)^{0.25}}{(2.4 + 0.3 V_s/V_w)^{0.50}}$$

Where:

N = 1.15 for one exhaust pipe

N = 0.86 for more than one exhaust pipe

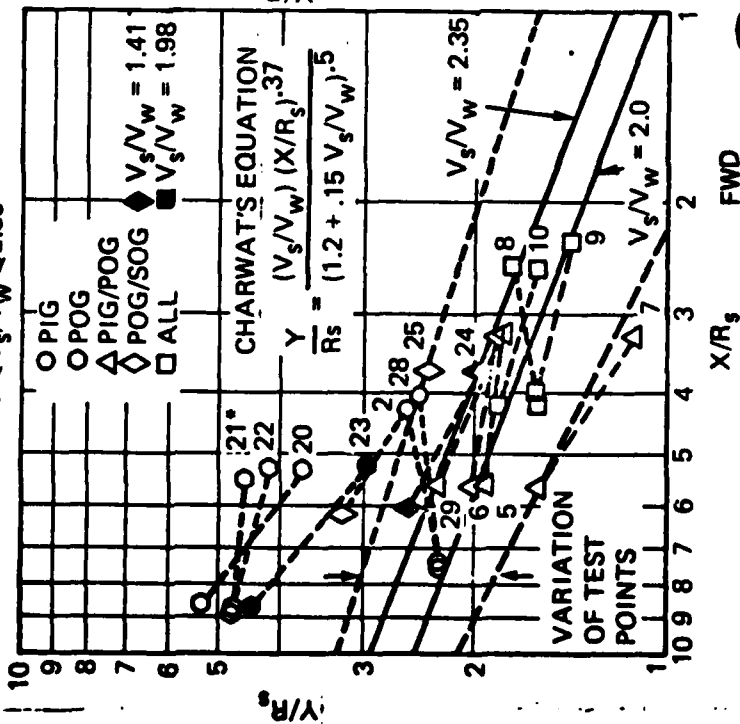
2.2.1.2 Plume Temperature - Equation 2.2 was derived during the design of the Sea Control Ship. This equation is plotted on Figure 2-12 along with the GLAMORGAN and LM2500 [14] full scale test data and Charwat's model test data. To use equation 2.2 it is necessary to know the plume length.

$$\phi = \frac{T_m - T_\infty}{T_s - T_\infty} = \frac{(V_s/V_w)^{0.25}}{s/D_s} \quad [2.2]$$

In many instances it is sufficient to plot the trajectory (using equation 2.1 [1]) and then measure the plume length with an appropriate graphical method. When a graphical solution is not appropriate equation 2.3 can be employed to determine S analytically. This equation is a direct application of Simpson's rule to the integral:

$$s = \int \sqrt{1 + x^2} \, dy$$

NON-DIMENSIONAL
PLUME TRAJECTORIES
GLAMORGAN TRIALS
 $20 \leq V_s/V_w \leq 2.35$



NON-DIMENSIONAL
PLUME TRAJECTORY
GLAMORGAN TRIALS
 $2.35 \leq V_s/V_w \leq 2.7$

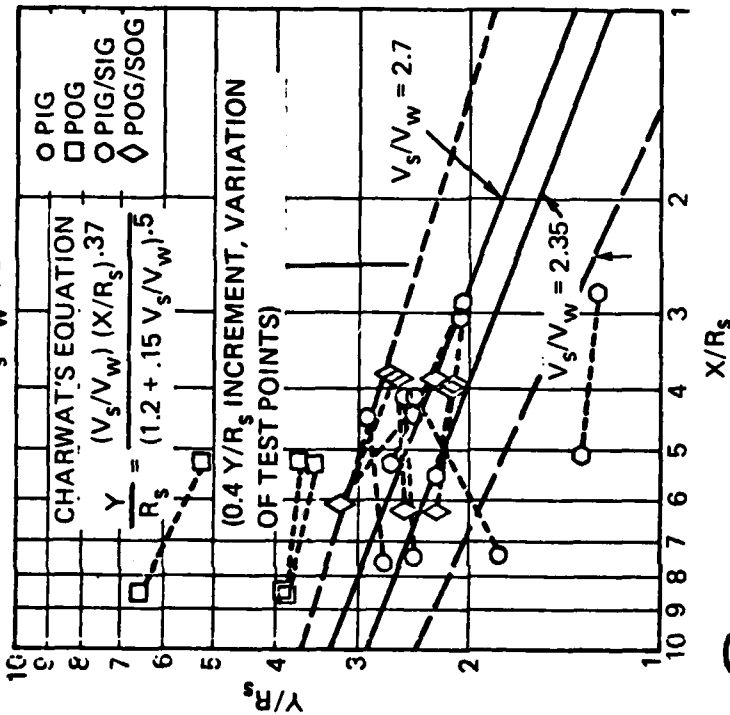


FIG. 2-11 CHARWAT'S EQUATION AND THE GLAMORGAN DATA

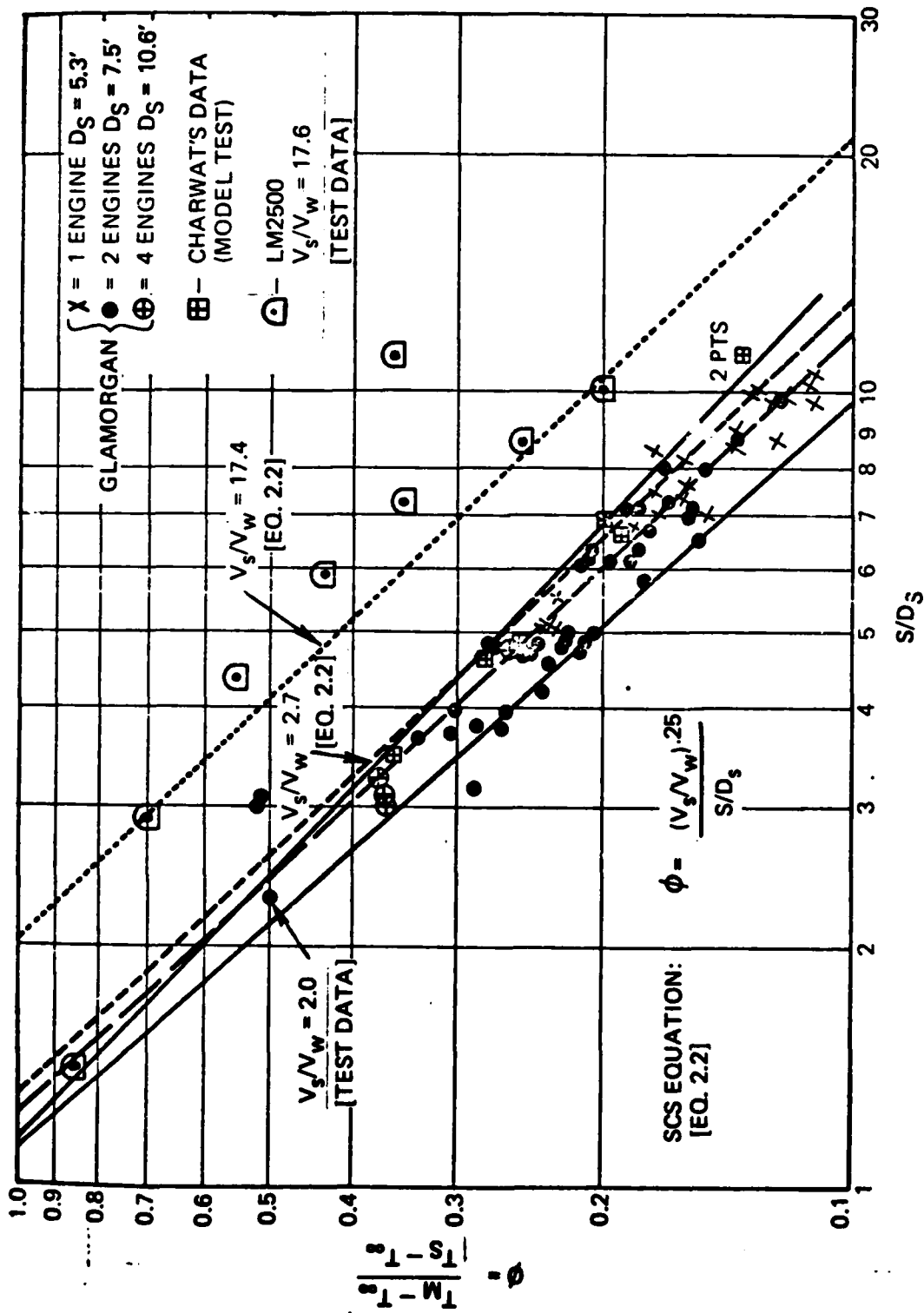


FIG. 2-12 PLUME TEMPERATURE EQ. 2.2 AND DATA FROM GLAMORGAN, LM2500, AND CHARWAT'S MODEL TEST.

$$\frac{s}{D_s} = \left(\frac{y}{6D_s}\right) [1 + 4(1 + .6906K)^{0.5} + (1 + 7.29K)^{0.5}] \quad [2.3]$$

where

$$K = \left[\frac{2.4 + 0.3 V_s/V_w}{0.914 (V_s/V_w)} \right]^{5.4} \left(\frac{y}{D_s}\right)^{3.4}$$

2.2.1.3 Plume Radius - Equation 2.4 presents the radius, r_o , of the plume as a function of plume centerline height. The equation was reported by Weil [6] who had based his theoretical work on Hoult, Fay and Forney [13].

$$r_o = R_s + [2 (.15 + 1.2/(V_s/V_w)) - 1/(2F_r^2)]y \quad [2.4]$$

where

$$F_r = V_s/[gR_s/((T_s - T_\infty)/T_\infty)]^{0.5}, T_\infty \text{ in } ^\circ R$$

Equation 2.5 (as reported by Stoner [15]) can be used to predict the temperature within the plume, T , at a given radius, r , given the maximum radius from equation 2.4 and the temperature at the plume centerline 2.2.

$$\frac{T - T_\infty}{T_m - T_\infty} = \left[1 - \left(\frac{r}{r_o}\right)^{1.5} \right] \quad [2.5]$$

2.2.2 Sources of Information - The following Tables (2-1) contain a summary of the essential sources of plume behavior theory upon which this text is based.

TABLE 2-1

PLUME BEHAVIOR THEORIES

AUTHOR	EQUATIONS	NOTES AND ASSUMPTIONS
<p>Hoult, Fay, Forney</p> <p>A Theory of Plume Rise Compared With Field Observations</p> <p>March 1963 [13]</p>	<p>If v_w is constant and $\frac{d\rho}{dy} = 0$, then for $x < x_c$</p> $\frac{y}{R_g} = \frac{(v_s/v_w)(x/R_g)^{1/2}}{(\beta + \alpha v_s/v_w)^{1/2}} \quad (1)$ <p>where x_c is given by:</p> $x_c = \left(\frac{2\beta^2}{3}\right)^{1/2} \frac{v_s/v_w}{(\beta + \alpha v_s/v_w)}, \quad \frac{L_m^2}{L_b^2} \quad (2)$ <p>For $x > x_c$ the trajectory is given by:</p> $y = \left(\frac{3}{2\beta^2}\right)^{1/2} L_b^{1/2} x^{2/3} \quad (3)$ <p>Stack exit Froude No.</p> $F_r = \frac{v_s}{[g(T_a - T_m)R_g]^{1/2}} \quad (4)$	<p>Trajectory equations are presented for two regions of flow. The work herein is derived for the case of a high stack so that atmospheric turbulence is minimum. In addition, if the momentum of the exhaust gas is sufficiently high, the effect of turbulence can be neglected. However, the final equations are derived assuming a constant crosswind.</p> <p>Lab work has shown that velocity profiles are locally similar within 10 orifice diameters. Hence it is likely that the shapes of the velocities and density profiles do not change except for a scaling factor as the plume moves downstream. Jordensen showed that the main factor in determining the trajectory of a plume is the rate at which it entrains mass from the ambient atmosphere. Thus plume trajectory can be determined from conservation of mass, momentum and energy by using the entrainment assumption to determine the rate of mass, momentum and energy addition to the plume.</p> <p>The length scales: (pure, jet length scale) L_m = momentum length scale $L_m = R_s v_s / v_w$ L_m^2 is proportional to the initial momentum of the jet L_b = buoyancy length scale, measures the length of a pure plume. (s)</p> <p>From equation (2) we note that L_m^2/L_b^2 is proportional to $(v_s/v_w)^2$. The results indicate that although y is a function of x^n, n is not a universal constant.</p> <p>Geometric similarity can exist if L_m/R_g and L_b/R_g are the same for two flows. However, usually the velocity ratio and stack Froude no., F_r, are used to judge similarity.</p>

PLUME BEHAVIOR THEORIES

AUTHOR	EQUATIONS	NOTES AND ASSUMPTIONS
Hoult, Fay, Forney (Cont.) Weil Model Ex- periments of High Stack Plume Aug., 1968 (6)	Plume radius is given by: $r = R_g + [2(\alpha + \beta V_w/V_g) - \frac{1}{2F_r^2}] y$ in the near field. $F_r = \frac{V_g}{[g(\rho_w - \rho_g) R_g]^{\frac{1}{2}}}$	From these scaling factors come values of α and β which are: $\alpha = 0.15$ (universal constant), β varies with V_g/V_w and F_r . β generally lies between 0.6 and 1.2 with a mean of 0.9 for the Tennessee Valley Authority Data. Contains equations 1-4 from above plus the radius equation. Model Test Series 1. Stack Reynold's number varied from 28 to 2800. $V_g/V_w = 4$ and $(\rho_w - \rho_g)/\rho_w = 0.4$ 2. Tests were conducted in a water tank. 3. Results: A. Values of optimum β for equations by Hoult, Fay and Forney 1. $\beta = 0.9$ for field cases 2. $\beta = 0.56$ for laboratory experiments B. Transition from laminar flow in the stack to full turbulent flow occurs when the local Reynold's number is of the order 1000. C. Plume behavior does not depend on stack Reynold's number.

PLUME BEHAVIOR THEORIES

AUTHOR	EQUATIONS	NOTES AND ASSUMPTIONS
<p>Charvat July 10, 1971</p>	$\frac{Y}{R_g} = \frac{(V_g/V_w)(x/R_g)^{1/2}}{(3 + \alpha V_g/V_w)^{1/2}}$ $\frac{Y}{R_g} = \frac{(V_g/V_w)(x/R_g)^{0.37}}{(1.2 + 0.15 V_g/V_w)^{1/2}}$ <p>Temperature equations:</p> $\phi = \frac{T_m - T_\infty}{T_g - T_\infty} = \frac{\gamma(x/R_g)^{0.63}}{1 + \gamma(x/R_g)^{0.63}}$	<p>This equation is the Hoult equation. Charvat modified it by using $\alpha = 0.15$ and $\beta = 1.2$ and adjusting the exponents until the equation fit his data.</p> <p>Charvat proposes that the difference between his data and theory is due to wind tunnel effects. Hoult states that although x^n is a controlling factor of plume rise, n can not be a universal constant.</p> <p>ϕ = mass averaged local plume temperature</p> $\gamma = (\beta + V_g / V_w)^{1/2}$
<p>Charvat July 28, 1971</p>	<p>Stack Eductor Study</p> $\phi = \frac{T_g - T_e}{T_g - T_\infty} = \frac{M}{1+M} ; M = \frac{\dot{m}_g}{\dot{m}_g}$ <p>Basic eductor performance characteristics</p> $\frac{SP}{BP + SP} = 2 \left(\frac{A_g}{A_e} \right)^2 \left[\frac{A_g}{A_e} - (1 + M) \left(1 + M \frac{T_\infty}{T_g} \right) \right]$	<p>T_e = gas-turbine exhaust temperature</p> <p>A mixing section is required, 6 to 10 diameters of the primary nozzle in length.</p> <p>SP = suction pressure difference</p> <p>BP = backpressure on primary gas generator</p> <p>A_e = area at gas turbine exhaust; A_g = area after mixing</p> <p>\dot{m} = mass flow</p>

PLUME BEHAVIOR THEORIES

AUTHOR	EQUATIONS	NOTES AND ASSUMPTIONS
<p>Cransfield Inst. of Technology from Glamorgan Report late 1960's [10]</p>	$\left(\frac{X}{D_s}\right)^3 = \left[\frac{\rho_i}{\rho_\infty} \left(\frac{V_s}{V_w}\right)^2\right]^{1.3} \left(\frac{Y}{D_s}\right)$ $\phi = \frac{K}{S/D_s}$	<p>Trajectory equation - this is a modification of "Ivanov's cubic".</p> <p>Plume Temperature = ϕ</p> <ol style="list-style-type: none"> 1. Effective diameter, D_g, based on stack exit area. 2. This substitution is valid $\frac{T_\infty}{T_i} = \frac{\rho_i}{\rho_\infty}$ 3. Values of K (shown to be independent of velocity ratio between the values of 2 and 5). <ol style="list-style-type: none"> a. Free-standing funnel discharging into free stream $K = 1.1$ b. Flush orifice, $K = 1.9$ c. 20° to vertical upwind and downwind are respectively $K = 1.2$ and $K = 2.1$

PLUME BEHAVIOR THEORIES

AUTHOR	EQUATIONS	NOTES AND ASSUMPTIONS
PF Gas Turbine Exhaust Stack Plume Trajectories and Temperature Distribution Sept. 1972 [23]	<p><u>Trajectory</u> DD-963 Charvat:</p> $\frac{Y}{D_s} = \frac{(V_g/V_w)(x/R_g)^{0.57}}{[2.4 + 0.3(V_g/V_w)]^{0.5}} \quad (1)$ <p><u>Cranfield:</u></p> $\frac{Y}{D_s} = \left[\left(\frac{T_w}{T_g} \right) \left(\frac{V_w}{V_g} \right)^2 \right]^{0.57} (x/D_s)^{0.57} \quad (2)$ <p><u>Temperature</u> DD-963 Charvat:</p> $\phi = \frac{0.8}{[0.72 + 1.4(V_w/V_g)^{0.57}(x/D_s)]^{0.57}} \quad (3)$ <p><u>Cranfield:</u></p> $\phi = \frac{1.9}{s/D_s} \quad (4)$ <p><u>Resulting equations: - Trajectory</u></p> $\frac{Y}{D_s} = \frac{(V_g/V_w) [1.7(x/D_s)]^{0.57}}{[2.4 + 0.3(V_g/V_w)]^{0.5}} \quad (5)$ <p><u>Temperature</u></p> $\phi = \frac{K}{[0.72 + 1.4(V_w/V_g)^{0.57}(x/D_s)]^{0.57}} \quad (6)$	<p><u>Model assumptions</u></p> <ol style="list-style-type: none"> The stack exit dynamic head loss necessary to generate the stack gas momentum needed to "pump through" the boundary layer is prohibitively large and unnecessary with a stack that is high enough to penetrate the boundary layer. Thus the model assumes that the cross flow is laminar at the stack exit and down stream. Wind direction does not change with altitude (y). Velocity profiles within the plume are locally similar within at least 10 diameters (D_g) downstream. No buoyancy effects accounted for. Shapes of velocity and density profiles are assumed to change only by a scaling factor to account for conservation of mass, ratio of mass entrainment, and conservation of energy (no heat transfer). <p>Report contains results of Devonshire test and LM-2500 tests and from the test results revises equations 1-4 to arrive at equations 5 and 6.</p> <p>K = 0.57 Dual stack operation; K = 0.44 single stack operation (when the dual stacks are closer than 1.5D_g).</p> <p>Note: Original equations were revised by a factor applied to the value of x for the trajectory equation and by a factor applied to φ for the temperature equation.</p> <p>Temperatures are absolute (°R).</p>

PLUME BEHAVIOR THEORIES

AUTHOR	EQUATIONS	NOTES AND ASSUMPTIONS
<p>Smith's Comments on the PF work Feb. 1973</p> <p>Memo - PF Exhaust Studies Dec. 1973 [16]</p>	<p>$T = T_m$ at $y = y_1$</p> <p>$T = T_m$ at $y = 3.3 y_1 / D_s$</p> <p>Radius of plume from Charvat</p> $r_0 = \left\{ \frac{7}{3\pi} \frac{A_s}{\psi} \left[\frac{T_m + 0.6(T_m - T_a)}{T_a (1 - \frac{y}{13l})} \right]^{0.5} (V_s / V_w) \right\}^{0.5}$ <p>The temperature within the plume is given by:</p> $\frac{T - T_m}{T_s - T_m} = 1 - \left(\frac{r}{r_0}\right)^{1.5}$ <p>Factors</p> <p>$K_1 = 1.3$ dual $= 1.7$ single</p> <p>$K_1 = 1.4$ dual $= 1.8$ single</p>	<p>From the work of PG Everaats (RNN) - the ratio is linear</p> <p>These equations are based on Schlichting and Charvat.</p> <p>r_0 = radius of the plume at which the temperature is at ambient</p> <p>A_s = Area of stack</p> <p>This equation is for a circular plume. The crosswind tends to flatten the resulting plume as it is bent.</p> <p>Temperatures are absolute, °R</p>
		<p>These are the K's required to obtain corresponding values of x in the respective plume trajectory equation as shown in the PF report. The value of K_1 in equation [5] uses the Devonshire data ($K_1 = 1.7$).</p> <p>Relationship of Devonshire Trials to Cranfield Institute Model Studies</p> <p>Relationship of Devonshire Trials to DD963 Model Studies.</p>

PLUME BEHAVIOR THEORIES

AUTHOR	EQUATIONS	NOTES AND ASSUMPTIONS
Pollitt, SCS, Stack Gas Air- flow Report Feb. 1974 [7]	Plume Trajectory $\left(\frac{Y}{D_s}\right)^2 = \left[\frac{T_m}{T_s} \left(\frac{V_s}{V_w}\right)^2 \right]^{1.3} (x/D_s)$ $\frac{Y}{D_s} = \frac{K (V_s/V_w) (x/R_s)^{0.37}}{[2.36 + 0.296 (V_s/V_w)]^{0.5}}$ Temperature Prediction $\phi = \frac{0.8 (V_s/V_w)^{0.35}}{s/K_1 D_s}$	Equation (1) and (2) were used to make predictions under the following conditions: Relative winds from ahead Equation (1) $V_s/V_w < 3$ Relative winds from astern Equation (2) $V_s/V_w < 4$ Equation (1) $V_s/V_w < 3, K = 1.3$ Equation (2) $V_s/V_w < 4, K = 1.3$
SCS-Airflow and Stack Gas Disper- sion Pre- diction [17]	Plume trajectory. The same as (2) above but with $K = 1$. $\phi = \frac{(V_s/V_w)^{0.25}}{s/D_s}$	Equation (3) was used to predict the T_m . $K_1 = 1$ for single stack, $K_1 = 2$ for two stacks. Equations based on GE LM2500 gas turbine data, HMS Glamorgan data, SCS model tests, DD963 model test data, PF design data and Cranfield model test data.

PLUME BEHAVIOR THEORIES

AUTHOR	EQUATIONS	NOTES AND ASSUMPTIONS
<p>M. Stoner Est. Prob. of Mast Overtemper- ature Due to Gas Turbine Ex- haust Plume 20 Oct. 1961 [15]</p>	<p>Plume trajectory: $\frac{x}{D_s} = \frac{n(V_s/V_w)(x/D_s)^{0.37}}{[2.36 + 0.296(V_s/V_w)]^{0.3}} \quad (1)$ <p>Temperature @ Plume $\phi = \frac{K}{[0.716 + 1.389(V_w/V_s)^{0.5}(x/D_s)]^{0.57}} \quad (2)$ <p>The outer radius of a circular plume $r_o = \left\{ \frac{7}{3\pi} \frac{\lambda_s}{\phi} \left[\frac{T_m + 0.6(T_m - T_s)}{T_s [1 - \frac{13}{9}\phi]} \right]^{0.5} (V_s/V_w)^{0.5} \right\} \quad (3)$ <p>Temperature within the plume $\frac{T - T_m}{T_m - T_s} = 1 - (r/r_o)^{1.5} \quad (4)$ </p> </p></p></p>	<p>Trajectory equation was derived by Charwat n is an "x" correction</p> <p>Temperature equation was derived from the wind tunnel data generated by Charwat K = 0.8</p> <p>In both equations (1) and (2) D_s is the hydraulic diameter of the stack exit</p> <p>Bracketed part of radius equation is an approximation for the density and velocity variation in the plume.</p>
<p>Don D'Arcoy DD 963 AEGIS</p>		<p>Equations (1) and (2) are used again. In this instance a relationship was derived before the Glamorgan test; n = 1.217, and K = 0.44 or 0.57. The Glamorgan data relationship was n = 1.12 and K = 0.61.</p> <p>Equations (3) and (4) are identical.</p> <p>Note in this paper the constants in equations (1) and (2) were rounded to two places.</p>

PLUME BEHAVIOR THEORIES

AUTHOR	EQUATIONS	NOTES AND ASSUMPTIONS
<p>D'Arcy (Cont.)</p>	$\frac{Y}{D_s} = \frac{N(V_s/V_w)(X/R_s)^{0.33}}{(2.4 + 0.3 V_s/V_w)^{0.33}}$	<p>Also the above equations were used to predict temperatures for eductors. However, these equations, notably (3) and (4), were derived for the case of a stack without eductors. No mention is made of the effect an eductor would have on these equations.</p> <p>Based on NAVSEC. Code 6136 review of the GLAMORGAN data and refinement of the curve fitting technique the plume trajectory equation was modified to the form shown</p> <p>N = 1.15 for one exhaust pipe N = 0.86 for more than one exhaust pipe</p>

2.3 Model Testing

2.3.1 Introduction

This chapter is included to aid the designer in choosing the proper technique and scope of smoke plume related model testing. Model testing to determine the characteristics of the stack gas flow has been employed for the last five decades.

Nolan's paper of 1946 [1] was one of the earliest to address the function of the smoke plume model test. He utilized two different types of model tests that are still in use today. The first of these tests was conducted with a ship model complete from the waterline up. This model was mounted on a flat turntable to simulate the ground plane and placed in a wind tunnel so that the yaw angle could be adjusted to any desired figure. The waterline model was used in two different investigations. The first was a determination of the height of the turbulent zone. For this test the ship stack need not be included since it has only a local effect on flow. The second purpose of the waterline model is to investigate stack performance. For this test gases are emitted from the stack at several yaw angles and velocity ratios.

Nolan conducted a second test series to investigate the downwash behind the stack. In these tests several stack shapes were mounted on a flat turntable. Simulated stack gas was emitted and each stack was rotated to examine downwash at different yaw angles. This arrangement allowed comparative studies of the stacks at higher Reynold's numbers than the ship model tests, and in a laminar cross flow.

Since Nolan's original work in a wind tunnel at Newport News, many tests have been conducted world wide in wind tunnels and water channels. These tests have shown modeling to be an invaluable tool in stack design which, considering the state of mathematical prediction techniques for plume behavior, is often necessary for a complete and thorough design effort. The following outline is a condensation of stack model testing information. The information contained herein will aid the designer in using model testing.

2.3.2 Fluid Flow in Test Channel - Both wind and water channels have been used in stack plume model tests. They suffer the common drawback of a zero velocity gradient with elevation change. Natural winds exhibit a velocity gradient.

Wind velocity increases to a constant value, V_R , several hundred feet, Z_R , above sea level. The velocity gradient follows this form:

$$V/V_R = (Z/Z_R)^{1/x} \quad (x \approx 7, x = f \text{ (temperature)}) \quad [2.6]$$

Large ships are largely within this gradient and experience a variation in the direction of the relative wind because of the change in the magnitude of true wind velocity. However, because of the difficulty of generating a stable meteorological wind profile in a tunnel, even unidirectional gradients are rarely examined.

Sea roughness also affects the wind profile. The usual modeling procedure is to mount the model on a smooth board, with no consideration for sea roughness (Thornton [2]).

Early model tests (Nolan [1] and Acker [2]) were usually conducted in wind tunnels; sometimes with heated plumes. More recently, tests for naval vessels have been conducted with inverted models mounted on the roofs of water channels. In these tests a denser fluid is injected to model buoyancy of the smoke plume. Water tunnels have the advantage of offering higher Reynolds number than wind tunnels for the same tunnel flow speed and model size. Generally the plume in a water tunnel can be made visible more easily than in a wind tunnel and photographed with greater facility.

2.3.3 Model Scaling Factors

2.3.3.1 Effect of Reynold's Number - Model testing can only be applied to design when the scale effect is understood and can therefore be accounted for properly. Geometric similarity does not imply flow similarity for model and ship. For low flow velocities (i.e., the range covered by stack flow model testing) similarity of flow patterns for ship and model would be assured if the ship length Reynold's number, Re , is maintained

where

$$Re = \frac{V_w L_{ship}}{v_w}$$

However, model size usually falls between 1/40 and 1/100 ship size and testing tunnel velocities are limited so that both

for air and for water the model length Reynold's number is much smaller than the ship length Reynold's number. This difference in Reynold's number has been investigated in various model tests and shown to have little, if any effect on ship models. Ower and Third [4] conducted three full scale tests to compare the heights of the turbulent zone of models and full scale ships. They found no appreciable difference even for a ship with a well rounded superstructure.

The effect of Reynold's number on the stack itself must be considered separately from the ship Reynold's number. It is the normal design practice to extend the stack above the turbulent zone. In this case the stack individually encounters a cross flow and the downwash behind the stack is the critical factor. When individual stacks are tested over a range of Reynold's number, a critical value of stack Reynold's number is encountered. Stack Reynold's number is,

$$Re_s = \frac{V_w D_s}{\nu_w} \quad [2.8]$$

Below this value the drag is higher and consequently the flow pattern is larger at values slightly above the critical Re_s . One would expect that the downwash behind the stack would be greatly affected by the stack Reynold's number. However, Ower and Third [4-5] have experimentally demonstrated that downwash behind the stack does not change as the stack Reynold's number traverses the critical range. These authors attributed the change in drag at critical stack Reynold's number to a reduction in the thickness of the turbulent region but saw no reduction in the extent of downwash along the stack casing axis.

A third very important scaling factor can be assessed through use of the local flow Reynold's number; which is

$$Re_L = \frac{V_s X}{\nu_w} \quad [2.9]$$

This Reynold's number is critical in determining the transition from laminar to turbulent flow in the plume. Above the critical Re_L , the plume size greatly increases because fully turbulent flow has developed within it. Below the critical Re_L , the turbulence within the plume does not fully develop and the plume is no longer geometrically similar to the full scale plume. Weil [6] has determined that the critical Reynold's number (Re_c) is approximately 10^3 . One should

note the implication of Re_c that the model gas flow adjacent to the stack is not modeled properly until the distance downstream, x , is large enough to raise Re_c above critical. Therefore, if the V_s is low enough the model plume will be too small for a significant distance downstream.

2.3.3.2 Plume Density - The plume from a ship is a mass of heated gas that is buoyant and this buoyancy will affect the plume trajectory. Buoyant forces become increasingly important at higher velocity ratios. Normally, the higher velocity ratios are not critical for stack performance because the plume tends to travel straight up and presents the least interference problem with other ship systems. The exclusion of temperature effects results in model tests that are conservative. It should be noted that the theoretical plume trajectory presented in this manual does not include a term for plume density since it is assumed that plume behavior near the stack, for reasonably low velocity ratios, is a function of stack gas and cross flow momentum and not stack gas buoyancy. In most literature plume density modeling is not recommended. However, the use of the following relationship will allow plume buoyancy scaling in a water channel if it is believed important to do so. For plume gases and air, density is proportional to temperature, hence, given the temperature of the exhaust gas at the stack and the cross flow temperature, it is possible to determine the density of the buoyant plume.

$$\begin{aligned} \left[\frac{\rho_\infty - \rho_s}{\rho_\infty} \right]_{\text{ship}} &= \left[\frac{T_s - T_\infty}{T_\infty} \right]_{\text{ship}} = \left[\frac{T_s - T_\infty}{T_\infty} \right]_{\text{model}} \\ &= \left[\frac{\rho_\infty - \rho_s}{\rho_\infty} \right]_{\text{model}} \end{aligned} \quad [2.10]$$

Air test exclude the use of heated air in the model because the above temperature relationship would require extremely high model gas temperatures which are not practical. Hence plume density modeling is limited to a water channel where the density of the plume can be controlled more easily.

2.3.4 Necessary Conditions for Plume Model Scaling

The following four conditions must be satisfied simultaneously to assure the similarity of the model plume with the full-scale plume.

- o Geometric similarity of model to ship - However, details such as rigging often are omitted since their effects are not significant.

- Relative wind direction - When the relative wind yaw angle of the ship model and the full scale ship are equivalent then the flow patterns will also be equivalent regardless of the magnitude of the relative wind. Usually individual stack performance gets increasingly worse with increasing yaw. A stack on a ship performs poorly from about 15° to 60° of yaw but performance improves from 60° to 90°. This is due to the vertical component of flow past the stack as the relative wind approaches the beam. The designer must remember the vertical component of flow past the stack changes with yaw and this affects downwash [3].
- The velocity ratio - When the velocity ratio of model and full scale vessel are equivalent then the momentum of vertical stack gases and the cross flow momentum will produce similar plume trajectories (see Section 2.3.3.2 on the plume density).
- The model local flow Reynold's number, which is $Re_L = \frac{V_S X}{v_w}$ must exceed 10^3 or plume diameter will not expand fully.

2.3.5 Effect of Tunnel Walls

Weil [6] has shown with model tests that the walls of the flow channel do not affect plume rise until the plume diameter is equal to the separation from the wall.

2.3.6 Methods of Making the Plume Visible and Determining the Height of the Turbulent Zone Models

2.3.6.1 Plume Visualization - The plume is usually colored by a dark dye or, in the case of a wind tunnel, smoke is ejected into the stack. Photographic techniques are very useful in assessing model performance, including short duration stills (with strobic illumination), longer duration stills (1/8 second to several seconds) and motion picture photography. Photography provides a permanent storage of data. However, many lighting techniques tend to overemphasize wisps of smoke so that notes should be included with photographs.

2.3.6.2 Boundary Layer Determination - The extent of the boundary layer can be determined from a ship waterline model by three methods. All of the methods make the gradual transition from laminar flow above the boundary layer to fully turbulent flow within the turbulent zone evident.

- Shadowgraph method - A trail of hot air from a fine wire probe is made visible by special lighting conditions. Outside the turbulent zone the trail is long and steady. When the probe enters the turbulent zone the trail behind the probe shortens and becomes unsteady. The probe is moved vertically and translated along the ship to map the entire turbulent region.
- Tufts - This method is similar to the shadowgraph but employs tufts on a probe to determine the flow characteristics.
- H₂S Method - This method can be used in various ways. It is based on the darkening of white lead acetate paint by H₂S in even minute quantities. Therefore, a probe painted with white lead acetate paint will become blackened when it enters a turbulent zone containing H₂S. The H₂S does not cross the boundary layer. A second method has been employed where the after part of the model is painted with lead acetate and a probe ejecting H₂S is lowered until it enters the turbulent zone and darkens the paint.

2.4 Theory Behind Stack Height Predictions

A technique for determining the minimum stack height for commercial ships was developed by Third and Ower [5] in a paper on funnel design. Their technique is formulated to give the lowest stack height possible for any given ship by allowing the plume to mix in the upper transitional part of the boundary layer. Flow in this region gradually degenerates from laminar to fully turbulent, decreasing with height, but, as long as the plume does not enter the fully turbulent region where a back flow has developed the plume will be carried free of the ship. To determine the minimum stack height there are two rules.

- o Rule 1 - The lower boundary of the smoke plume may be allowed to penetrate the zone of turbulence created by the ship's superstructure to a vertical depth in accordance with Figure 2-13, in headwinds and winds up to a maximum of 20 degrees yaw.

TABLE 2-2
PLUME INTERPENETRATION

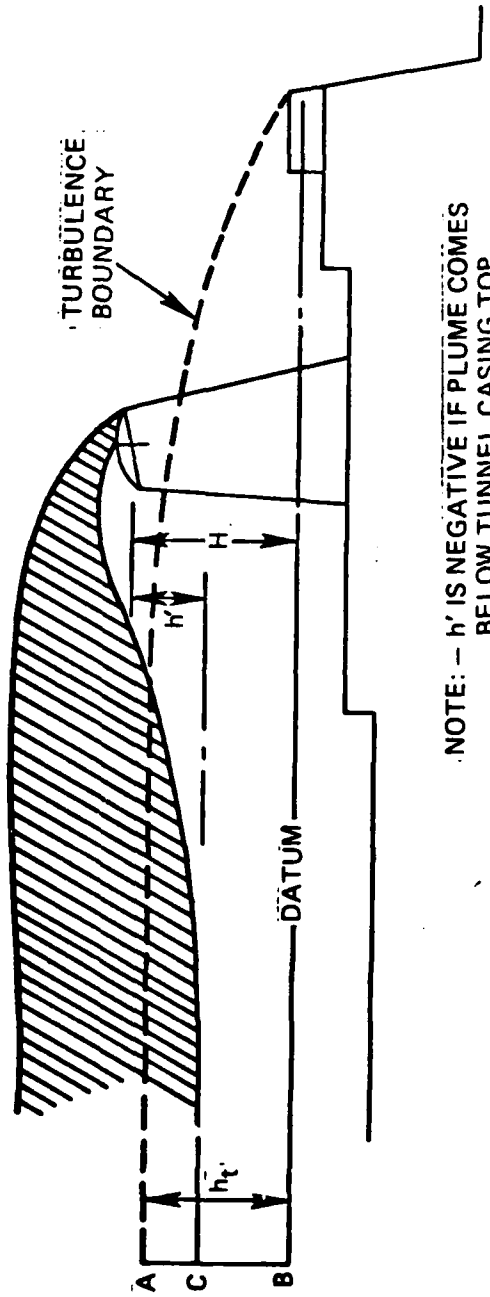
Interpenetration (h')	Interpenetration Fraction Allowed (p)
above - 0.5	0.35
From -0.5 to -1.5	0.50
Below -1.5	0.70

Expressed analytically, Rule 1 will yield the following equation:

$$H = h_t(1 - p) - h' \quad [2.11]$$

where:

- H = stack height above datum of turbulent zone
- h_t = maximum height of boundary layer above datum
- h = stack outlet height above lowest plume boundary
- p = interpenetration fraction of Table 2-2



NOTE: -- h' IS NEGATIVE IF PLUME COMES BELOW TUNNEL CASING TOP

FIG. 2-13 INTERPENETRATION OF PLUME (THIRD AND OWER [5])

In their paper Third and Ower realized that the smoke must be kept from entering intakes at all wind speeds. Intakes are usually located only a few degrees off the centerline. The authors assumed that the problem of intake ingestion could be adequately solved by designing for a high velocity ratio at the yaw angles that directed smoke over the engine intakes. However, for higher yaw angles, Third and Ower suggested that a lower wind speed of 15 to 20 knots could be used. In the North Atlantic 15 and 20 knots are annually exceeded 70 and 30 percent of the time, respectively. On the other hand 30 knots is exceeded annually only 3 percent of the time. The wind speed of 30 knots also falls on the wind distribution curve where it levels off with respect to probability while both 15 and 20 knots are in the steepest region, (Figure 2-14). It is therefore suggested when applying Rule 1, that a value of 30 knots be used for the maximum yaw angle and 40 knots be used for the yaw angle that directs the flow over intakes or antennae.

Ship speed and true wind speed must be added vectorially to obtain relative wind speed. This addition is represented in Figure 2-15 and by equation 2-12. Once the V_w has been determined, this value can be used to calculate V_g/V_w . With this ratio and a selected casing type, h' can be obtained from Figure 2-16 or 2-17.

$$V_w = \frac{\sin [180 - (\theta + \arcsin ((\sin \theta) (V_A/V_T)))]}{\sin \theta / V_T} \quad [2.12]$$

where

V_w = relative wind speed,

V_T = true wind speed

V_A = ship speed, and

θ = angle of relative wind

The value of h' is used to determine the interpenetration fraction from Table 2-2 and Equation 2.11 is then used to calculate the stack height, H .

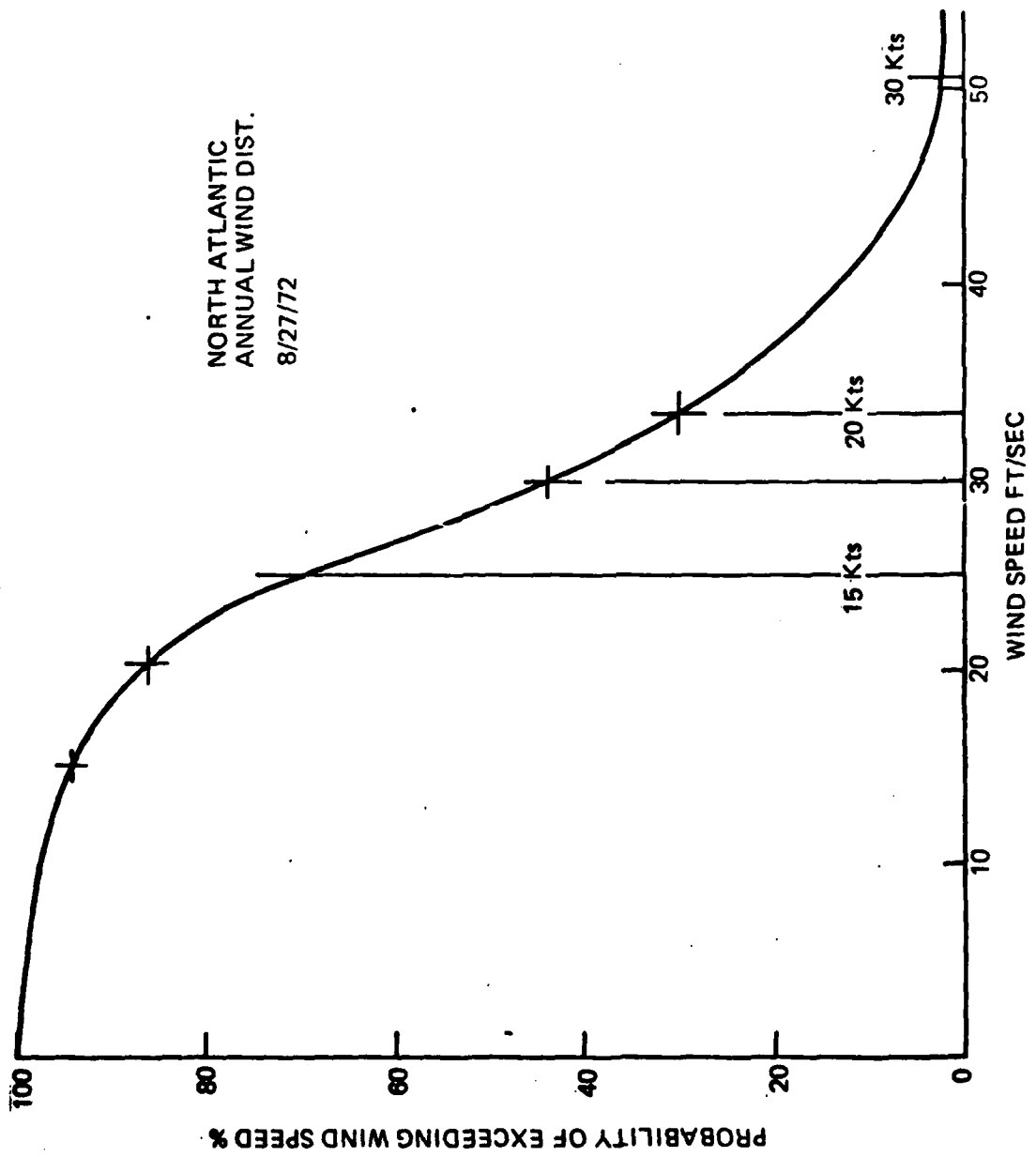


FIG. 2-14 (REFERENCE [7])

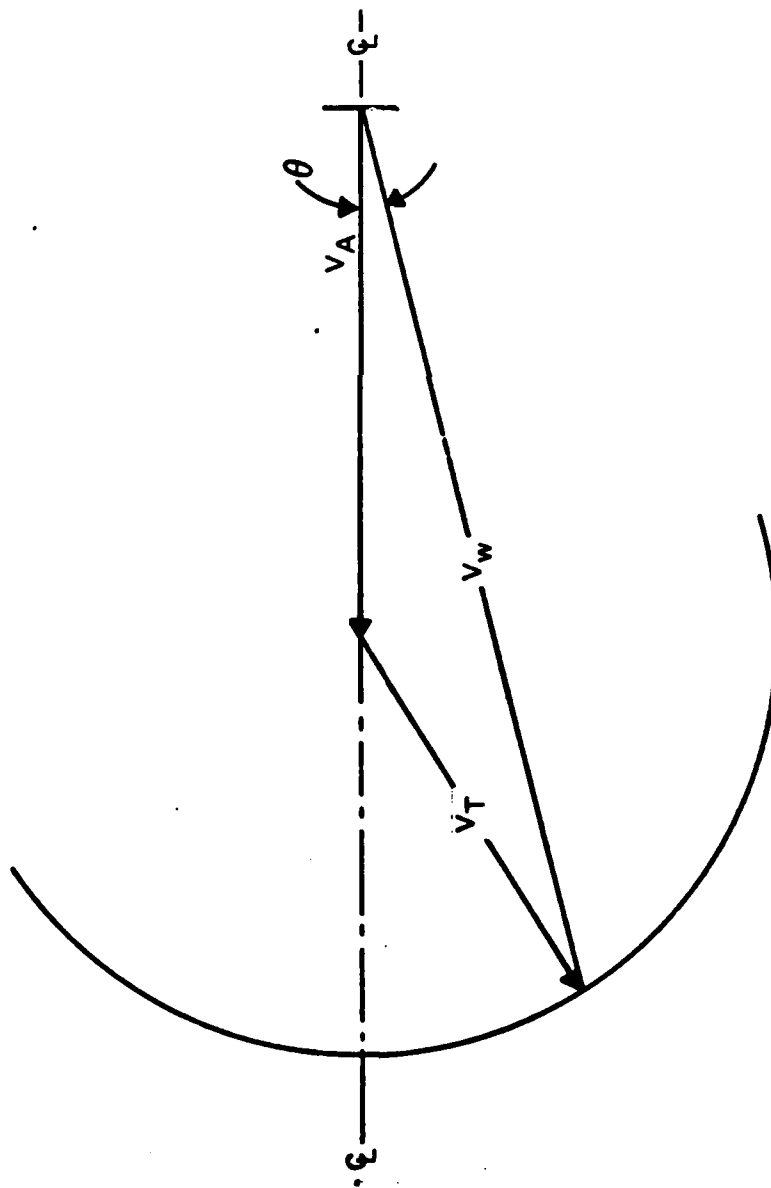
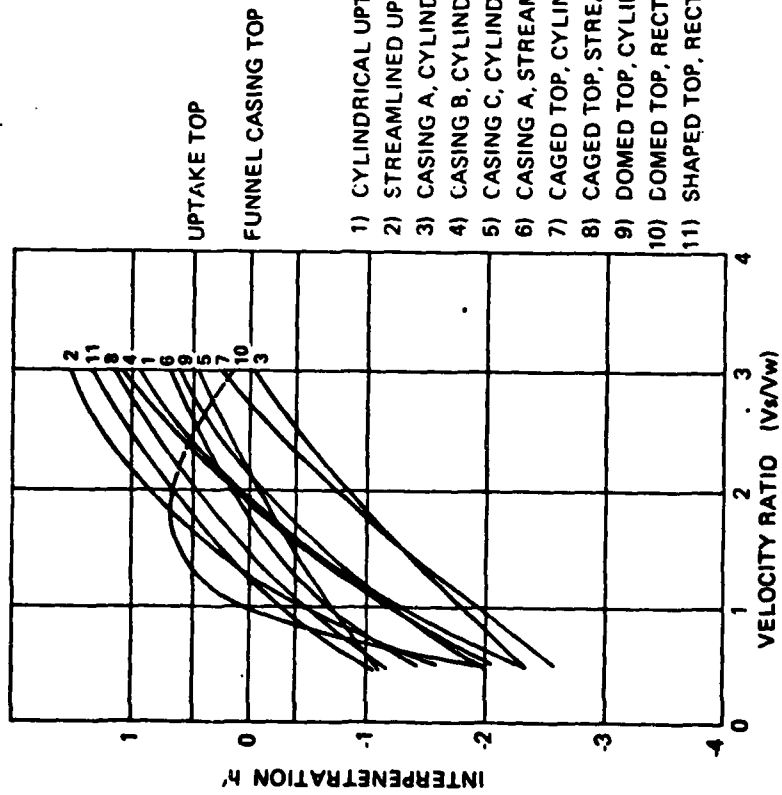


FIGURE FIG. 2-15 VECTOR DIAGRAM OF THE VELOCITIES



- 1) CYLINDRICAL UPTAKE ALONE
- 2) STREAMLINED UPTAKE ALONE
- 3) CASING A, CYLINDRICAL UPTAKE FORWARD
- 4) CASING B, CYLINDRICAL UPTAKE FORWARD
- 5) CASING C, CYLINDRICAL UPTAKE FORWARD
- 6) CASING A, STREAMLINED UPTAKE FORWARD
- 7) CAGED TOP, CYLINDRICAL UPTAKE
- 8) CAGED TOP, STREAMLINED UPTAKE
- 9) DOMED TOP, CYLINDRICAL UPTAKE ANGLED 22% DEG.
- 10) DOMED TOP, RECTANGULAR UPTAKE ANGLED 22% DEG.
- 11) SHAPED TOP, RECTANGULAR UPTAKE ANGLED 22% DEG.

FIGURE 2-16 INFLUENCE OF STACK DESIGN ON INTERPENETRATION n'
 $\phi = 0.475$ (APPROX.), 0 DEG. YAW (FOR DEFINITIONS OF SYMBOLS SEE FIGURE 1-2)

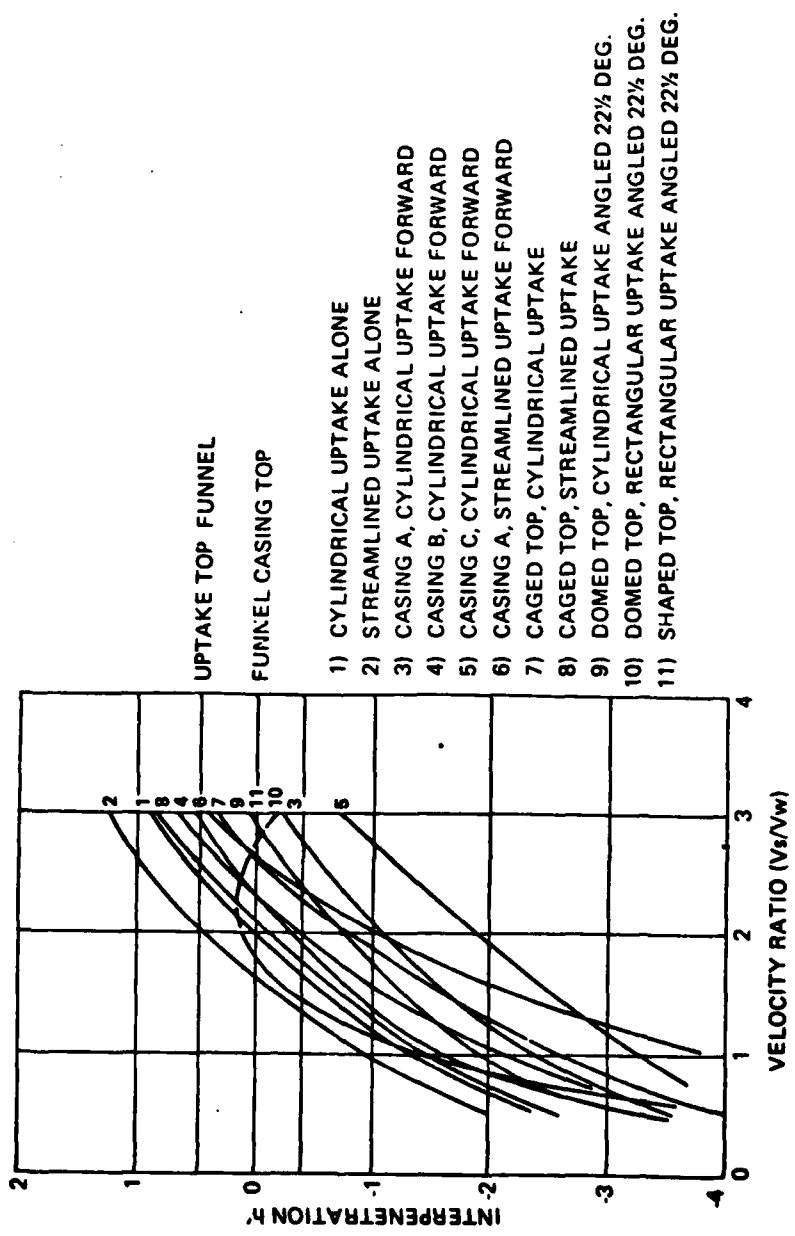


FIGURE 2-17 INFLUENCE OF STACK DESIGN ON INTERPENETRATION h'
 $\theta = 0.475$ (APPROX.), 20 DEG. YAW (FOR DEFINITIONS OF SYMBOLS SEE FIGURE 1-2)

- o Rule 2 - The lower boundary of the smoke plume must not descend below the funnel casing top by a distance equivalent to more than twice the breadth of the casing. When the height of the funnel is less than this distance, the allowable descent of the plume is reduced accordingly. This rule is applicable to all angles of yaw up to 30 degrees.

Table III in Reference [5] contains the minimum values of V_s/V_w to comply with Rule 2 for various stacks.

In most instances Rule 1 and Rule 2 are both applied and the highest stack height from either becomes the design height. Both rules are applied only over limited yaw angles ($< 30^\circ$) because the turbulent zone calculation in Appendix A has no meaning for large yaw angles. There are special cases where Rule 1 is not applied at all or where the yaw angle for which Rule 1 should be applied is limited.

The following discussion (of the maximum yaw angle for Rule 1) refers to Figure 2-18. Rule 1 should not be applied when the line ac, which passes through the top of the stack at 20° from the horizontal, clears the ship aft. If line ac intersects the deck of the ship in question then the maximum yaw angle for Rule 1 is determined in the following manner. The circle with its center point a and radius ab will intersect the deck at d. If the angle θ formed by the lines ab and ad is less than 20° then θ is the maximum yaw angle for Rule 1. If θ exceeds 20° then Rule 1 is applied for 20° of yaw.

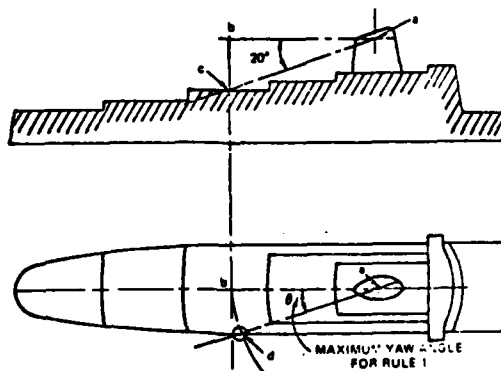


FIGURE 2-18
MAXIMUM YAW ANGLE FOR RULE 1 [5]

REFERENCES

1. Nolan, Robert W., "Design of Stacks to Minimize Smoke Nuisance," SNAME Transactions, Vol. 54, 1946.
2. Thornton, C.P., "Ship Smoke Stacks: A Review of Aerodynamic Factors and Wind Tunnel Methods" DME/NAE Quarterly Bulletin, 1962(4).
3. Acker, H.C., Stack Design to Avoid Smoke Nuisance," SNAME Transactions, Vol. 60, 1952.
4. Ower, E., and A.D. Third, "Superstructure Design in Relation to the Descent of Funnel Smoke," Transactions, Institute of Marine Engineers (London), Vol. 1, 1959.
5. Third, A.D., and E. Ower, "Funnel Design and the Smoke Plume," Transactions, Institute of Marine Engineers (London), Vol. 72, 1962.
6. Weil, Jeffery C., "Model Experiments of High Stack Plumes," MIT Master's Thesis, August 1968.
7. Pollitt, G., D. N. McCallum and T. C. Harrington, "Sea Control Ship (SCS) Stack Gas Air Flow Report (Confidential), NAVSEC Code 6136, Hyattsville, Md. February 1974.
8. Sherlock, R. H., and E. A. Stalker, "A Study of Flow Phenomena in the Wake of Smokestacks," Engineering Research Bulletin No. 29, Department of Engineering Research, University of Michigan, Ann Arbor, March 1941.
9. Gordier, Robert L., "Studies on Fluid Jets Discharging Normally into Moving Liquid," St. Anthony Falls Hydraulic Lab., Minneapolis, Minnesota, August 1959.
10. "Gas Turbine Funnel Plume Temperature Trials, (HMS GLAMORGAN)" AMEE Technical Report No. 27/72 (British), Project No. 2103, September 1972.
11. Schultz, and Matthew, "Wind Tunnel Investigation of Smokestack Annulus Parameters," NSRDC, Technical Report, August 1967.
12. Rains, Dean A., "DD 963 Power Plant," Marine Technology, Volume 12, No. 1, January 1975.

13. Hoult, David D., James A. Fay, and Larry J. Forney, "A Theory of Plume Rise Compared with Field Observations," Fluid Mechanics Lab., Department of Mechanical Engineering, MIT, March 1963.
14. Exhaust Plume Temperature Survey, DD 963 Propulsion Gas Turbine Module, Test Report, General Electric Aircraft Engine Group, Document No. PF-1-100, Lynn, Mass/Cincinnati, Ohio, September 1972.
15. Stoner, W., "Estimated Probabilities of Mast Overtemperature Due to the Gas Turbine Exhaust Plumes," Office Correspondence to D. A. Rains, October 1971.
16. NAVSEC, Code 6136, Memo: Patrol Frigate-Exhaust Plume Studies, Hyattsville, Maryland, December 1973.
17. NAVSEC, Code 6136, "Sea Control Ship, Air Flow and Stack Gas Dispersion Prediction," Hyattsville, Maryland, January 1973.
18. Frazier, T. and G. Baham, "A0177 Class Air Flow and Stack Gas Dispersion Report," George Sharp, Inc., June 1974.
19. "Clydebank Funnel," The Marine Engineer and Naval Architect, March 1954.
20. Pollitt, G., and D. McCallum, "Mean Stack Gas Velocity Ratios and Probabilities of Relative Wind Direction for Known Ship Speed Characteristics," Sec. 6136 August 1974.
21. "AO 177 Air Flow and Stack Gas Dispersion Report," Naval Ship Engineering Center, Code 6136, June 1964.
22. Hampton, Gary A., "Stack-Gas Studies for a Patrol Frigate (PF) represented by Model 5282", NSRDC Carderock, Report 495-H-03, September 1972.
23. NAVSEC, Code 6110, PF Project Report 5079, "Patrol Frigate Gas Turbine Exhaust Stack Plume Trajectories and Temperature Distribution", 22 September, 1972.
24. Westinghouse Letter Report 827-15-1, "Effects of Elevated Ambient Temperature or Mast Mounted Equipment for Sea Control Ship", 28 July 1972.

APPENDIX A
"SUPERSTRUCTURE DESIGN IN RELATION TO THE
DESCENT OF FUNNEL SMOKE"

by
Ower and Third

Reprinted from the Transactions of the Institute of Marine
Engineers, Vol. 1, 1959.

Superstructure Design in Relation to the Descent of Funnel Smoke

E. OWER, B.Sc., A.C.G.I., F.R.Ae.S.,* and A. D. THIRD, B.Sc., Ph.D., A.R.C.S.T.†

One of the factors that determines the necessary height of a funnel casing is the height of the zone of disturbed air flow due to the superstructure. This paper provides formulæ and diagrams which enable the height of the zone to be calculated from the ship's drawings alone, without recourse to experiments.

The data were obtained from wind tunnel tests with model ships. The methods used are described; and an account is given of comparative tests carried out on ships at sea, which showed that wind tunnel experiments of this kind accurately reproduce full-scale conditions. No direct confirmation of the validity of wind tunnel tests to the aerodynamics of superstructure design had previously been obtained.

Finally, consideration is given to the problem of smuts, which is essentially different from that of smoke. It is shown that it should be possible to prevent smuts from being ejected from the funnel by introducing, somewhere in the exhaust ducting between the boiler and the outlet of the uptake, a vertical length of enlarged section and about 12ft. high in which the gas velocity will be reduced to about 10ft. per sec.

INTRODUCTION

General

The factors responsible for the descent of funnel smoke on to the decks and superstructures of ships were discussed in an earlier paper⁽¹⁾. It was there shown that the movement of air over the bows and superstructure due to a combination of ship speed and wind speed sets up a region of disturbed flow over the ship. The height of this disturbed region, which has come to be called the turbulent zone, depends mainly on the shape and size of the superstructure; and the efflux from the funnel must be carried clear of the turbulent zone if the ship is to be free from smoke trouble. Two main factors determine whether this condition will be fulfilled, namely the height of the upper boundary of the turbulent zone—the turbulence boundary—and the design of the funnel, including the speed at which the smoke is emitted.

Scope of Research

A general research is being carried out for the British Shipbuilding Research Association to investigate both these factors. Its ultimate object is to enable the naval architect to predict, from an inspection of the ship's drawings alone, and without recourse to experiments, either model or full-scale, whether a projected design of ship is likely to be free from smoke trouble. To do this, he will require data from which he can estimate (a) the probable height of the turbulence boundary, and (b) how much his particular type of funnel should project above the boundary to ensure that, with the efflux speed he can allow, the smoke shall not be drawn down into the turbulent zone.

* Director, British Thermostat Co., Ltd.

† Director of Research of Thermostat, Ltd.

‡ See Appendix I for an explanation of the meaning of "turbulence" in the present context.

Part I of the paper is intended to supply the designer with information of type (a) in the form of diagrams and formulæ from which he can calculate the height of the turbulence boundary above the superstructure. Work on problems of type (b) is still in progress. Two earlier American researches^(2,3) have dealt with both these aspects, but the results are not sufficiently systematic or comprehensive for the purpose stated in the preceding paragraph.

Full-scale Work

The results given in Part I were obtained entirely from tests of models in a wind tunnel. Experiments of this kind are much easier to conduct and less costly than tests on actual ships; and the method has been widely used by Nolan⁽²⁾ and Acker⁽³⁾ and for numerous *ad hoc* investigations on the smoke problem extending over many years. The disparity in scale and speed between model and full-scale conditions, however, is so great that doubts have sometimes been expressed about the applicability of the model results to actual ships. Hitherto it has been possible to counter these doubts only by the statement that ships modified or designed on the basis of the results of smoke tests in the wind tunnel have usually been found trouble free in service; no direct quantitative comparison between the air flow pattern over a full-scale ship and its model had been made.

It was thought desirable, therefore, to include a comparison of this kind in the present research; and tests were accordingly made on three ships and their models for this purpose. The work is described in Part II of the paper.

Smuts

To avoid misunderstanding it should be stated here that, although the data given in Part I will be of assistance to the

Superstructure Design in Relation to the Descent of Funnel Smoke

naval architect in respect of the smoke problem, they will not enable him to prevent smuts or soot from falling on to the ship, or even to reduce troubles due to this cause. Smoke and smuts present two entirely different problems, although they are often confused. Smoke consists of very fine solid particles which in still air would eventually fall on to the deck, but so slowly that they can be regarded as virtually in suspension. Smuts are much heavier than smoke particles and, if they are ejected from the funnel at all, they will fall to deck level much more quickly. If by then the ship has not travelled far enough, or the relative wind is not strong enough, to carry them clear, they will fall on to the deck. A possible method, which was suggested by a shipowner, of preventing the ejection of smuts is discussed in Part III.

ACKNOWLEDGEMENTS

The whole of the research was undertaken for the British Shipbuilding Research Association, and the authors wish to thank the Director of Research and the Council of the Association for permission to publish this account of it. Thanks are also due to the British Transport Commission for making available a cross-channel ship (ship A) on which the pioneer work in developing the full-scale technique was carried out, and for most valuable co-operation in these and subsequent tests; to Thos. and Jno. Brocklebank, Ltd., and to the Port Line, Ltd., for making available ships (B and C) for further full-scale work; and to the Ministry of Supply and the Chemical Defence Experimental Establishment for developing and providing special smoke generators for the full-scale work.

PART I—DETERMINATION OF THE TURBULENCE BOUNDARY ON MODELS OF TYPICAL SUPERSTRUCTURES

1. 1. EXPERIMENTS

All the model work was done at an air speed of 12ft. per sec. in the wind tunnel of Thermotank, Ltd., which has a rectangular working section 3ft. (vertical) by 4ft., in which the flow is horizontal. After a satisfactory method of test had been established it was used to determine the height of the turbulent zone above each of a series of models ranging from simple rectangular blocks to shapes representative of different types of superstructures. The hull on which these blocks were mounted was a model to a scale of 1/64 of the above-water

stained black when exposed to even small traces of hydrogen sulphide gas, H₂S.

1. 1. 2. Range of Tests

The chemical reaction or H₂S method was used to trace the turbulence boundaries over a series of blocks representing typical shapes of superstructure. The main cause of the formation of the turbulent zone is the frontal obstruction to the flow presented by the superstructure, which, in its simplest form, is a rectangular, sharp edged structure with its forward

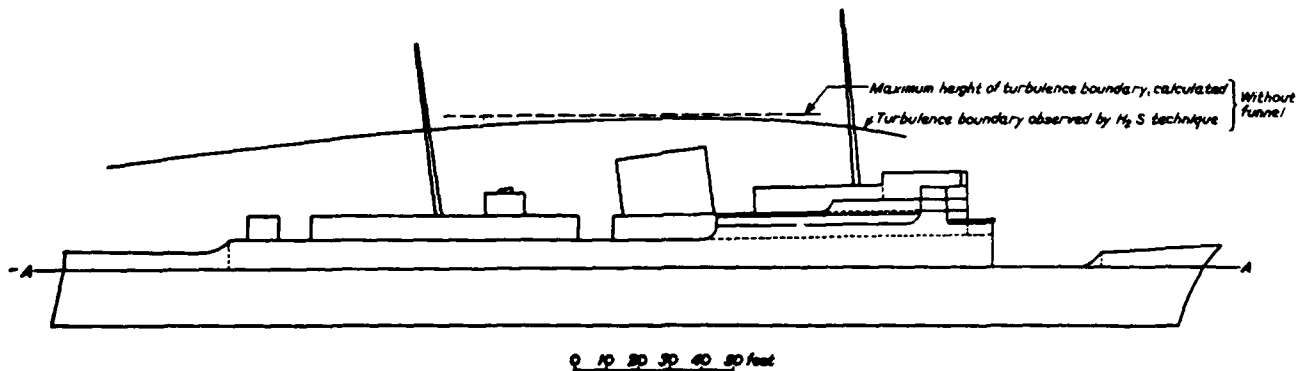


FIG. 1

hull of the cross-channel ship A (see Fig. 1), which was adopted as the standard ship for this research because it was the one made available for the first of the model-full-scale comparisons mentioned above and described in Part II.

1. 1. 1. Methods of Test

The method used in most previous investigations of this kind has been to introduce smoke somewhere within the turbulent zone or upstream of it, and to attempt to define the limits of the zone by visual observation or by photography of the subsequent behaviour of the smoke. It was found impossible to obtain consistent results by this method, and other methods were therefore sought; two of these are described in Appendix 2. In the first, trails of hot air behind fine, electrically heated wires supported in the air stream are made visible by appropriate illumination, and their appearance indicates whether or not the wires from which they spring are situated in smooth or turbulent flow. This method will be referred to as the "shadowgraph" method. The second method, called the "chemical reaction" method, proved more convenient; it makes use of the property whereby white lead acetate paint is rapidly

face rising vertically from the deck. A simple, rectangular block was therefore taken as the basic form of superstructure; and, first of all, the relation between the height of the turbulence boundary and changes in length and height of the block were determined. The third variable, i.e. breadth, was taken into account by expressing all dimensions, including the height of the turbulence boundary, in terms of the breadth which, for convenience, was kept constant. Then the effects of various modifications were examined, namely rounding of the forward face in plan and in elevation, both separately and together, sloping and stepped-back fronts, and additions representing bridges and wheelhouses of different forms.

In all these tests, the appropriate blocks were substituted for the whole of the superstructure of the model above the flat deck denoted by A-A in Fig. 1.

1. 1. 3. Results

All the tests carried out with the blocks on the model hull are recorded in Table I, which shows the various combinations and modifications tested, together with the maximum height *h* of the turbulence boundary observed in

Superstructure Design in Relation to the Descent of Funnel Smoke

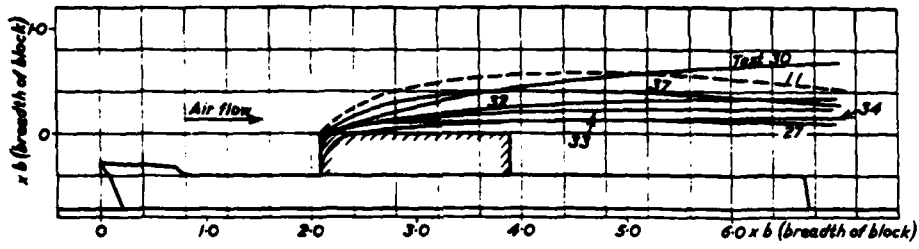


FIG. 2

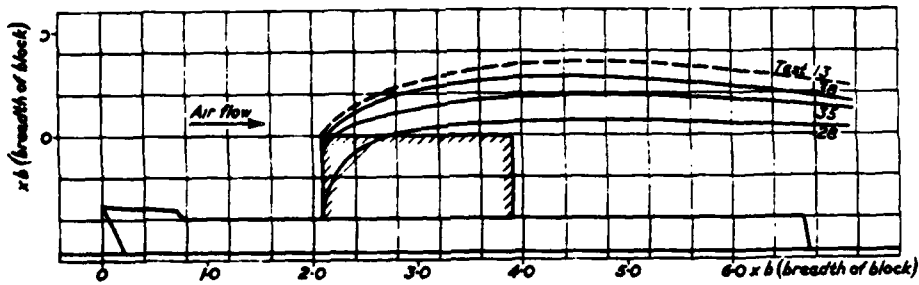


FIG. 3

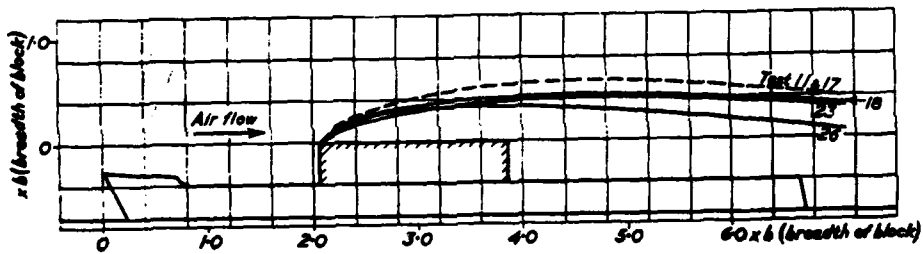


FIG. 4

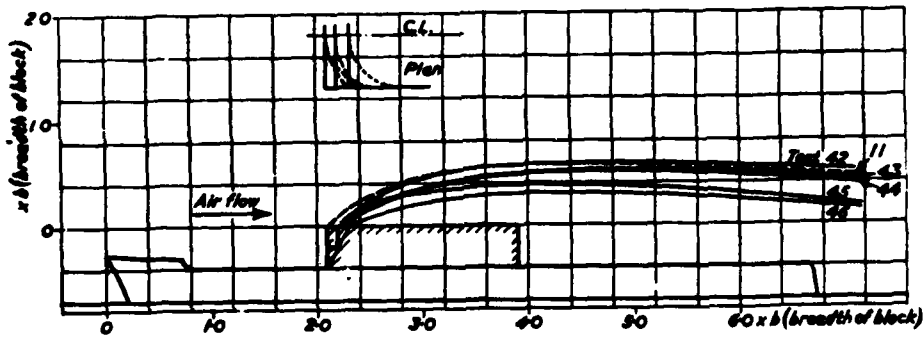


FIG. 5

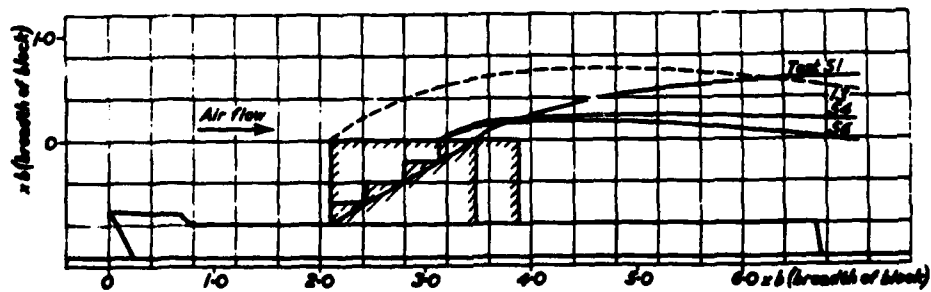


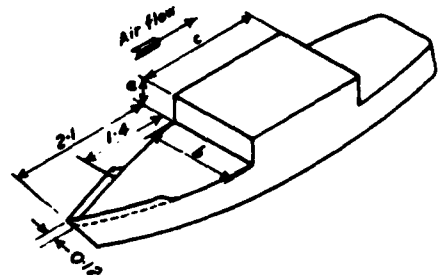
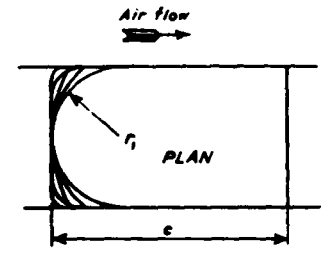
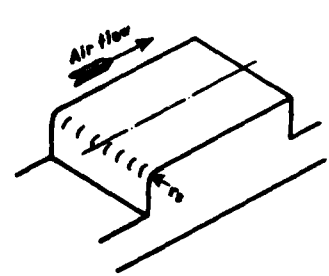
FIG. 6

Superstructure Design in Relation to the Descent of Funnel Smoke

TABLE I

* Measured from top edge of plate.

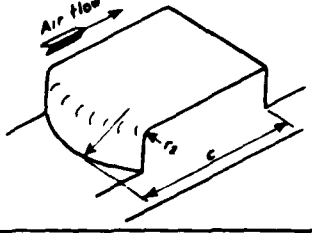
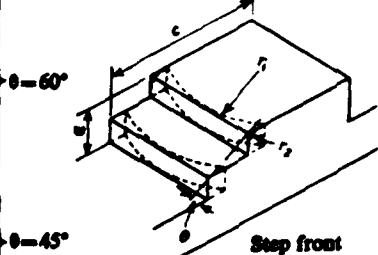
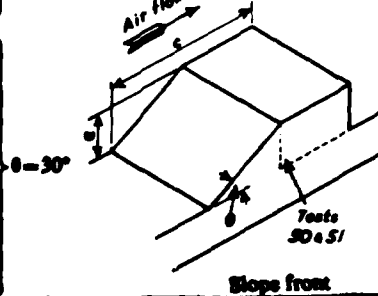
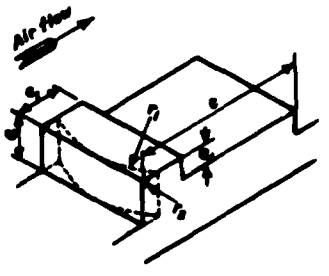
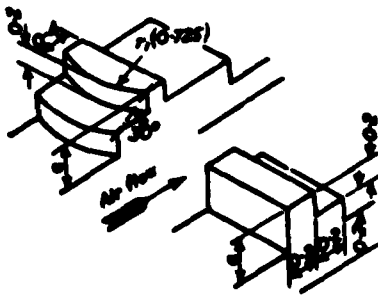
Notes: All dimensions in terms of beam $b (= 1.0)$.
All tests at zero yaw except 89-99 (see page 115).

Test number	a	c	h	Superstructure form		
1	0.4	0	0.69*	Vertical plate		
2	0.2	0.4	0.35			
3	0.4	0.4	0.64			
4	0.6	0.4	0.67			
5	0.8	0.4	0.69			
6	0	1.0	0.32			
7	0.4	1.0	0.30			
8	0.6	1.0	0.60			
9	0.8	1.0	0.68			
10	0.2	1.8	0.37			
11	0.4	1.8	0.58			
12	0.6	1.8	0.65			
13	0.8	1.8	0.69			
14	0.4	1.8	0.52			
15	0.6	1.8	0.58	$r_1 = 0.2$ (edge radius)		
16	0.8	1.8	0.58			
17	0.4	1.8	0.58	$r_1 = 0.1$ (edge radius)		
18	0.4	1.8	0.45	$r_1 = 1.0$ (full radius)		
19	0.4	0	0.54*			Curved plate
20	0.4	0.4	0.49			
21	0.4	1.0	0.40			
22	0.2	1.8	0.30	$r_1 = 0.725$ (full radius)		
23	0.4	1.8	0.41			
24	0.6	1.8	0.43			
25	0.8	1.8	0.43			
26	0.4	1.8	0.34	$r_1 = 0.5$ (full radius)		
27	0.4	1.8	0.12			$r_2 = 0.4$
28	0.8	1.8	0.15	$r_2 = 0.9$		
29	0.2	1.8	0.14			
30	0.4	0.4	0.66	$r_2 = 0.2$		
31	0.6	1.8	0.37			
32	0.4	0.6	0.34			
33	0.4	1.0	0.25			
34	0.4	1.8	0.16			
35	0.8	1.8	0.37			
36	0.2	1.8	0.20	$r_2 = 0.05$		
37	0.4	1.8	0.40			
38	0.8	1.8	0.56			

Rectangular block, with dimensions of hull used in tests 1 to 75 and 89 to 107

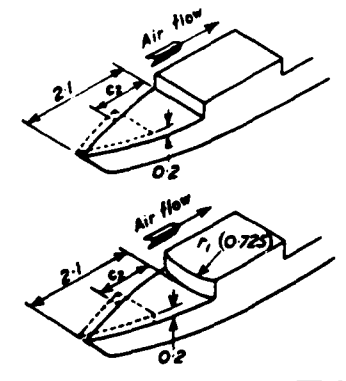
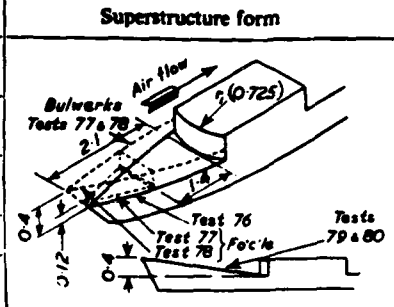
Block rectangular
in elevation
and rounded in plan

Superstructure Design in Relation to the Descent of Funnel Smoke

Test number	a	c	h		Superstructure form
39	0.4	1.8	0.20	$r_1=0.725$ $r_2=0.2$	
40	0.4	1.8	0.35	$r_1=0.725$ $r_2=0.05$	
41	0.8	1.8	0.36		
42	0.4	1.8	0.58	Step front	
43	0.4	1.8	0.52	Step front, $r_2=0.05$	
44	0.4	1.8	0.51	Slope front	
45	0.4	1.8	0.38	Step front, $r_1=0.725$	
46	0.4	1.8	0.30	Slope front, $r_1=0.5$	
47	0.4	1.8	0.48	Step front	
48	0.4	1.8	0.44	Slope front	
49	0.4	1.8	0.40	Step front, $r_1=0.725$	
50	0.4	0.69	0.67	Slope front	
51	0.8	1.38	0.60		
52	0.4	1.8	0.22	Step front	
53	0.4	1.8	0.29	Slope front	
54	0.8	1.8	0.23	Step front	
55	0.4	1.8	0.24	Step front, $r_1=0.725$	
56	0.8	1.8	0.20		
57	0.4	1.8	0.42	$a_1=0.3$ $c_1=0.4$ $r_2=0.2$	
58	0.4	1.8	0.63	$a_1=0.3$ $c_1=0.4$ $r_2=0.05$	
59	0.4	1.8	0.67	$a_1=0.2$ $c_1=0.4$	
60	0.4	1.8	0.56	$a_1=0.2$ $c_1=0.4$ $r_1=0.725$	
61	0.4	1.8	0.34	$a_1=0.2$ $c_1=0.4$ $r_2=0.2$	
62	0.6	1.8	0.71	$a_1=0.2$ $c_1=0.4$	
63	0.4	1.8	0.24		
64	0.4	0.4	0.72		

Superstructure Design in Relation to the Descent of Funnel Smoke

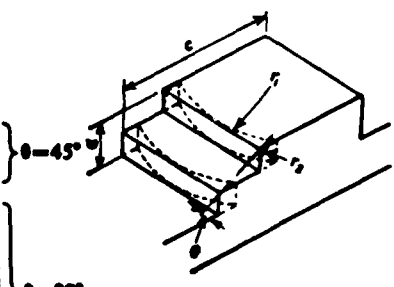
Test number	<i>a</i>	<i>c</i>	<i>h</i>	Superstructure form	
76	0.4	1.8	0.42	No forecastle or bulwarks	
77	0.4	1.8	0.35	0.12 forecastle and bulwarks	
78	0.4	1.8	0.29	0.4 forecastle and bulwarks	
79	0.4	1.8	0.27	0.4 sheer	
80	0.4	1.8	0.21	0.4 sheer, with well-rounded bow	
81	0.4	1.8	0.37	$c_2 = 1.2$	
82	0.4	1.8	0.29	$c_2 = 0.4$	
83	0.4	1.8	0.42	$c_2 = 0$	
84	0.4	1.8	0.37	$c_2 = 1.7$	
85	0.4	1.8	0.29	$c_2 = 1.2$	
86	0.4	1.8	0.22	$c_2 = 0.8$	
87	0.4	1.8	0.22	$c_2 = 0.4$	
88	0.4	1.8	0.30	$c_2 = 0$	
89	0.4	0.4	0.32	Rectangular block	
90	0.4	1.8	0.25		
91	0.6	1.8	0.18		
92	0.2	1.8	0.39		
93	0.4	1.8	0.18		$r_2 = 0.2$
94	0.8	1.8	0.11		
95	0.4	1.8	0.29		$r_1 = 1.0$
96	0.4	1.8	0.22		$r_1 = 0.5$
97	0.4	1.8	0.23		30° step front $r_1 = 0.725$
98	0.4	1.8	0.29		60° step front $r_1 = 0.725$
99	0.4	1.8	0.30	Deckhouse as for Test 68 $r_1 = 1.0$	
100	0.2	0	0.36°	Vertical plate	
101	0.6	0	0.74°		
102	0.8	0	0.76°		
103	0.8	1.8	0.45	Step front	
104	0.8	1.8	0.40	Step front, $r_1 = 0.725$	
105	0.4	0.6	0.38	Step front, $r_1 = 0.725$	
106	0.6	1.8	0.23	Step front	
107	0.6	1.8	0.21	Step front, $r_1 = 0.725$	



20° yaw

θ = 45°

θ = 30°



* Measured from top edge of plate.

Superstructure Design in Relation to the Descent of Funnel Smoke

each case. The dimensions a , b and c (see first sketch in Table I) denote respectively the height, breadth and length of the block, all expressed in terms of the breadth b , which was the same for all of them and equal to the beam of the hull (10 in. on the wind tunnel model). Thus, for all the tests, $b = 1$. It should be noted that h in the tables is measured above the uppermost block surface, i.e. above the deckhouse top in those models where there was a deckhouse on the superstructure (Tests 63 to 71).

For each combination tested, a complete plot of the turbulence boundary was made, extending over the full length of the ship aft of the forward face of the superstructure block. In most instances, the maximum height h of the turbulence boundary, which is recorded in the tables, was well forward of the stern. Typical plots of the observed turbulence boundaries are given in Figs. 2 to 6.

1. 1. 4. Discussion of Results

The results show a number of features of some interest.

(a) Rounded Fronts

Considerable improvement (lowering of the turbulence boundary) can be obtained by rounding the sharp edges of the superstructure, particularly in elevation (Figs. 2 and 3) even when the radius is only one-eighth of the superstructure height (Test 37). The effect of rounding in plan (Fig. 4) is also appreciable, provided that the whole front is rounded (compare Tests 11, 18, 23 and 26) and not only the sharp, vertical edges (Tests 11, 14 and 17).

(b) Sloping or Stepped-back Fronts

Sloping or stepped-back fronts produce an appreciable improvement if the angle of slope or step-back^o is less than 60 degrees to the horizontal (Tests 42-56).

Figs. 5 and 6 show the turbulence boundaries obtained at slopes of 60 degrees and 30 degrees respectively. The apparently anomalous behaviour of the boundary for Test 51, in which the length of the superstructure was very short, is an example of the effect discussed in the next paragraph.

(c) Effect of Length of Superstructure

The advantage of fronts adequately rounded in elevation or sloped or stepped-back tends to be lost if the length of the superstructure is less than the beam b . The turbulence boundary then rises steeply until it is as high as, or even higher than, that with the sharp edged, vertical front (see Figs. 2 and 6, and the values of h in the tables for Tests 30, 32, 33 and 34). This effect is also seen in the results for rectangular superstructures (Fig. 7), particularly the lower

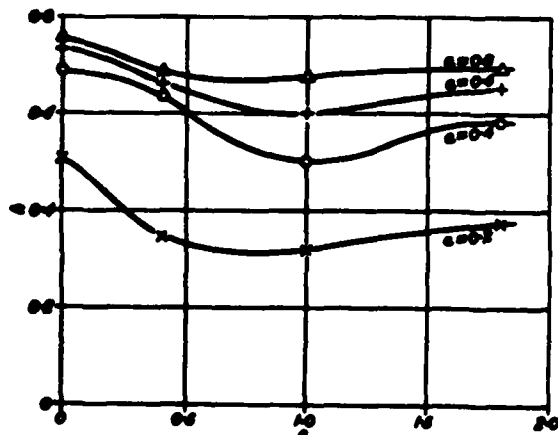


FIG. 7—Values of h for flat fronted superstructures

* The sketches for Tests 42-56 and 103-107 in Table I show how the angle of slope θ is defined.

ones; and in Tests 68 and 69, and 70 and 71, where a set-back deckhouse of given length produces a lower boundary when it is farther back than when it is well forward.

These results suggest that, if the disturbance produced by the superstructure is not too great, as with a low superstructure or one with a well rounded or stepped front, conditions can be greatly improved by arranging for there to be no space close behind the disturbing edge in which large eddies can form. One way of ensuring this is to have a sufficiently long superstructure (length at least equal to its beam). But if the initial disturbance is too great, filling in the space in this way produces no improvement.

(d) Effect of Forecastle Deck

An example of the same effect is shown by Tests 81-88 on the influence of the forecastle deck, the length of which, in successive tests, was increased until it reached the bridge. One would have expected a gradual fall in the height of the turbulent zone with this change, culminating in a value the same as for a bridge front of height equal to the difference in deck levels. Instead, the height of the zone fell to a minimum much below this value, when the intervening well deck length was about 0.5 (Fig. 8). The same trend was observed both with square and rounded bridge fronts.

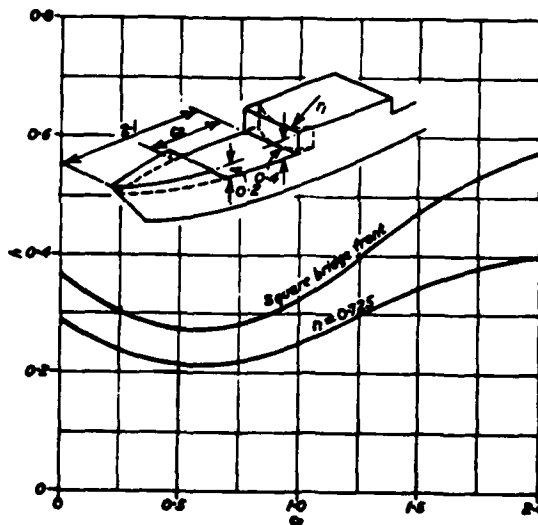


FIG. 8—Effect of length of forecastle deck on height of turbulent zone

The explanation of this unexpected effect is that, as with the short superstructure followed by a step-down, so with the short forecastle deck followed by the well deck, the disturbance produced in the air flow is greater than with a longer structure. Thus it happens that, over a range of lengths of forecastle deck, the turbulence boundary due to the air meeting the forecastle itself is higher than it is when the forecastle deck is longer and the well deck correspondingly shorter. The higher turbulence boundary may pass right over the superstructure, but in any case will reduce the effective height it presents to the full air stream; and so, for certain combinations, the turbulence boundary above the superstructure will be lower than when there is no well deck.

(e) Miscellaneous Tests

A number of miscellaneous additions (Tests 57-75) to the basic blocks were tested to examine the effects of "step-down" and of superstructures not of constant width. In addition, the effect of sheer and bulwarks was investigated (Tests 76-80). The bulwark as fitted to the standard ship (see first sketch in Table I) terminated well forward of the bridge front and produced a negligible effect (compare Tests 23 and 76).

Superstructure Design in Relation to the Descent of Funnel Smoke

(f) Effect of Yaw

A few tests were done at an angle of yaw of 20 degrees (Tests 89-99) and also at 10 degrees. These showed that in general the maximum heights of the turbulent zone were no greater than they were in a head wind, except for the lowest superstructures which would not, in any case, be likely to cause smoke trouble.

1. 2. ESTIMATION OF HEIGHT OF BOUNDARY OF TURBULENT ZONE

1. 2. 1. Application of Test Results

The results obtained from these tests may be used to predict the height of the turbulence boundary from the geometry of the superstructure. To simplify the procedure as much as possible, the data have been generalized, in some cases perhaps more than is strictly justified. But many more experiments would be needed to provide design rules free from this admitted fault. And it can be said that, as regards the more important effects, the rules have been framed by using some of the data only, and have been tested by using them to predict some of the other observed results. This will be made clear in the following notes, and it will be seen that the agreement is usually close enough for practical purposes.

1. 2. 2. Determination of Effective Deck Height

(a) Effect of Forecastle, Bulwarks and Sheer

The first step in estimating the zone height from the drawings of a ship is to determine the level above which the height a of the superstructure is to be measured. If there is no sheer of the deck forward of the superstructure and no forecastle deck, a is measured above deck level; but if there is sheer or a forecastle, a must be measured from some level above deck level since the superstructure front is then partly shielded.

A comparison between the results of some preliminary tests with the blocks on the tunnel floor and those on the model hull showed that the form of the bows themselves had little effect on the height of the turbulence boundary; this was confirmed by Test 80 with bows of exaggerated bluntness rounded to a radius of $0.5b$. It is unlikely, therefore, that the results obtained for different arrangements of sheer, bulwarks, forecastle and length of well deck (Tests 76-88) with the hull form selected for this investigation will be markedly different for other hulls. The effect of bulwarks only can be neglected, as already noted.

The effect of length of forecastle and well deck can be deduced from Fig 8, but the results indicate that a simple working formula, easy to apply, will give all the accuracy required, and that it can be used as well to allow for the effect of sheer. If it is assumed that the shielding due to sheer or forecastle raises the effective base of the superstructure to a height a_1 above deck level (see Figs 9(a) and 9(b)), a can be calculated from the following formula:—

For sheer

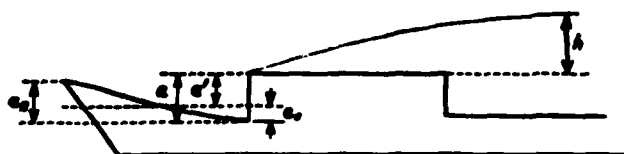


FIG. 9 (a)

$$a_1 = \frac{1}{2}a$$

For forecastle

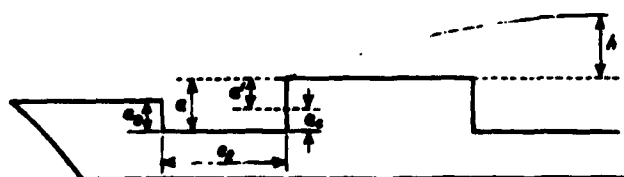


FIG. 9 (b)

(i) When c_1 is less than 1.25

$$a_1 = a$$

(ii) When c_1 is greater than 1.25

$$a_1 = \frac{1}{2}a$$

When the forecastle is sheered, a_1 should be taken as the average height of the forecastle deck.

Applying this rule to calculate the effect of the exaggerated sheer examined in Test 79, in which the deck rose at the bow to the same level as the superstructure, it is found that the observed value of h should be the same as that for the superstructure of the same shape but half the height, i.e. Test 22. The values of h observed were 0.30 for Test 22 and 0.27 for Test 79, so that the rule seems satisfactory.

(b) Effect of Deckhouse

The tests with deckhouses of various widths and flush with the bridge front (Tests 62 and 65-67) indicate that the structure can be represented with sufficient accuracy by taking an effective height

$$a' = a + a_1 b,$$

where a is the height of the deckhouse above the superstructure of full width, and then finding the zone height h from the curves for a full-width superstructure of height a' and a similar form in other respects. It is important to note that the datum from which h is measured when using this formula is the top of this imaginary superstructure of height a' .

When the wheelhouse is set back at an angle less than 60 degrees to the horizontal, it becomes enveloped within the turbulent zone, and so ceases to influence the zone height appreciably.

Various forms of superstructure fronts with and without bridge wings were tested (Tests 72-75). The results show that the effective height a' of the superstructure for such cases can be obtained sufficiently accurately by taking a as the height up to which the superstructure is of full width b (neglecting any wing projections beyond this width), and then applying the formula

$$a' = a + a_1 b,$$

previously quoted to allow for portions of less than full width above this.

1. 2. 3. Determination of h

The preceding section shows how the effective height a' of the superstructure is obtained when the real height has to be corrected for fronts not of constant width (bridges, deckhouses, etc.), and the level above which it should be measured to allow for the effect of forecastle and sheer. Frequently

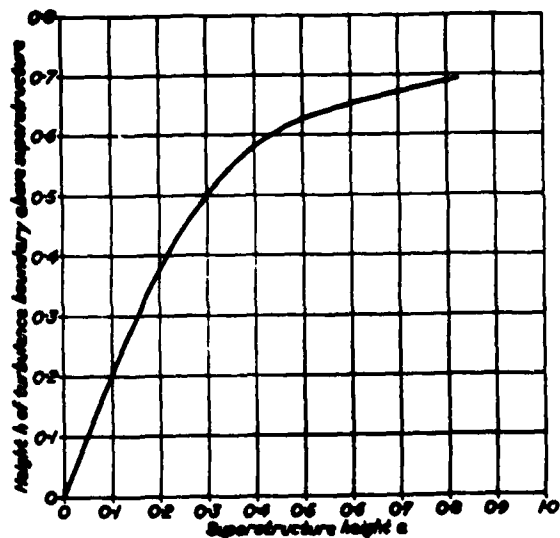


FIG. 10

(All dimensions are expressed as decimal fractions of beam b)

Superstructure Design in Relation to the Descent of Funnel Smoke

these corrections will not be necessary, and a' can be taken as the height of the superstructure itself measured from deck level. The value of h can now be calculated; it will depend mainly on five variables: rounding in plan, rounding in elevation, angle of slope or step-back, length of superstructure, and intermediate step-down (see sketches for Tests 57-62 and 64).

The basic condition is taken as a flat, vertical fronted superstructure, rounded neither in plan nor elevation (Tests 1-13). The height h of the turbulent zone measured above the top surface of this superstructure varies with the height a and also with the length c of the superstructure. But as c increases and becomes greater than about 1.5, h tends to become constant (Fig. 7). The basic condition in these tests is therefore taken to be a flat fronted superstructure of the greatest length tested in this series, namely $c = 1.8$. The values of h for this basic superstructure are shown in Fig. 10. The procedure is now to correct this basic h , as necessary, for each of the five variables mentioned in the preceding paragraph.

(1) Effect of Rounding in Plan (Tests 14-26)

Since an edge radius has little effect, only rounding extending over the full front is considered. Each value of h observed in the relevant tests (Nos. 18-26) has been divided by the corresponding value of h (Nos. 10-13) for the sharp edged superstructure of the same height to give a factor f_r . Thus for Test 24, for example,

$$f_r = \frac{0.43}{0.65} = 0.66$$

Fig. 11 has been derived from the data in this way; it shows the values of f_r for different superstructure heights and for various values of $1/r$, where r is the radius of the rounded front. It can be used to estimate the height of the turbulence zone for any height of superstructure, by interpolation if necessary, and for any degree of rounding in plan, within a range that will cover most existing ships.

Thus, for a superstructure of height 0.35, for example, and length 1.8, with a front curved in plan to a radius 0.8 times the beam, $1/r = \frac{1}{0.8} = 1.25$; and from Fig. 11 the value of f_r is 0.68. From Fig. 10, h for the corresponding flat fronted superstructure is 0.55.

Hence, for the rounded superstructure
 $h = 0.68 \times 0.55 = 0.37$

Although Fig. 11 has been derived for a superstructure length c of 1.8, it can probably be used, within reason, for

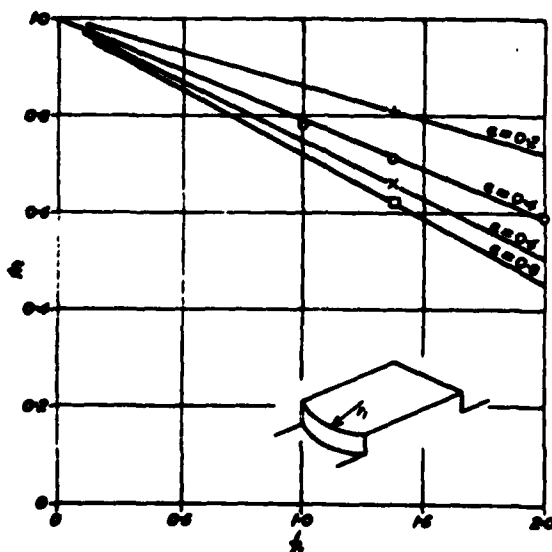


FIG. 11—Front rounded in plan

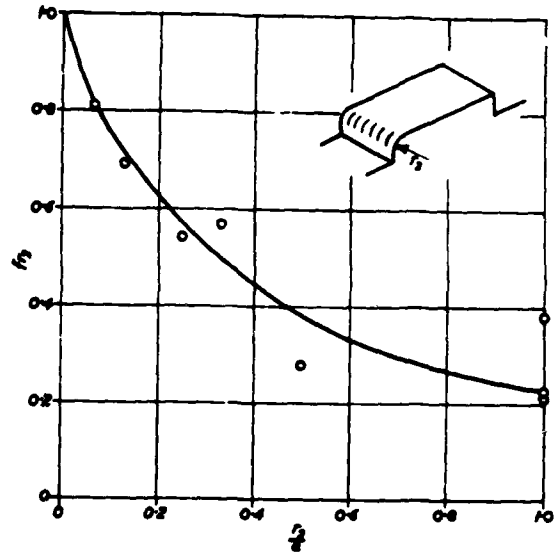


FIG. 12—Front rounded in elevation

different values of c . Thus, applying the above procedure to the conditions for Tests 20 and 21, in which $c = 0.4$ and 1.0 respectively, calculated values are obtained for h of 0.45 and 0.35 as against observed values of 0.49 and 0.40. This agreement is well within practical requirements.

(2) Effect of Rounding in Elevation (Tests 27-38)

For any generalization of this effect to be possible, it appears reasonable to assume that the ratio of the radius of rounding to the superstructure height (r/a), rather than the radius r alone, is the governing factor. On this assumption, Fig. 12 has been derived from the results, showing the factor f_e by which the value of h for a flat fronted superstructure must be multiplied to calculate h for the corresponding superstructure rounded in elevation. This curve, which was derived for a superstructure length of c of 1.8, cannot be used for short superstructures because of the effect already noted in § 1. 1. 4(d). The effect of length for superstructures rounded in elevation is discussed in § 1. 2. 3(5).

(3) Combined Effect of Rounding in Plan and Elevation (Tests 39-41)

For a superstructure of reasonable length, rounded both

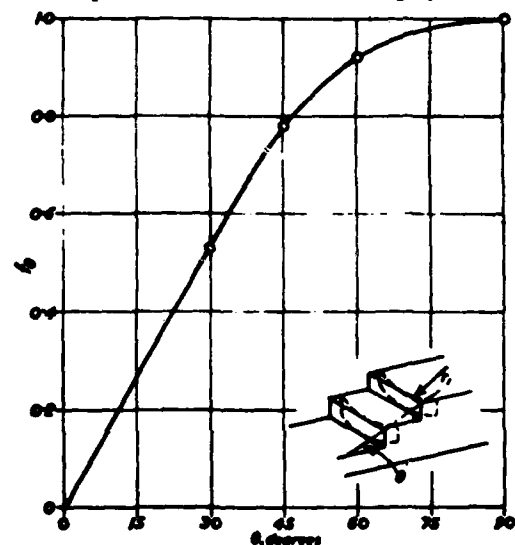


FIG. 13—Step or slope front

Superstructure Design in Relation to the Descent of Funnel Smoke

in plan (r_1) and elevation (r_2), the value of h can be obtained by multiplying the basic h in turn by factors f_1 and f_2 , obtained from Figs. 11 and 12.

(4) Stepped-back or Sloping Superstructure (Tests 42-56)

The results show that h for a sloping-back front does not differ much from that for a stepped-back front of the same angle of slope (θ), defined as the angle to the horizontal of the line joining the extreme edge of the steps in side view. A factor f_0 has been derived from the data, which is applied in the same way as the factors f_1 and f_2 to the basic value of h to obtain the effect of slope. A curve of f_0 is plotted in Fig. 13 on a base of θ . This curve was derived from the data for one height of superstructure only, namely $a = 0.4$. The supplementary tests afterwards made (103, 104, 106 and 107) provided data for other superstructure heights, which were found to be in reasonably good agreement with values of h obtained by multiplying the appropriate basic h by factors f_0 obtained from Fig. 13, and also where necessary, by f_1 obtained from Fig. 11.

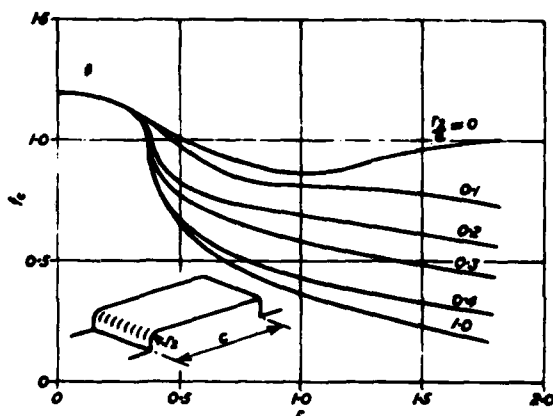


FIG. 14—Effect of length of superstructure and radius r_1 .

Tests 42 and 43 show that the effect of rounding sloped or stepped-back fronts in elevation is considerably less than for a vertical front. It is therefore suggested that the allowance

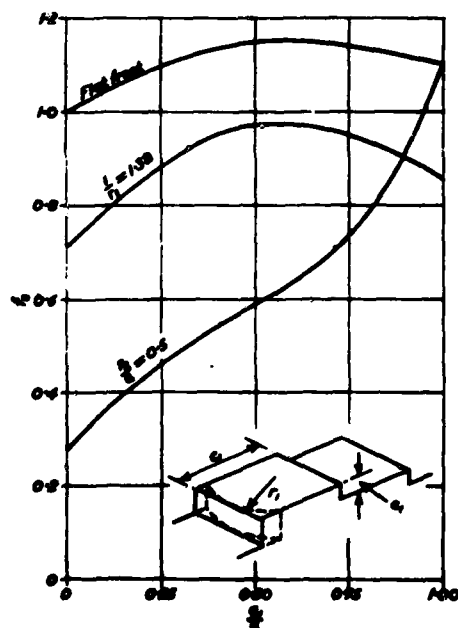


FIG. 15—Typical curves for intermediate step down

for rounding in elevation should be made only for fronts sloping at more than 60 degrees to the horizontal.

(5) Effect of Superstructure Length

Fig. 14, which has been derived from the results of Tests 1, 3, 7, 11, 27, 30, 32, 33, 34 and 37, shows values of a length factor f_c for superstructures of various lengths c and degrees of rounding r_1/a . Only the results for a height $a = 0.4$ were used in deriving this diagram, but, applying the factors there given to the conditions of Tests 28 and 29, in which a was 0.8 and 0.2 respectively, calculated values of h of 0.12 and 0.07 are obtained as compared with the measured values of 0.15 and 0.14. The agreement is good enough for practical purposes.

It should be noted that the factor f_c includes the allowance for rounding in elevation. Therefore, when it is necessary to use this factor, no separate allowance (factor f_2) should be made for rounding in elevation.

(6) Effect of Intermediate Step-down (Tests 57-62)

The results are not sufficiently numerous to define this effect with certainty, but Fig. 15, which relates to a superstructure height of 0.4, can be used as a guide. The effect is significant only for superstructures rounded in elevation. For such superstructures, and probably also for well-sloped or stepped-back fronts, it is clear that an appreciable intermediate step-down will destroy much of the improvement due to rounding or slope.

1. 2. 4. Application of the Method to Actual Ships

As examples of the application of the method of estimating the height of the turbulence boundary, calculations have been made of the heights of the boundary for the three ships A, B and C which were used for the full-scale-model comparisons previously mentioned and described in Part II. For each of these ships, the actual height of the turbulence boundary was also determined by model tests, using the H. S. method, so that three direct checks of the method have been obtained. The calculated heights are compared with the observed turbulence boundaries for the three ships in Figs. 1, 16(a) and 16(b), and it will be seen that in each case remarkably good agreement was obtained. In all three cases the difference between estimated and observed height was within 3ft. full scale.

It should be noted that the method of calculation makes no allowance for the effect of the funnel on the height of the turbulence boundary. As shown by the work described in Part II, this is local and very small. But in order to make a true comparison between the results of the calculations and the observations, the funnels were removed from the three ship models when the heights of the turbulence boundaries were being measured in the wind tunnel.

The dimensions required for applying the method were scaled from drawings of the three ships. Details of the calculations for Ship A are as follows:—

The breadth of the superstructure, which increased slightly for some distance aft, is taken as the breadth at the front face. The various dimensions, in terms of the symbols shown in Fig. 17, are as follows:—

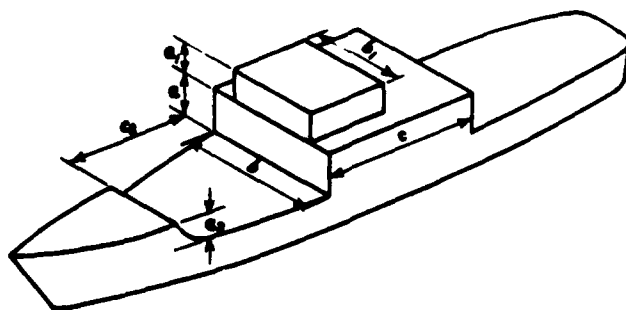
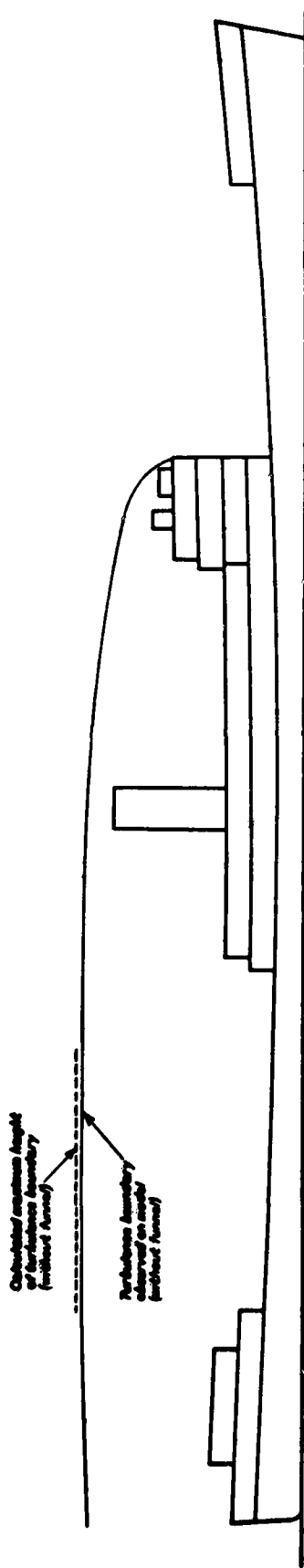


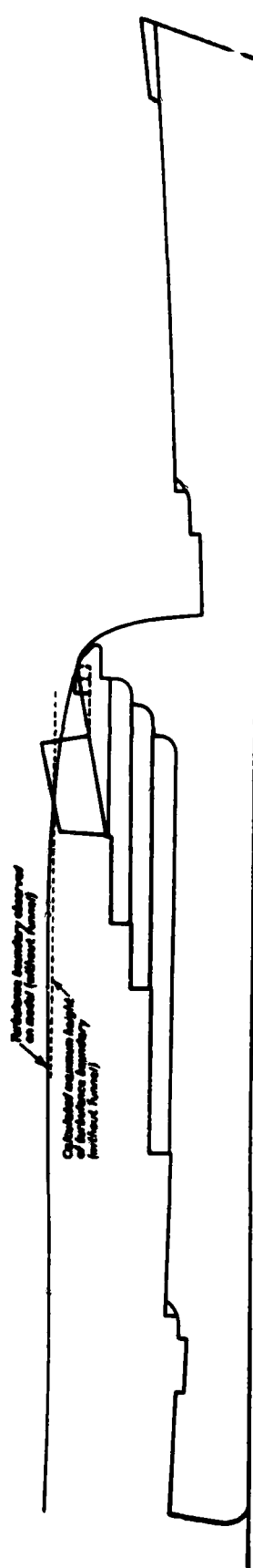
FIG. 17

Superstructure Design in Relation to the Descent of Funnel Smoke



0 10 20 30 40 50 feet

FIG. 16(e)



0 10 20 30 40 50 feet

FIG. 16(b)

Superstructure Design in Relation to the Descent of Funnel Smoke

a = height of superstructure of full width = 0.54,
 a_1 = 0.103,
 a_2 = 0.14,
 b_1 = 0.43,
 c_1 = 0.7

In the same notation
 $b = 1.0$

(1) *Determination of the Effective Height a' of the Superstructure*

(i) Allowance for forecastle and sheer.

Since c_1 is less than 1.25

$$a_1 = a_2 = 0.14$$

(ii) Allowance for wheelhouse, which is flush with front of superstructure.

$$\begin{aligned}
 a' &= a - a_1 + a_1 b_1 \\
 &= 0.54 - 0.14 + 0.103 \times 0.43 \\
 &= 0.44
 \end{aligned}$$

(2) *Allowance for Rounding in Plan*

r_1 (measured on drawing) = 1.1,

i.e. $1/r_1 = 0.9$

and $f_1 = 0.8$ from Fig. 11

(3) *Allowance for Rounding in Elevation*
 None.

(4) *Allowance for Stepped-back Front*

The angle θ measured from the drawing is about 60 degrees,

$$f_2 = 0.92 \text{ from Fig. 13.}$$

(5) *Allowance for Length of Superstructure*

The length of the superstructure is somewhat uncertain

because of variations of height, but it is at least 1.8;
 $f_2 = 1.0$ from Fig. 14.

(6) *Determination of h*

$$h = h_{\text{basic}} \times f_1 \times f_2 \times f_3$$

From Fig. 10 it is found that for $a' = 0.44$,

$$h_{\text{basic}} = 0.6$$

$$\text{Hence } h = 0.6 \times 0.8 \times 0.92 \times 1.0$$

$$= 0.44$$

This is measured from the top of the imaginary superstructure of height a' . This imaginary superstructure is lower than the actual superstructure (which is assumed to extend to the wheelhouse top) by the amount $a_1 - a_1 b_1$, i.e. 0.06.

Hence h measured above wheelhouse top

$$= 0.44 - 0.06$$

$$= 0.38$$

This height is shown by the dotted line in Fig. 1 in comparison with the H, S line.

1. 3. CONCLUSIONS TO BE DRAWN FROM PART I

A method has been developed for estimating, from drawings of the ship, the height of the turbulence boundary. The method is based on the use of simple formulae and diagrams; and comparisons with observations on three different ships have shown that it enables accurate predictions to be made of the height of the turbulence boundary.

The height of the boundary can be considerably reduced by suitable rounding of the edges of the superstructure, particularly in elevation.

Superstructures of length less than their breadth give rise to higher turbulence boundaries than longer superstructures, and the beneficial effect of rounding the edges is lost if the superstructure is too short.

PART II—COMPARISON BETWEEN MODEL AND FULL-SCALE OBSERVATIONS OF THE HEIGHT OF THE TURBULENCE BOUNDARY

The reasons for making full-scale checks of the wind tunnel results have already been explained in the introduction to the paper. Three ships were selected for the purpose; the turbulence boundary for each was traced by the H, S method on a model in the wind tunnel, and the heights of the turbulence boundaries on the ships themselves were observed at sea at two points for Ships A and B and at one point for Ship C. The choice of the ships was governed by their availability for short voyages, since the observations, once the technique had been established, did not take long to complete; and by their suitability for carrying the equipment, the main requirement being two masts of adequate height. Ship A, on which the technique was developed, was a cross-channel ship and as such was admirably suited to the purpose. Although, as is shown below, the model and full-scale results on this ship agreed closely, it was thought desirable to carry out a second check on another ship, Ship B, for which equally good agreement was found.

Both these ships, however, had more or less bluff, sharp edged superstructures; and general hydrodynamic experience indicates that if there is any Reynolds-number effect whereby model and full-scale flow patterns differ, it is more likely to be found in rounded than in sharp edged forms. A third model-full-scale comparison was therefore made, this time with a more modern, "streamlined" ship (C) having a superstructure well rounded both in plan and elevation. Unfortunately, the choice of a such a ship was restricted for various reasons, one being the present trend to have one mast only. It eventually proved necessary to use a single-masted ship, and therefore, for reasons that will shortly be apparent, the height of the turbulence boundary could be observed only at one point on the ship itself.

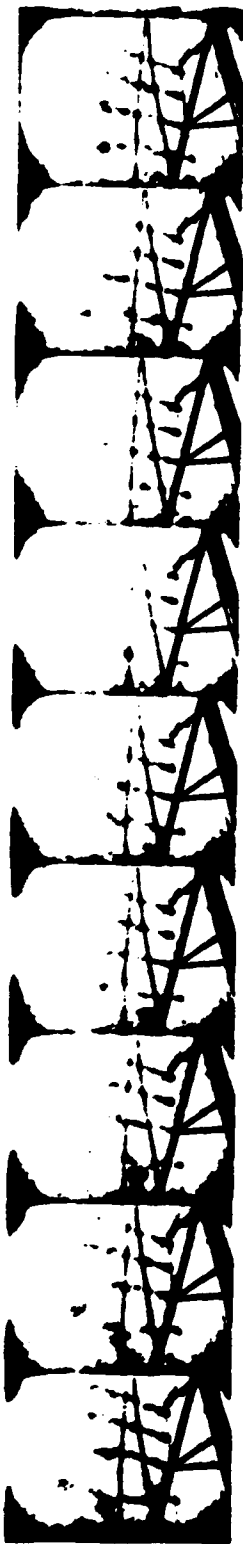
2. 1. METHOD OF EXPERIMENT

Initial attempts to use streamers were not entirely satisfactory, and, with the help of the Chemical Defence Experimental Establishment (C.D.E.E.), Ministry of Supply, a successful method depending on the use of smoke was devised. A small smoke generator which emits a jet of dense orange smoke for about three minutes was developed by C.D.E.E., and proved entirely satisfactory. For observations on the ship at sea, a number, usually six, of these generators, spaced four or five feet apart, were fixed on a cable which was suspended from a yard attached to the mast on Ship A, and from an overhead cable stretched between the mastheads on Ship B and the single mast and two kingposts on Ship C. Two vertical lines of generators were used on Ships A and B and one on Ship C. Each generator consisted of the pyrotechnic mixture developed by C.D.E.E., enclosed, with an igniter, in an ordinary tin can of about 2 in. diameter and 4 in. height. The igniters were electrically actuated from a 6-volt dry battery.

Before each experiment, the ship was headed into wind; the smoke generators were then ignited, and visual and cinematograph observations were made of the smoke trails from the six generators. In the undisturbed flow, these trails persisted as comparatively steady jets for some 6-10 ft. down stream; but the trails from the generators in the turbulent zone were less steady, the degree of unsteadiness increasing progressively the lower the height of the generator. The visible length also decreased as the unsteadiness increased.

Since the sole purpose of this investigation was to compare model and full-scale results, the experiments were done for one relative-wind direction only, namely wind ahead, because this was the easiest to set on the full scale.

Superstructure Design in Relation to the Descent of Funnel Smoke



(5)

FIG. 18

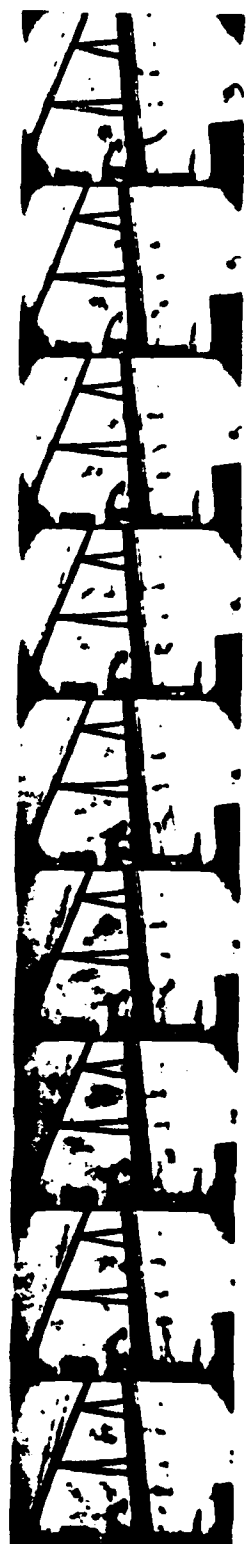


(6)



(7)

FIG. 19



(8)

Superstructure Design in Relation to the Descent of Funnel Smoke

2. 2. TESTS ON SHIP A

2. 2. 1. Results of Tests

Typical sets of cinematograph records at the foremast of Ship A are shown in Figs. 18(a) and 18(b). Since it was not possible to find a position on the ship from which to photograph the smoke trails from all the smoke generators simultaneously, the upper and lower trails were photographed separately. They can be identified if it is remembered that No. 2, the second from the top, appears in Fig. 18 to be at the level of the upper triangular bracing of the mast. There were six generators at heights of 31, 28, 24, 20, 16 and 12ft. above the foot of the foremast, and six also abreast of the mainmast at heights of 28, 24, 20, 16, 12 and 8ft.

The two highest trails at the foremast showed that the flow at 31ft. and 28ft. was steady, and the two lowest that at 16ft. and 12ft. turbulence was strongly developed, with frequent reversals in direction at 12ft. and some at 16ft. There was occasional disturbance of the third trail at 24ft. and

at the mainmast experienced some disturbance for 20 or 30 per cent of the time, unsteadiness did not begin to develop to any appreciable extent above the level of No. 3, and was predominant at the heights of the two lowest trails. From the observed fact that smoke would be sucked down from the level of about generator No. 4 on the foremast, where the percentage of U-disturbances was 6, it would seem that the corresponding position at the mainmast would be about generator No. 3 (20ft. above the foot of the mast) where the U-percentage was 8. It should be noted, however, that since the mainmast is much nearer the stern, it does not necessarily follow that smoke would descend to deck level within the length of the ship aft of the mast.

2. 2. 2. Comparison with Wind Tunnel Results

Fig. 20 shows the heights of the turbulence boundary on a model of Ship A, determined by the two methods described in Appendix 2. Three shadowgraph boundaries (full lines)

TABLE II—ANALYSIS OF RECORDS

Trail number	Foremast				Mainmast			
	Number of records examined	Percentage of total number in category			Number of records examined	Percentage of total number in category		
		S	D	U		S	D	U
1	155	100	0	0	551	77	23	0
2	140	94	6	0	625	67	30	3
3	710	79	21	0	688	51	41	8
4	710	40	54	6	760	12	47	41
5	560	0	37	63	748	1	21	78
6	361	0	4	96	543	0	18	82

distinct turbulence at 20ft. (smoke generator No. 4). Subsequent visual observations with the generators 2, 3 and 4 only in action showed that smoke from No. 4 occasionally drifted forward to the bridge. It thus appears that the effective height of the turbulence boundary at the position of the foremast is at about the level of generator No. 4.

Some of the results obtained at the mainmast are shown in Figs. 19(a) and 19(b), the former for the three upper generators separately, and the latter for the three lower. It was not as easy as for the foremast position to distinguish clear cut differences in the behaviour of the three upper trails from one another. Although for most of the time trails 1 and 2 were steady, as in the upper frames of Fig. 18(a), there were times when even No. 1 became somewhat disturbed, as in the three lowest frames.

A simple statistical analysis was therefore undertaken of the records, dividing the trails into three categories: S (steady), D (occasionally disturbed), and U (unsteady). For the sake of comparison, a similar analysis was made of the records from the foremast. The results are given in Table II.

This analysis shows that, although the two upper trails

are shown in Fig. 20, corresponding to the criteria indicated at the left-hand side of the diagram. For practical purposes, it may be said that the second shadowgraph line from the top represents the boundary at which appreciable turbulence begins. Within the zone between this line and the one above it, the shadows of the hot-air trails are only slightly disturbed at infrequent intervals and not perceptibly shortened. The frequency and degree of disturbance, however, increase somewhat towards the lower boundary of this zone.

Except near the forward edge of the bridge, the second shadowgraph line agrees well with the upper dotted line, which represents the height at which turbulence begins to spread downwards, as indicated by the chemical reaction (H₂S) method. The lower of the two dotted lines* marks the height above which H₂S must be introduced if it is to be kept clear of the stern of the ship; any H₂S introduced below this line will descend to deck level at the stern (Appendix 2).

It is clear from the wind tunnel results that the change from smooth flow to strong turbulence takes place not at

* There are two "lower" lines in Fig. 20, one for the model with the funnel and one without.

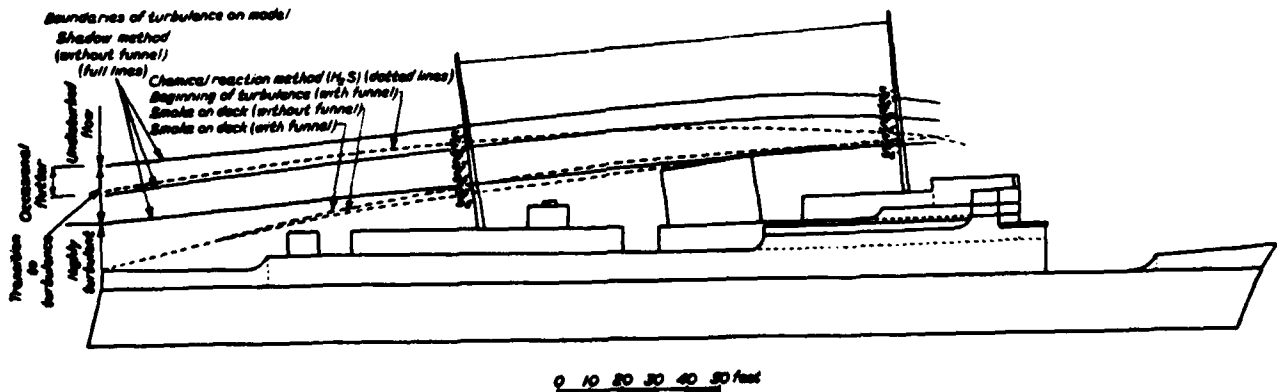


FIG. 20

Superstructure Design in Relation to the Descent of Funnel Smoke

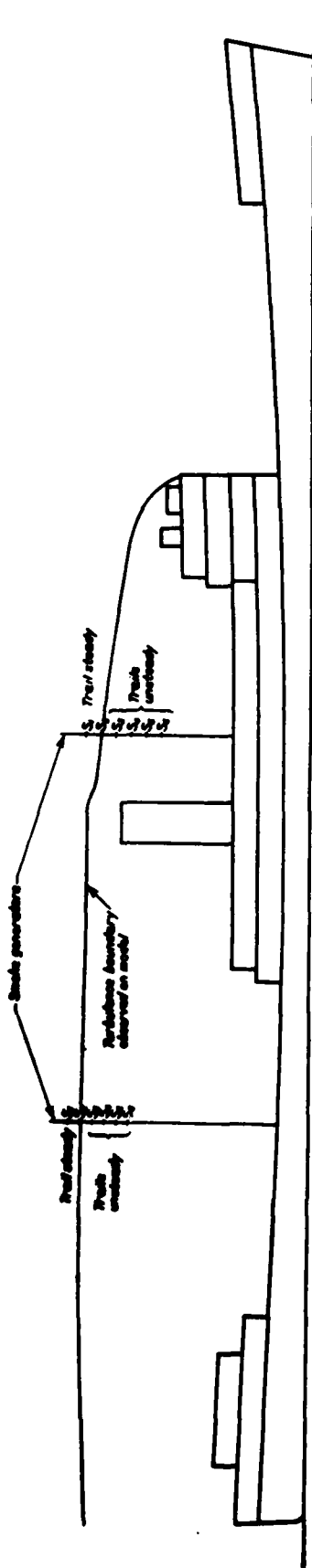


FIG. 21(a)

0 10 20 30 40 50 feet

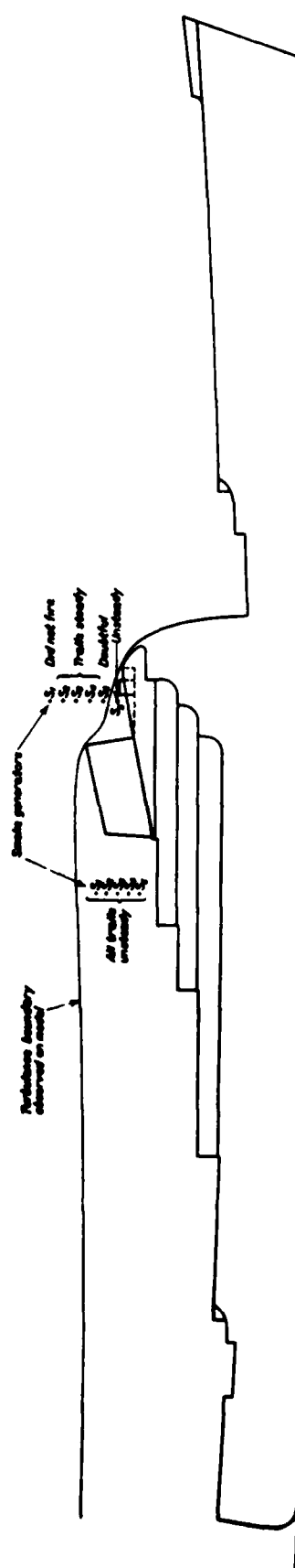


FIG. 21(b)

0 10 20 30 40 50 feet

Superstructure Design in Relation to the Descent of Funnel Smoke

any sharply defined line, but over a transition zone of some depth, which is greater aft than forward. The results obtained with the smoke generators show that this is true also for the full-scale ship.

The positions of the six smoke generators are denoted in Fig. 20 by the points S_1, S_2, \dots, S_6 at each mast. At the foremast, turbulence was found to be appreciable on the full scale at about S_1 , and this comes well within the transition band as determined on the model by shadowgraph. It also agrees satisfactorily with the H.S. results: as already mentioned, smoke from generator S_1 , 20ft. above the foot of the mast, could be just detected by smell on the bridge forward of the mast; and comparative experiments in the wind tunnel with the H.S. technique showed that the smoke would be carried forward to the bridge when emitted from a point at the foremast of the model corresponding to a full-scale height of 18ft. above the mast foot. It will also be seen from Figs. 18 and 20 that the full-scale results agree well with the model shadowgraph results in showing that at the foremast there was practically no turbulence at S_1 and S_2 , that S_3 was occasionally disturbed, and that turbulence was pronounced at S_4 and S_5 .

This agreement between model and full-scale is equally good for the results at the mainmast.

PART III—PREVENTING THE EJECTION OF SMUTS BY REDUCING THE GAS VELOCITY

As already remarked in the introduction, smuts ejected from the funnel must eventually fall to deck level; and whether or not they will fall on to the ship will depend on the speed at which they are ejected, the height they reach before beginning to fall, and the speed and direction of the relative wind. Higher funnels or increased efflux velocities from the funnel uptakes—measures that may cure the smoke problem entirely—can only be regarded as palliatives as regards smuts. They will cause some improvement by increasing the time taken by the smuts to fall to deck level; but they will be ineffective in light winds or at slow speeds of travel, or when the ship is at rest.

It has been suggested that if at some section of the exhaust ducting between the boiler and the exit end of the uptake a length of vertical piping of larger diameter is introduced, in which the upward velocity of the gases is low enough, the smuts will fall out of the stream inside the uptake and so will not be ejected at all. For this suggestion to be effective, the upward velocity of the gases in this section of piping must be less than the natural rate of fall of the smuts in still air; also, the section must be long enough to give the smuts time to lose any excess velocity with which they enter it.

The practical implications of these requirements are discussed below.

3. 1. DISCUSSION OF THE PROBLEM

The exhaust gases, travelling at speed V , in the main uptake (Fig. 22), enter the enlarged section where their velocity drops to V_1 . Let $V_1 = pV$, and $V_2 = qV_1$, where V_1 is the natural rate of fall of the smuts in still air (the terminal velocity). Then the upward velocity of the smuts in the main uptake is $V_1(p-1)$ and in the enlarged section $V_1(q-1)$. It is assumed that the velocity changes instantaneously when the gases enter the enlarged section.

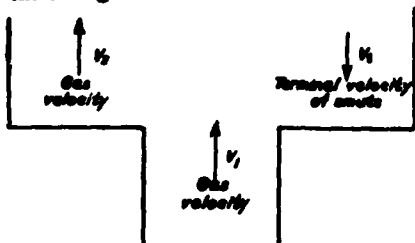


FIG. 22

2. 3. TESTS WITH SHIPS B AND C

Figs. 21(a) and 21(b) show the turbulence boundaries obtained by the H.S. technique on models of Ships B and C, together with the positions of the smoke generators used in the full-scale tests. The behaviour of the smoke trails is also noted on the diagrams, and it will be seen that there is again good agreement between the height of the turbulence boundary (model) and that of the smoke generator at which turbulence set in on the full-scale. Because of the absence of a mainmast, it was not possible on Ship C to straddle the turbulence boundary with the smoke generators, which were all below the boundary.

2. 4. CONCLUSIONS DRAWN FROM PART II

The type of flow over a ship model as determined in a wind tunnel agrees well with that existing on the ship itself in regard to the wide transition zone over which the flow changes from smooth to turbulent, to the heights of the boundaries of this zone above the ship, and to the limiting height above which smoke must be emitted if it is to clear the decks. The results of such wind tunnel experiments can therefore be applied directly to the design of funnels and superstructures.

If the smuts are to come to rest, V_1 must be less than V_2 , i.e. q must be less than 1. The motion of the smuts can be considered in two stages:—

- (i) The velocity of the smuts drops to V_1 .
- (ii) The velocity of the smuts drops from V_1 to zero.

In the first stage, a smut is moving upwards relatively to the gases, and the force on it due to the resistance to motion through the gases is downwards; in the second stage, the smut is moving more slowly than the gases and the resistance acts upwards.

The following solutions have been obtained by Dr. J. E. Richards for the equation of motion for a smut in each of the two stages:—

Stage (i)

$$h_1 = \frac{V_1^2}{g} \left[q \tan^{-1} (p - q - 1) - \log_e \sqrt{\frac{1}{1 + (q - p + 1)^2}} \right] \dots \dots \dots (1)$$

Stage (ii)

$$h_2 = \frac{V_1^2}{g} \left[q \tanh^{-1} q - \log_e \sqrt{\frac{1}{1 - q^2}} \right] \dots \dots \dots (2)$$

Equation (1) gives the height h_1 necessary for the velocity of the smut to drop to the speed V_1 of the gases in the enlarged section, and equation (2) the additional height h_2 required for the particle to come to rest, i.e. to fall out of the stream. The total height of the enlarged section of the uptake required is therefore $h_1 + h_2$.

If the terminal velocity V_1 of the smuts is known, equations (1) and (2) can be used to calculate h_1 and h_2 for various values of the gas velocities V_1 and V_2 , i.e. for various values of p and q .

3. 2. TERMINAL VELOCITY V_1 OF THE SMUTS

The terminal velocity V_1 of the smuts from a certain ship was determined in two ways: firstly by calculation from the sizes and total weight of a large number of smuts collected from the decks, and secondly by measuring the times of descent of a number of smuts through known heights. Details of both methods are given in Appendix 3, from which it will be seen that the most probable value of V_1 was 11.8ft. per sec. at atmospheric temperature. The calculations and one set of dropping tests both gave this value independently. Another set of dropping tests made under different conditions gave 8.1ft. per sec.

If the temperature of the gases in the uptake is 360 deg. F.

Superstructure Design in Relation to the Descent of Funnel Smoke

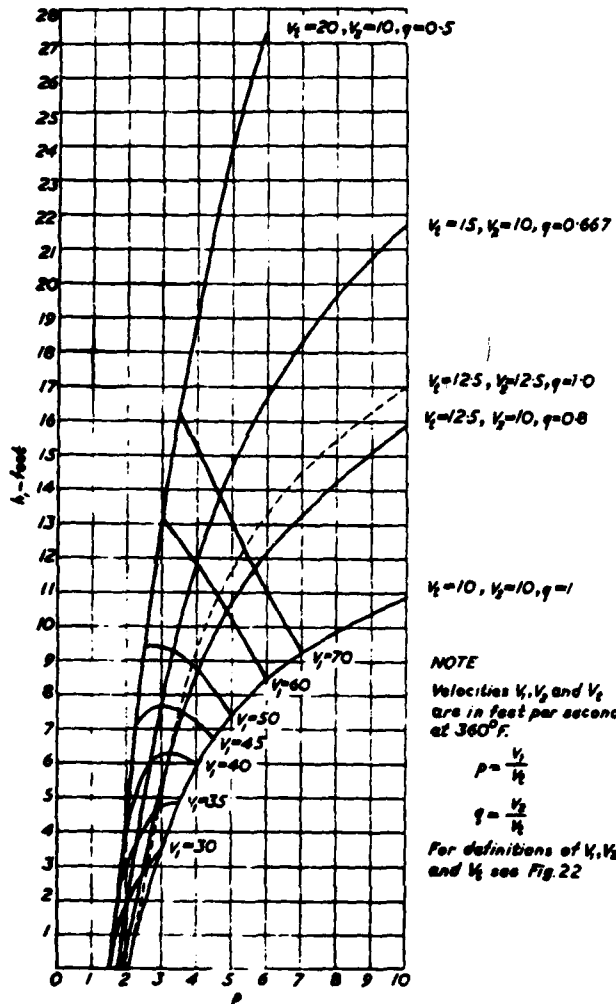


FIG. 23

and the air temperature is 60 deg. F., these dropping speeds will be increased in the ratio $\sqrt{\frac{820}{320}}$. Hence we may take V_1 as 15ft. per sec. or 10ft. per sec. The reason for the difference has not been explained, but, as the following calculations show, the effect is not serious for our present purpose.

3. 3. CALCULATIONS OF REQUIRED HEIGHT OF EXPANDED UPTAKE

(a) Calculation of h_1

Equation (1) has been used to derive Fig. 23, which gives values of h_1 for various values of the velocities V_1 and V_2 . The four full curves for different values of V_1 all relate to a velocity V_2 in the expanded section of 10ft. per sec., and the dotted curve is for $V_2 = 12.5$ ft. per sec. Each of the cross curves relates to the constant value of V_1 indicated. The practical range of V_1 is probably within the limiting values of 10 and 20ft. per sec. included in Fig. 23; and it is seen that, if the velocity V_1 , with which the gases enter the expansion is not greater than 45ft. per sec. the requisite height of the expansion is less than 8ft. Comparison of the dotted curve with the one immediately below it shows that this conclusion is practically unaffected by quite large changes in V_2 .

(b) Calculation of h_2

Equation (2) shows that h_2 depends only on the value of q , as it must do, since the equation gives the height in which the particle comes to rest after its upward velocity has become equal to the velocity V_1 of the gases in the expansion.

Thus, for each value of q , h_2 is a constant height to be added to h_1 as obtained from equation (1) or Fig. 23. The values to be added, obtained from equation (2), are 1.4, 1.8 and 2.2ft. for values of q of 0.5, 0.8, and 0.99 respectively.

3. 4. DISCUSSION OF RESULTS

Although there is some doubt about the terminal velocity of the smuts, it seems unlikely that it will exceed 20ft. per sec. or be less than 10ft. per sec. in gases at a temperature of 360 deg. F. If that is so, and provided that the velocity of the gases in the expanded uptake is not greater than 45ft. per sec., the total height of uptake required is about 7.7ft. for stage (i) and 2.2ft. for stage (ii), or a total of about 10ft. To allow a margin of safety, it is suggested that a height of 12ft. be taken as a minimum practical requirement.

3. 5. CONCLUSIONS FROM PART III

It appears probable that the ejection of smuts can be prevented by including in the uptake a vertical section in which the gas velocity is reduced. If this velocity does not exceed 10ft. per sec. and the velocity ahead of the expansion is not greater than 45ft. per sec., the total height of the expanded section should be about 12ft.

REFERENCES

- (1) OWER, E., and BURGE, C. H. 1950. "Funnel Design and Smoke Abatement". Trans.I.Mar.E., Vol. 62, p. J.19.
- (2) NOLAN, R. W. 1946. "Design of Stacks to Minimise Smoke Nuisance". Trans.Am.S.N.A.M.E., Vol. 54, p. 42.
- (3) ACKER, H. G. 1952. "Stack Design to Avoid Smoke Nuisance". Trans.Am.S.N.A.M.E., Vol. 60, p. 566.

APPENDIX I

NOTE ON THE MEANING OF "TURBULENCE" AS HERE USED

The meaning attached in this paper to the term "turbulence" in connexion with the region of disturbed flow due directly to the air flow over the above-water structure of a ship is rather different from the more general meaning attached to the term in hydrodynamics.

By turbulence in the present paper is meant all the disturbances introduced by the above-water ship's structure; and the turbulence boundary is the boundary between these disturbances and the undisturbed flow outside the zone affected by the structure. In the sense in which turbulence is used in hydrodynamics, the flow in this undisturbed region is generally itself turbulent as well; that is to say, there are relatively small fluctuating velocity components, parallel and perpendicular to the direction of general streaming, super-

imposed on the average velocity in that direction. But, except possibly in rough weather, the scale of this turbulence over the open sea is much smaller than that caused by the superstructure. The essential difference is that, whereas in the free turbulence the fluctuating longitudinal velocity components are hardly ever large enough to cause a reversal of flow, the turbulent zone of disturbances due to the ship's structure almost always contains regions of reversal.

Briefly, the turbulent zone is a region of disturbances which are entirely due to the air flow over the above-water structure of the ship; these disturbances generally include eddies or rotating masses of air, which are large in relation to the eddies outside the disturbed region and probably always cause a reversal of flow somewhere within the zone.

Superstructure Design in Relation to the Descent of Funnel Smoke

APPENDIX 2

METHODS USED IN THE WIND TUNNEL TO DETERMINE THE TURBULENCE BOUNDARY

(a) Shadowgraph Method

Details of the platinum wire assembly used to generate the trails of hot air are shown in Fig. 24. The heating current was supplied through the vertical metal supports to which the ends of the wires were soldered, and adjusted until the wires

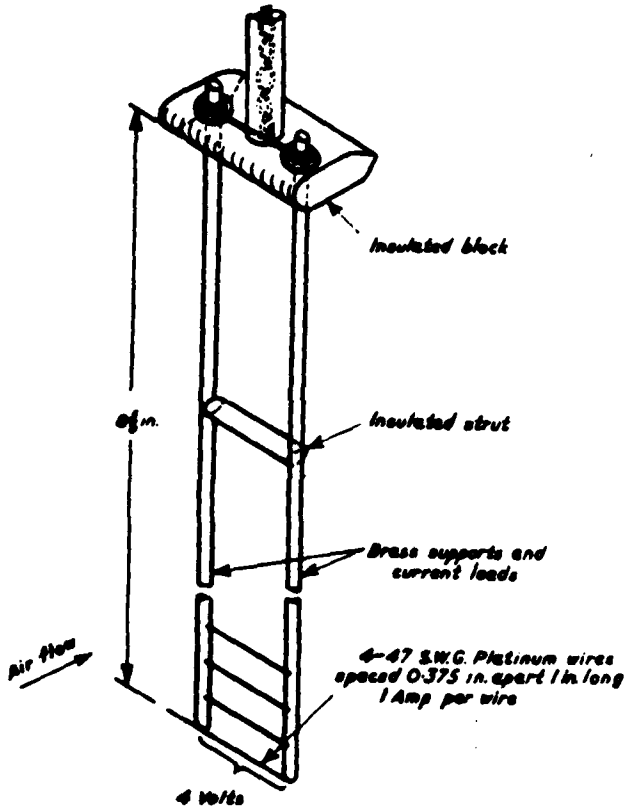


Fig. 24

glowed in still air. The whole assembly was mounted from the roof of the wind tunnel in such a manner that it could be traversed vertically through a sufficient height to cover the zone to be explored.

Moving with the assembly, but outside the tunnel, was an arc lamp from which a horizontal beam of light, shining through a glass window let into one side of the tunnel, cast a side-view shadow of the assembly on to a sheet of white paper pinned to the inside of the opposite wall. When the wires were in a region unaffected by the presence of the model in the tunnel, the trail of hot air from each wire was clearly visible as a dark "shadow" on the paper, quite steady and about 6 in. long. In turbulent flow, however, the shadows became unsteady and shorter to an extent depending on the amount of turbulence (Fig. 25). When the flow was highly turbulent, the shadows became very short stumps, which were violently agitated and sometimes reversed their directions.

(b) Chemical Reaction or H_2S Method

This method can be used in two ways. In the first, the after part of the deck of the model is painted with lead acetate paint, and H_2S from a Kipp's apparatus outside the tunnel is introduced through a fine tube of 1/32-in. bore, which projects vertically downwards through the roof of the tunnel into the air stream, the last inch being bent horizontal and pointing downstream. Starting well above the turbulent zone, the tube is lowered in stages until the first signs of blackening are observed at the stern of the model. The height of the point of emission of the H_2S is measured, and this gives a point on the lower dotted line in Fig. 20. Turbulence at the height indicated by any point on that line is thus sufficiently high to suck the H_2S down to deck level; and it will be seen that this lower H_2S line agrees well over most of its length with the lowest shadowgraph line which indicates fully-developed turbulence. The two lines diverge towards the stern because, although smoke may be sucked down by the fully developed turbulence, it need not necessarily reach deck level before it has travelled past the stern; the lower H_2S line, by the manner in which it is determined, must necessarily pass through the stern point, whereas the lowest shadowgraph line does not.



Fig. 25

Superstructure Design in Relation to the Descent of Funnel Smoke

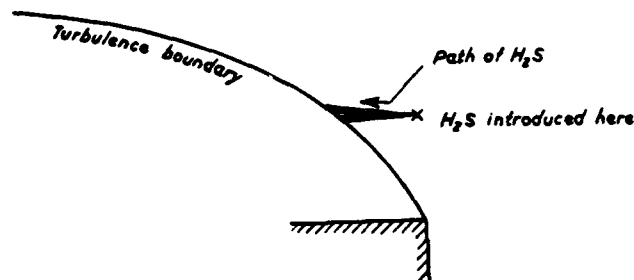


Fig. 26

The upper dotted line, indicating the beginning of turbulence as determined by the H_2S method, is obtained by using a small vertical streamlined strut one inch downstream of the H_2S jet. The strut is mounted on the same support as the jet and moves vertically with it. It is painted with lead acetate, and as long as the jet is above the turbulent zone the lower edge of the black stain that occurs where the H_2S impinges on

the strut does not move up or down the strut as the jet and strut are gradually lowered. But at a certain position of the jet, the lower edge of the stain moves downwards quite sharply, giving a point on the upper dotted line in Fig. 20; and this is taken as the height at which turbulence begins, i.e. the upper boundary of the turbulent zone.

This position is much more easily determined than the corresponding shadowgraph point and is much more definite; different observers obtain the same readings within close limits. It will be seen from Fig. 20 that, except well forward, the upper H_2S line agrees well with the second shadowgraph line, which marks the height at which turbulence begins to be appreciable and the heated-air shadows begin to shorten. The divergence of the two lines forward has not yet been explained.

One further point should be noted: it will be seen that the two H_2S lines approach one another near the foremost. The reason for this is that H_2S introduced at a point above the turbulence boundary can still enter the turbulent zone and find its way to deck level if the boundary is rising behind the point of emission of the H_2S (see Fig. 26).

APPENDIX 3

THE TERMINAL VELOCITIES OF SMUTS

1. Determination of V_t , the Terminal Velocity of a Smut, by Calculation

If the weight of a smut is known, the terminal velocity can be calculated as follows:—

When the smut is falling freely in still air at its terminal velocity, its weight is equal to the air resistance,

$$\text{i.e. } mg = \frac{1}{2} \rho A V_t^2 C_D \quad \dots\dots\dots(3)$$

where m = mass of smut,
 ρ = air density = 0.0765 lb./cu. ft. at about 60 deg. F. and 30 in. of Hg,
 A = cross-sectional area of smut,
 C_D = a resistance coefficient.

The value of C_D depends on the shape of the smut. This approximates to a flat disk, for which it is known that C_D is about 1.0. Using this value of C_D in equation (3), the following equation is obtained for V_t :—

$$V_t = \frac{2 mg}{\rho A} \quad \dots\dots\dots(4)$$

The most obvious assumption regarding the weight of a smut is that it is proportional to the cube of the diameter; and, since A is proportional to the square of the diameter, equation (4) shows that if this assumption is correct the terminal velocity V_t will be proportional to the square root of the diameter. But the dropping experiments carried out later (see (2) below) showed conclusively that the terminal velocity was independent of the size of the smut.

A possible explanation of this is that the smuts are all of the same thickness t . For then the weight of any particular smut is equal to σAt , where σ is the density of the soot; and inserting this value of the weight mg in (3) one gets

$$V_t = \frac{2\sigma t}{\rho}$$

which is constant, since σ , t and ρ are constant.

It appears probable therefore that the smuts are all of constant thickness and are formed by the break up of a deposit or layer of soot on some surface.

To calculate V_t by means of equation (4), a knowledge of m , the mass of a smut, is required. This was obtained as follows:—

The chief engineer of a certain ship supplied a sample of soot collected from the decks, made up as follows:—

- 10 smuts of $\frac{1}{16}$ in. diameter
- 1 smut of $\frac{1}{8}$ in. diameter
- 40 smuts of $\frac{1}{32}$ in. diameter

- 10 smuts of $\frac{1}{16}$ in. diameter
- 7 smuts of $\frac{1}{8}$ in. diameter
- 2 smuts of $\frac{1}{4}$ in. diameter

These were reduced to the equivalent number of $\frac{1}{16}$ -in. diameter smuts on the assumption that the smuts were of constant thickness, i.e. that the weight was proportional to the square of the diameter. The total equivalent number of $\frac{1}{16}$ -in. smuts was thus calculated as 446; the total weight of the sample was found to be 2.85 gm., so that the weight of one $\frac{1}{16}$ -in. diameter smut was 1.41×10^{-5} lb.

Inserting this value of m in equation (4), one gets
 $V_t = 11.8$ ft. per sec. in air at about 60 deg. F.

2. Determination of V_t by Timing the Drop of Smuts through a Measured Height

The equation of motion of a freely falling smut is

$$m \frac{d^2 h}{dt^2} = mg - 2\rho A C_D \left(\frac{dh}{dt} \right)^2$$

where h is the height from the starting point.

If the smut starts from rest, the solution of this equation is

$$\frac{dh}{dt} = V = \sqrt{\frac{gm}{K}} \left[\frac{e^{2\sqrt{\frac{Kt}{m}}} - 1}{e^{2\sqrt{\frac{Kt}{m}}} + 1} \right] \quad \dots\dots\dots(5)$$

where $K = \frac{1}{2} \rho A C_D$
 $= \frac{1}{2} \rho A$ if, as before, it is assumed that $C_D = 1$,
 and V is the velocity of the smut at time t .

The terminal velocity is obtained by putting $t = \infty$;

$$\text{i.e. } V_t = \sqrt{\frac{gm}{K}} \quad \dots\dots\dots(6)$$

Hence

$$\frac{V}{V_t} = \frac{e^{2\sqrt{\frac{Kt}{m}}} - 1}{e^{2\sqrt{\frac{Kt}{m}}} + 1} \quad \dots\dots\dots(7)$$

When the numerical values of m , g , and K are inserted, equation (7) becomes

$$\frac{V}{V_t} = \frac{e^{5.46t} - 1}{e^{5.46t} + 1} \quad \dots\dots\dots(8)$$

Equation (8) gives the rate of drop of the smut at any time t as a ratio of the terminal velocity. A curve of this ratio

Discussion

plotted against t shows that at the end of one second the velocity is over 99 per cent of the terminal velocity. This curve also enables us to calculate the terminal velocity from the average velocity over any interval starting from rest; and the average velocity can be obtained by observing the time taken for a particle to fall a known height.

Observations were made on the ship of the time taken by smuts of various sizes between $\frac{1}{4}$ -in. and $\frac{1}{2}$ -in. diameter to fall through a height of 21.5ft. Eight observations in all were made, and the average time of fall was 2.1 sec., giving an average velocity over this period of 10.25 per sec.

The curve of V/V_1 , obtained from equation (8) showed that the ratio of the terminal velocity to the average velocity over 2.1 sec. was 1.14; hence

$$V_1 = 1.14 \times 10.25 = 11.7\text{ft. per sec.}$$

The very close agreement between this value and that obtained by calculation (11.8, see (1) above) is probably partly

accidental, but it shows that the values obtained for V_1 and the assumed value of C_D are of the right order.

Some further observations were made the next day with smuts that had been lying on deck all night. On this occasion the vessel was berthed and the smuts were dropped over the side through a height of 52.25ft. to water level. Again, smuts of various sizes fell at the same rate, but the terminal velocity obtained in the same way as for the previous day was 8.1ft. per sec.

The reason for this difference has not been explained. In making the calculations, the value of the mass m of the smuts was assumed to be the same as that used in the earlier calculations. This mass may have been different, or there may have been an up-draught up the ship's side. However, as pointed out in the main text, the discrepancy does not affect the conclusions to any material extent.

Discussion

MR. J. P. CAMPBELL (Member of Council) said he was privileged to be at sea with one of the authors of this excellent paper, when he carried out some of his ship tests for the purpose of checking the records he had obtained from wind tunnel tests.

He had previously been advised of what was expected to happen when a head wind was encountered, and for the first test streamers were rigged forward and aft of the vessel. Unfortunately a strong head wind caused the streamers to flap about too rapidly and no reliable results were obtained. At a later date, when the smoke generators were introduced, the smoke trails noticed confirmed the model test results.

The publication of this paper gave shipowners and shipbuilders valuable information on how to prevent fumes getting into accommodation or on to the after deck of a ship.

To obtain reliable films of the tests, it had been suggested that a photographer should take the photographs from a helicopter. It was decided to try taking the photographs from a vantage point on the ship before resorting to this expedient. One of the authors was able to take the photographs by using a ciné camera whilst standing in a lifeboat—a hazardous position at sea. This gave some idea of the lengths research workers were prepared to go to get confirmation of the experiments.

The short answer to the funnel smoke problem was still to make the funnel high enough and in this paper, possibly with great diplomacy, the authors avoided the discussion of funnels. There was a time when funnels on ships were known as "smoke stacks" and were used solely for emitting the fumes from boilers and many years ago these fumes were emitted as high up in the atmosphere as was reasonably possible, especially in the days of natural draught, coal burning boilers, and in those days the funnels were invariably of circular section. Since then they had seen funnel casings of oval, square, gothic and other sections and the stage had been reached where a side elevation usually showed a conic frustrum. On most ships today the funnel casing contained a number of essential parts, some of which might be said to overflow from the machinery spaces, such as silencers, ventilating fans, etc. There were ships afloat where the masters' accommodation was sited in a funnel.

On the ships on which he had seen the tests carried out the actual area of the exhaust pipes accounted for only 7 per cent of the funnel top area and many people were under the impression today that funnel casings on ships were more for appearance than utility.

Many ships could be seen today with what might be called unconventional tops to their funnels, the designs of which were attributable to the shipbuilders and were considered to assist in obviating the smoke nuisance. There were cases on record where shipowners had tried to reduce the smoke nuisance by coning the funnel tops and also increasing the air supply to the boilers; and, incidentally, increasing their fuel consumption in consequence.

When the wind veered round towards the beam the superstructure ceased to have any effect on funnel fumes. As with a yaw of 30 degrees the fumes on the leeward side of a modern funnel casing came down to near deck level. To obviate this many vessels could be seen with an exhaust pipe extending above the top of the funnel casing.

Mr. Ower had given a previous paper on funnels but it was unfortunate that there was no appendix in this paper on funnel cross-section area and shape because this would be of great interest.

In connexion with the smut nuisance, he would have thought that a swirling effect in the flow of the exhaust gas would be more effective in guiding any smuts formed to the outer diameter of the casing of the low velocity gas chamber, as centrifugal force would tend to throw the smuts out to the perimeter where they could be collected. On one of the ships in which he was interested, smut trouble was traced to a small automatic auxiliary boiler operating in a closed stokehold with the air supply trunked from another compartment. In fairness to the designer of the burning equipment, the boiler was burning a higher viscosity fuel than that for which it was designed. To reduce this trouble to a minimum, it had been necessary to resort to continual cleaning of the fire side of the boiler. As a point of interest, this trouble had been entirely eliminated by the introduction of a fuel additive.

Smuts were always of great nuisance value to shipowners in so far as they were very corrosive, containing a lot of sulphur, and when they landed on deck could cause considerable

Superstructure Design in Relation to the Descent of Funnel Smoke

damage to passengers' clothing, tarpaulins, lifeboats, etc. Arresting smuts in funnels by water washing, or methods of straining and retaining them in funnel tops, proved extremely expensive in maintenance repairs, but there was no doubt they could be arrested, but this resulted in extremely rapid corrosion of steelwork. The best way to prevent smuts from landing on deck was to eliminate them at source. Experts on oil burning would confirm that if the CO₂ content in the exhaust gases was increased to 14½ per cent, the smut trouble was eliminated.

He would like to thank Mr. Ower and Dr. Third for this extremely interesting information. Only the authors would know the extensive tests and research that had been necessary before this paper could be published.

MR. C. H. BURGE said the authors should be congratulated on their lucid presentation of the results of their experiments to determine the course of the turbulence boundary. It would be regrettable that the investigation was to be continued and if this was so the authors had provided themselves with a weapon to annihilate their critics inasmuch as the parts of the paper subject to criticism might still lie within the scope of the work yet to be done. Nevertheless, the paper would have been of great value to the naval architect had the authors included photographs of the performance of a model funnel designed on the lines recommended.

The experiment so far had been limited to the wind ahead condition and the results presented in the paper should appeal specially to constructors in the Department of Naval Construction of the Admiralty, whose problems from descending funnel gases mostly arose in winds between 0 deg. and 10 deg. off the bow. Naval architects engaged in the design of passenger vessels would gain very little assistance from the paper, because their ships did not meet with adverse conditions of smoke until the relative wind was between 17 deg. and 20 deg. off the bow. In this respect, the authors' statement on the effect of yawed winds was misleading. It gave the impression that a funnel with a satisfactory performance at wind ahead would be equally satisfactory in winds off the bow. In these days of high maintenance cost it was important to avoid damage from the acid constituents in the funnel gases and, in many ships, lifeboats and lifeboat covers suffered heavily from this form of contamination. Obviously the damage occurred mostly in winds off the bow. Other requirements of modern times demanded that the funnel itself should be free from smoke discoloration and that the oily odours of ventilated waste air should not descend to deck level. Both requirements applied to all directions of relative wind.

When the wind was dead ahead, the airflow pattern was symmetrical to port and starboard of the middle line, both above and below the turbulence boundary. When the funnel gases were discharged clear of the local aerodynamic interference of the funnel itself, the plume would disperse symmetrically, whether or not it remained above the turbulence boundary. The symmetry of the air flow pattern was destroyed as soon as the ship began to turn across the wind. Wind tunnel experiments on a number of model ships and funnels had shown that a critical condition in the funnel wake was reached when the relative wind was in the region of 17 to 25 deg. off the bow. Here the lower boundary of the plume suddenly descended over the leeward face of the funnel, even when the funnel top was above the turbulence boundary. Some of the turbulence to leeward of the funnel was due to the air flow over the ship from windward mixing with both the air flow along the leeward side of the superstructure and an air stream crossing the deck from the windward face of the superstructure, but the major effects came from the presence of the funnel casing itself. Over the range of adverse wind direction the airflow over the top of the funnel mixed with the eddies shed from the windward side of the funnel casing. This produced either a large eddy or a sheet of small eddies into which the lower boundary of the plume descended and then returned upstream to the funnel casing. In this manner, smoke would

return to the funnel from a distance as far as two funnel widths down stream.

There were several ways of dealing with this situation and so far the remedy had been discovered mostly by model experiment. At the moment, this would appear to be the quickest, cheapest and most satisfactory means of providing the naval architect with the right answer.

It was interesting to learn of the authors' success in correlating model and full-scale results from observations taken on a cross-channel ship. In coastal waters the presence of land masses introduced such inconsistent fluctuations in the velocity and direction of the natural wind that there was no time when the air flow over the ship was in a steady state long enough for observations to be taken.

Accordingly one prayed fervently for calm conditions on such occasions when the relative wind would be wholly from dead ahead and equal to the ship speed. This would then correspond with the wind tunnel conditions where there was no velocity gradient. Because of the fluctuation in the natural airflow in coastal waters, wind tunnel results were regarded as being applicable to open sea conditions, but only scanty full-scale evidence was yet available for correlation with measurements taken on the model. Nevertheless, it would appear that there was close agreement between model and full scale over those parts of the ship forward of the funnel, but downwind of the funnel the temperature of the heated surfaces, funnel gases and ventilated waste air introduced buoyancy effects which changed the pattern of the air flow from that experienced on the model. Accordingly one might expect the paths of the turbulence boundaries downwind of the funnel to be slightly above those drawn for the model conditions in Figs. 2 to 6.

It was impracticable to study the descent of smuts by means of model experiments and generally it was accepted that their own momentum on emission would cause them to follow a higher trajectory than that of the lower boundary of the plume. The method suggested in the paper for trapping the smuts was ingenious but modern ships at service speed discharged the funnel gases at high velocity and it was probable therefore that the necessary length of expanded uptake between the induced draught fan and the outlet might be too long to be accommodated conveniently within the funnel casing. The outlet area would be around 60 per cent of the inlet area and it might be expected that the diffusion of the effluent within the enlargement would, at all times, follow the pattern of a free jet rather than expand instantaneously to the full diameter of the enlargement. Therefore, the heights given for the enlargement by the curves of Fig. 23 would have to be increased for the condition V, to be attained.

Referring to Tests 74 and 75 it was interesting to note that the wings of the navigating bridge had so much effect on the height of the turbulence boundary at wind ahead.

Comparing Test 75 with Tests 68 and 70 it was important to bear in mind that a "monkey" bridge set back from the frontal face of the superstructure was almost untenable in high velocity relative winds by comparison with one set flush with the frontal edge.

MR. W. MCCLIMONT, B.Sc. (Member) pointed out that in the last paragraph of Appendix 2 the authors made a significant statement concerning their wind tunnel tests which had equal significance on the ship itself, yet was not noted anywhere in the paper. It was pointed out that hydrogen sulphide introduced at a point above the turbulence boundary could still enter the turbulent zone and find its way to deck level if the boundary was rising behind the point of emission of the hydrogen sulphide. Fig. 26 was included to demonstrate the point. The same remarks would apply if for "hydrogen sulphide" one put in "funnel gas". In other words, if the funnel was forward of the highest point of the turbulent zone, it would probably be necessary to arrange for the efflux from the funnel to be carried at least as high as the maximum height of the turbulent zone and not just to a point above

Discussion

the local turbulence boundary. Of course, if the funnel were aft of the highest point of the turbulent zone, there was no need to carry the funnel gas to a point any higher than the local boundary position.

These observations led to the question whether the position of the highest point of the turbulence boundary had not some practical significance. It was notable that no effort had been made to include the estimation of its position, and attention had been concentrated exclusively on determining the maximum height of the boundary. Figs. 2 to 6 suggested that the line of the boundary was so flat behind the highest point that the neglect of the position of the peak was justified but one wondered if in fact this was so with all arrangements.

All the model tests were done at one wind speed, which was equivalent to a ship speed of about 7½ knots in still air. Had the authors satisfied themselves that there would be no variation of the height of the boundary layer with wind speed and why was this particular speed chosen?

One thing which did not appear to have been varied during the tests with blocks on the model hull was the distance from the forepeak to the bridge front which remained at a length 2.1 times the beam right through the whole series of tests, if he read them aright. This particular dimension could vary to an appreciable extent on ships; for instance, it appeared to be about half as big again on ship C as on ship B. It was difficult to see that this dimension had no significance, especially since allowance was made for the effect of forecastle and sheer. On ship A, which was the hull form used for the model tests, this dimension appeared to be approximately 1.0. Had the authors any reason for increasing this dimension for their tests and why did they choose 2.1?

Fig. 15, which gave typical curves for intermediate step-down, was—he was afraid—incomprehensible to him. The factor f_s appeared to include the effect of other variables than step-down. For instance, the curve marked $r_s/a = 0.5$ appeared to include the factor f_{s0} , although this was not stated anywhere in the text. In doing so, however, it used the isolated point in Fig. 12 for this value of r_s/a and not the value which would be obtained from the curve. And furthermore in the sketch in Fig. 15 there was a dimension C, shown for length which was not referred to in the text dealing with the method of estimation. Was it intended that a minimum value of C, should be specified, above which there would be no effect from an intermediate step-down?

Looking at Figs. 14 and 15 together, in Fig. 14 the curve marked $r_s/a = 0$ represented the flat front condition, which again appeared as the top curve in Fig. 15. In the latter figure $a_s/a = 1.00$ represented the condition where c_s in Fig. 15 became the same as c in Fig. 14; that was to say, the step-down had become complete and was the same as the termination of the superstructure. At that particular point the value of f_c in Fig. 14 and the value of f_s in Fig. 15 should be exactly the same and should be 1.1. This could only occur in Fig. 14 when c was less than 0.4. Having worked all this out, he took another and much closer look at tests 57-62 and discovered that all these tests had been done with a value of $c_s = 0.4$. But the sketch in Fig. 15 was very misleading, because at c_s it looked as though the length was more like 1.4.

In the conclusions to be drawn from Part I of the paper, it was stated that accurate predictions could be made of the height of the turbulence boundary. This word "accurate" was rather worrying. Elsewhere prediction to within 3 feet on the full scale was claimed, and in yet another place it was stated that an agreement to within 4½ feet between measured and calculated values was good enough for practical purposes. (This was deduced by applying a variation of h of 0.07 in section 1.2.3(5) at the top of page 119 to a ship of 64ft. beam.) Could the authors indicate quite specifically the accuracy this method of estimation was expected to attain, and also state their view on the accuracy that was necessary in such a method to make the use of the turbulence boundary position a really practical feature in the design of funnels and superstructures?

How closely did one need to know the answer? 4½ft. seemed a large range in settling funnel height.

Turning to the use which could be made of the information set out in the paper, one would have thought that the calculation of the boundary height for a wide range of ships would be the most useful next step. An analysis of the relationship between the relative position of funnel efflux and boundary height and the known freedom or otherwise of the ship from smoke trouble, would give a fair indication of whether this method had a future.

Finally, what did the authors consider smuts to consist of, when did they think the smuts were ejected, and why did they occur? His own answer to these questions, which would probably not agree with that of many other people, was that smuts in the main were pieces of soot blown out by the soot-blowers and that generally the only time they were ejected was during soot blowing. That being so, had the authors considered the velocity conditions in the uptake during soot blowing, and if so had they found the enlarged uptake section a feasible arrangement under these soot blowing conditions?

Mr. W. F. STOOT, M.Sc., said that the efficacy of ship models for the purpose of producing an effective design of superstructure so as to prevent the descent of funnel smoke was indeed pertinent, and the authors were to be congratulated on making a substantial contribution to the subject. Of particular interest were the experiments carried out in full-size ships. It was well known that the correlation of model tests with the performances of actual ships was definitely still a subject of controversy. These full-scale tests carried out by the authors were therefore important.

It might be of value if the authors could give some idea of the ship and wind speeds experienced at the time of the experiment. Perhaps he had overlooked this information in the paper, but he did not think so.

With regard to the actual comparison between model and ship, a rational basis would be to use the same Reynolds number for ship and model. This was, however, impracticable due to the high wind velocities involved in the wind tunnel. It was assumed that the view of the authors was that the flow of disturbed air round the model at the low velocities they used in their wind tunnel experiments was of the same pattern as that found at the ship. The smoke trails in the full-scale tests seemed to indicate that this might be true. Any information the authors could give, which had been published, of work done on wind tunnel tests on similar models of different scale would be of great interest.

The empirical formula for working out the height of the turbulent zone was very important, and its success to some extent had been demonstrated. It must be borne in mind that the formula was based on results from highly simplified models, which did not precisely simulate the ship, even assuming that the basis of the correlation between model and ship was correct. However, it appeared from the later tests that this did not matter. He would not suggest that it did not matter, because the height of the turbulent zone was ill defined.

Before the publication of the paper it had been assumed that due to the varieties of superstructures of different complexities the production of an empirical formula would be next to impossible. The authors, however, had refuted this in a most convincing manner.

From the designer's point of view, having estimated the height of this turbulent zone, he had still to ascertain if there were going to be any interaction with the smoke from the funnel—as previous speakers had said—at all angles of incidence of the wind. It would seem necessary to resort to a model test to find an efficient answer to this. The ship could be simulated fairly well in a model test, except possibly for the rigging. By the use of coloured smoke a solution would almost invariably be found. The true importance of the paper could not be assessed until the results of the forthcoming work on funnel interaction were published.

There was one good aspect of the paper in that the

Superstructure Design in Relation to the Descent of Funnel Smoke

designer was supplied with sufficient data to keep his turbulent zone at a minimum. It must not be forgotten, when considering the smoke nuisance, that there is another factor, that for ships travelling at speeds over 25 knots the wind resistance could be considerable. To naval architects and from the engineer's point of view, the zone of turbulence might seem to be a zone of lost energy. From the shipowner's point of view it might be a zone of lost money and the shipowner appeared to be suffering from a surfeit of such difficulties in these days.

Mr. K. F. McGREGOR said that the authors had presented a very interesting paper on superstructure design and the problem of smoke falling on the deck. It had been practically admitted, however, that the design of superstructure could not prevent smuts falling on the deck and it was thought that smuts could be prevented from leaving ships' funnels merely by enlarging a section of the upgoing flue. It was appreciated that an effort had been made to substantiate this by calculation and observation of the terminal velocity of the smuts in question, and that the design of the enlarged section of the flue was probably theoretically correct but in practice would be far from sufficient.

Consider a ship with an oil-fired boiler of approximately 100,000lb. per hr. evaporation. This would produce a gas volume of something like 36,000 c.f.m. at 360 deg. F. For 45ft. per sec. gas velocity the flue would be about 4ft. in diameter, and the diameter of the enlarged section to give 10ft. per sec. would be about 8ft.

Before considering the behaviour of smuts having terminal velocities of about 10ft. per sec. one must be sure that the velocity distribution across the enlarged section was good. In normal measuring and sampling in ducts, a general rule to ensure good distribution was that the measuring point should be about six diameters downstream from the previous change of section or direction, which—if applied to this case—meant that the enlarged section must be at least 6ft. \times 8ft., i.e. 52ft. high, followed by the necessary 12ft. for the settling of the particles. This might be taking things to extremes but certainly 12ft. would not be sufficient for the smuts to settle out. Bad eddies would be formed at the entrance to the enlargement and would make themselves felt a considerable way up. Thus many particles would be carried over in vertical velocity components of the eddy currents greater than 10ft. per sec.

As to the amount of soot to be dealt with, the probable emission might be of the order of one ton per day. Using an enlarged section or separating chamber, as suggested, a fog of smuts and soot would build up in the chamber and means would have to be found to extract it. The arrangement as it was might stop some of the smuts temporarily but would not catch them and permit disposal.

It was necessary to make provision not only to arrest the particles but to collect them. This could be done fairly simply by passing the upgoing gases through a vane ring, so that the particles would be thrown to the wall of the chamber. The chamber could also be enlarged to reduce the upgoing velocity and the centrifugal forces would push the particles and smuts

out to the side. These could be skimmed off the wall of the body through a vertical slot and immediately passed tangentially into a small cyclone collector integral with the main body. In this cyclone the dust, now spinning in the opposite hand, would slide down the walls and be collected in a suitable hopper for disposal. The secondary gas carried over with the dust would be discharged through the top of the cyclone and passed back to the main gas stream. For the conditions under consideration, the pressure drop across the collector would be about 1.7in. w.g.

The enlargement suggested was about 9ft. in diameter and 12ft. high. For the type of collector now considered, the main body would be about 7ft. in diameter with an integral secondary cyclone of 27in. diameter with overall height of about 10ft. Fig. 27 showed the two arrangements to the same scale.

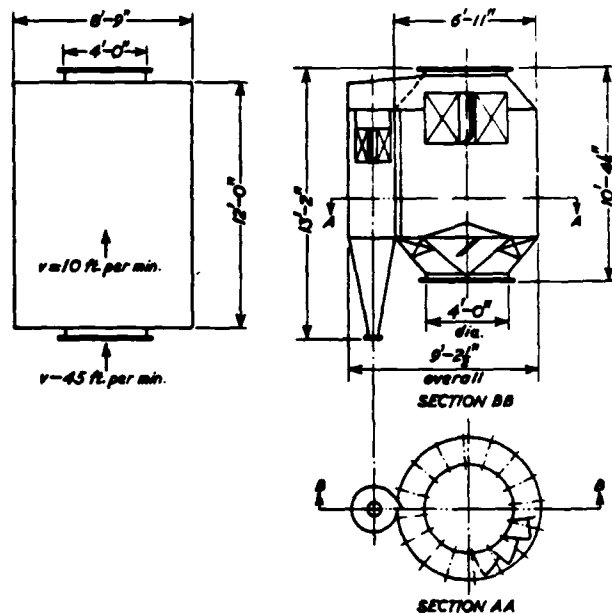


FIG. 27

This type of collector would most certainly catch the smuts and some of the finer particles which formed smuts, but not all of them. Some of the small fine particles that passed the collector and were not caught would settle on any cooler surfaces between the collector outlet and funnel discharge, forming more smuts. These would eventually be blown off and come down on deck. The ducting between the collector outlet and the funnel outlet must therefore be kept to a minimum.

Another way was to improve the collector efficiency for the very fine smut-forming particles. This, however, was a difficult and expensive thing to do.

Correspondence

Mr. R. W. CHOMARTY (Vice-President) thought the authors did well to emphasize early in the paper the difference between smoke and what they called "smuts".

Smoke had only comparatively recently become a problem, chiefly due to superstructure design, and in modern steamers to the low exit velocity of their boiler products of combustion. One new oil burning steamer in the London Docks was seen to have the smoke actually spilling over the edge of the funnel down to the deck. What a contrast to the natural draught coal burning steamer! The older members of the Institute

would recall these "old timers" with their smoke belching proudly upwards and well clear of the ship. In the Indian Ocean in calm weather the smoke plume could be seen floating well up in the sky and stretching for many miles—not the same colour, of course, but not unlike the vapour trail frequently seen in the sky today from aeroplanes.

The early Diesel engine, too, gave few smoke problems but it did have its "smut" problem. Just like a house chimney which was not kept swept, the accumulations of carbon in the exhaust system would fire or break away and suddenly shower

Discussion

out of the funnel. This problem came very much to the fore during the war years, aggravated by the necessity for fast Diesel-engined ships to keep station in slow convoys. Before other measures were evolved, convoy commodores permitted such ships in daylight hours to break convoy and race around at full power to burn up oil and blow out the loose carbon from their exhaust systems. If they did not, the risk was that a "chimney" would suddenly "catch alight" during the night and produce an enormous "Roman candle", advertising far and wide to any lurking submarine the exact whereabouts of the convoy.

This danger was overcome in his Company's ships by removing the cast iron nozzle at the top of the silencers, thus reducing the exit velocity, and fitting over this exit an inverted cone against which the red hot cokes impinged and were deflected down into the funnel top. A water spray was fitted to quench these red hot cokes and by washing them away prevented the accumulation of a destructive red hot mass of carbon. Those who had raked on to a stokehold floor plate ashes from a coal-fired boiler or carbon from the back ends of an oil-fired boiler would fully appreciate the problem. The quantity of cokes and smuts that did accumulate on the funnel top was most surprising.

Figs. 28 and 29 showed the arrangement described. The

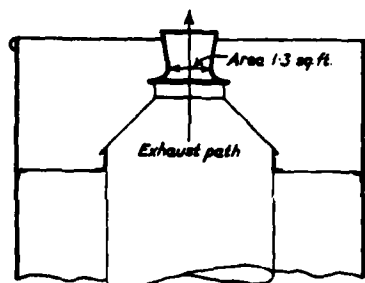


FIG. 28

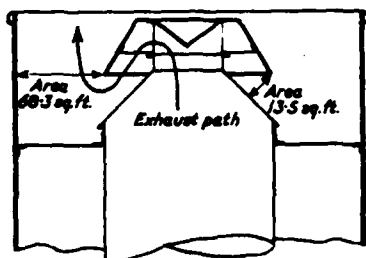


FIG. 29

dimensions of the inverted cone were restricted, of course, by the existing funnel top but it was generally found possible to arrange the exit area to be not less than ten times the exit area at the top of the silencers. This improvised solution of an urgent war problem compared well with the more scientific approach of Part III and Appendix 3 of this paper. Smuts of $\frac{1}{2}$ in. diameter mentioned in Appendix 3 must be rare phenomena and recalled the early days of Diesel engines when a chief engineer, tired of the incessant nagging of a captain to stop cokes and smuts falling on his beautiful holystoned tank decks and well scrubbed white canvas awnings, made up a large number of cheese balls (up to 2 in. diameter) soaked them in purifier dirt and one dark night scattered them over the deck. The next morning the amazed captain collected them all up in tins which he duly presented to his owners, who passed them on to the engine builders who at the time were his (Mr. Cromarty's) employers. Like the captain they were amazed to see such huge cokes (or smuts) for they had apparently come out of a silencer in which the baffles were perforated plates of $\frac{1}{2}$ in. diameter.

As the authors kindly mentioned in their acknowledgements, his Company had willingly, but in a small way, cooperated in the investigations which gave the Institute this most informative and helpful paper. Some ten years ago his Company's directors decided that the time had arrived to break away from the traditional profile of their ships. The profile had altered little from that of their coal-burning steamers. Improvements in crew accommodation and in the amenities provided required for many reasons that everyone be housed amidships. To maintain the cargo carrying capacity, no crew space could be allowed below the weather deck and so eventually the profile shown in Fig. 21(b) in the paper was evolved. The traditional profile had been not unlike that shown in Fig. 21(a) except that instead of the continuous amidships house shown there was a bridge house (accommodating the navigating officers and twelve passengers) and a separate amidships house (accommodating the engineer officers and stewards), separated by a cargo hatch on the weather deck; the crew were forward on the forecabin with the petty officers aft in the poop.

Examining these two profiles (Figs. 21(a) and 21(b)) it would be seen that whilst the funnel heights above the water levels were much the same, the funnel of Fig. 21(b) appeared by comparison to be hemmed in by the superstructure. The funnel of Fig. 21(a) on the other hand stuck up well into the air like the spouts on the top of some recent ships. But it would be noticed that by careful design the turbulence boundary height was practically the same and in service the streamlined superstructure ships had given no smoke problem. Which was precisely as was anticipated, the owners and the builders having taken advantage of the offer by Thermotank, Ltd., to test a model in their wind tunnel before finalizing the new profile.

Also, as the main engines and auxiliaries were Diesels, the smoke exit velocities at the funnel top were such as to clear the turbulence boundary. The silencers were designed to collect coke and smuts. When an oil-fired donkey boiler was in use, the smoke tended to "hang" to the top after end of the funnel and "roll" aft just under the line of the turbulence boundary, gradually falling to, but rarely reaching, the poop deck.

Prior to and since the above wind tunnel test the systematic tests, as detailed in the paper, had been carried out, from which a most useful method had been evolved by the authors for estimating the height of the turbulence boundary and also from which the advantages of streamlining were clearly proved.

The authors were to be congratulated on this lucid exposition of their researches and their thanks were due to their Principals for their permission to the authors to make these researches available to the Institute.

MR. M. HARPER (Member) thought the authors were to be congratulated on a very instructive and valuable paper which should lead to a more precise determination of funnel heights and so avoid the sooting of the upper decks of vessels which, in the case of passenger liners, could be most objectionable and possibly react unfavourably on the popularity of the vessel.

The decision to divide the subject into two parts was commendable for this was exactly the manner in which the problem confronted naval architects and machinery designers, with the addition, of course, of ensuring good combustion.

The close agreement of the calculated turbulent zone and the full scale results was very encouraging, although it was noted as being dependent on the superstructure lines being accurately known at an early stage of the design. However, with the clearance of the stream of funnel gas over the after portion of the vessel, there emerged the second part of the problem, that of the prevention of emission of smuts from the funnel and subsequent fall-out from the gas trail.

Mr. Harper had had some little experience of this trouble and believed that the authors' scheme of a zone of low velocity before final exit satisfactorily cured the trouble.

Superstructure Design in Relation to the Descent of Funnel Smoke

In several cases with which he was familiar soot nuisance was avoided by maintaining an area of the uptake from the economizer top to the base of the funnel so that the gas velocity was of the order of 18ft. per sec., the length of this uptake portion being 40ft. Inside the funnel the uptake area was reduced to give a gas velocity of 100ft. per sec. with the object of giving effective discharge to the funnel gases.

With reference to the authors' "Conclusions from Part III", on page 126, perhaps they would care to comment on the effect of increasing the gas velocity after leaving the expansion in the uptake, as this was necessary on some vessels due to restrictions imposed by the area through the funnel. Would the calculated height of the expansion in uptake be affected by an increase in gas velocity after the expansion?

MR. K. F. MCGREGOR, in a further contribution, wrote that it appeared that Mr. Ower believed that the turbulence in the enlarged section of the upgoing flue would not be so serious as to upset the prevention of emission of smuts whose terminal velocity was that of the mean vertical velocity in the enlarged section.

This was contrary to practical experience, as the following typical examples confirmed:

- (a) A paper entitled "The Collection of Representative Flue Dust Samples"* dealt, *inter alia*, with velocity gradients after a restriction.

In this paper plots were made showing the velocity distribution at a quarter area orifice restriction and at one, two, four and six diameters downstream from it. After one diameter, the maximum and minimum velocities were measured to be 20ft./sec. to over 40ft./sec. for a mean duct velocity of 30ft./sec. At six diameters downstream the maximum and minimum were about 25 and 35ft./sec. It was seen, therefore, that even after six diameters the maximum velocity was 16 per cent in excess of the mean. It should be noted that these measurements were made in a 10-in. square duct at laboratory temperatures: thus there was no thermal disturbance.

In the case of the vertical flue there would be thermal disturbance due to cooling at the walls and changes in boiler load, which would also alter the volume flowing and hence the mean velocity.

A further effect causing turbulence in the flue would be the chimney or funnel effect due to cross winds over the funnel outlet.

- (b) Tests recently conducted by the writer in a small horizontal settling chamber with very low gas velocities down to about 3ft./sec. showed that only 30 per cent of the particles which should theoretically fall out, in fact did so.

There was no doubt that the enlarged section, as suggested in the paper, would be of little use in the prevention of smut emission.

MR. W. MCARTHUR MORISON, C.B.E., found that the paper presented the result of a most interesting investigation into this problem and in a simple geometric way which should be of great assistance when scheming a layout of the superstructure and casings. For a ship with machinery amidship it appeared to cover all possible combinations of deck houses, bridge, etc.

The writer had not experienced any trouble from such types, possibly because the layout included a funnel which was sufficiently high to carry the smoke well above the turbulent zone, but on two vessels with turbine machinery aft, for which wind tunnel tests were available, an application of this method showed a close approximation in the wind ahead and astern conditions to those in the tunnel, and in service.

While it was not part of these experiments to check the conditions with a funnel in position, it was interesting to note

the effect in the above two tests of relatively small alterations. With the outer funnel of full height and the inner funnel well aft and extending about one foot above the top, there was a distinct tendency for the smoke to be drawn down at least to half its height in the eddy. By reducing the height of the outer funnel sufficiently to leave space inside for the necessary fittings and leaving the inner funnel protruding at centre to the original height, this tendency was eliminated, as was also any fouling at angles of yaw up to 30 degrees.

This method might not meet with approval in all cases but after all it was economical and followed domestic practice over the centuries.

MR. C. F. MORRIS considered that the paper provided information which could be used to produce answers good enough for a ship having simple forms of superstructure but for large passenger liners having complex shapes, including wells in the decks, the wind tunnel was the only way to approach the problem.

The effect of yaw, mentioned on page 117, was shown in almost every case to be at its worst at approximately 20 degrees in the case of a large passenger liner model tested recently.

MR. F. K. WYNN (Member) wrote that the method suggested of preventing the emission of smuts in funnel smoke had been put into practice successfully by the writer in two land installations of oil fired boilers.

It was the writer's experience that attention to combustion in the furnace would not solve the problem. In fact, after many months' experimenting with burners, air directors and furnace fronts, smut emission was observed during combustion trials in which a very high standard of combustion was maintained.

In any case burners, air directors and quarls deteriorated in service, and with the human element involved it was virtually impossible to maintain ideal combustion at all times, so that sooner or later soot was produced.

An attempt to produce smut deliberately by bad combustion, obtained by lowering the oil temperature and restricting the air supply, failed completely.

Fuel oil contained matter, non-combustible in the conditions obtained in the normal boiler furnace, varying between 0.185 per cent and 0.36 per cent of its weight. Assuming that the fuel used contained no more than 0.2 per cent of this matter, a burner consuming fuel at the rate of 500lb. per hr. would produce 24lb. of soot or dust per day.

If in practice 10 per cent of this was deposited in the tubes or adhered to brickwork, etc., 90 per cent, or approximately 21½lb. per day, would be emitted in the funnel gases as dust, but this was also potential smut.

The writer concluded, therefore, that all attempts to eliminate smut by attention to combustion were doomed to failure.

The theory that low acid dewpoint of the oil flue gases caused moisture condensation on the internal surface of the stack to which soot adhered was also suspect; the surface temperature of the stack was measured on a wet and windy day and found to be little above the ambient temperature, and yet no smuts appeared, nor could be produced by deliberately causing smoke for several hours.

Additives failed to produce any improvement, and a three months' run on 200 seconds viscosity oil also failed.

The writer suggested that smut was produced in the flues, uptakes and funnel in a similar manner to the phenomenon which took place in a ventilation system in which no filters were fitted. Fine dust adhered and built up on the walls of the duct and gave no trouble for years; it then paid off suddenly and was discharged into the ventilated space in lumps. Something similar could take place in the uptakes and funnel; some of the fine dust in the flue gas deposited on suitable surfaces and built up until its bulk overcame the initial surface attraction, when it peeled off and was emitted as smut.

* Fitton, A., and Saylor, C. P. "Engineering", 22nd and 29th February 1932.

Discussion

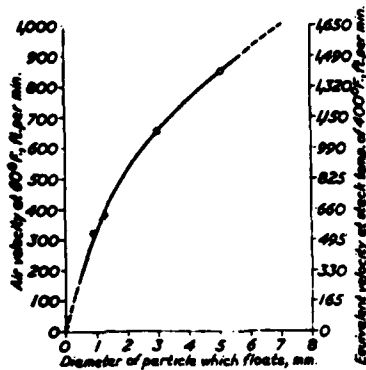


FIG. 30

To catch the smut before it could be emitted, arresters of the type used for grit emission were tried. Whilst these intercepted particles which were obviously produced by imperfect combustion, the dust of which smut was composed passed by and smut emission continued.

If the hypothesis of dust in the flue gas adhering to surfaces and peeling off to form smut were accepted, it became obvious that no surface above the arrester, upon which the dust could deposit, was permissible.

A model transparent chimney was attached to a fan, the speed of which could be adjusted to give a range of velocities of air in the model chimney. Smuts of various sizes were then introduced and the velocity adjusted until the smut floated in the air stream without being emitted.

The results were plotted in Fig. 30.

The size of smut which could be tolerated when emitted must be decided and the arrester designed accordingly.

A chimney, of course, could be built of sufficient diameter for its full height; this, however, would be expensive.

If the chimney were suddenly enlarged, a considerable length of the enlarged portion performed the function of a diffuser. This could be achieved more economically by tapering the stack and finally distributing the gases over the full area by a baffle.

A baffle was also advisable to check the puff of gas which occurred when a burner was lit or failed to light for an instant, and then lit with a small explosion producing a puff which would cause an emission of smut if not checked.

In the successful installation, a whirl of smut could be seen near the top of the chimney. The portion performing

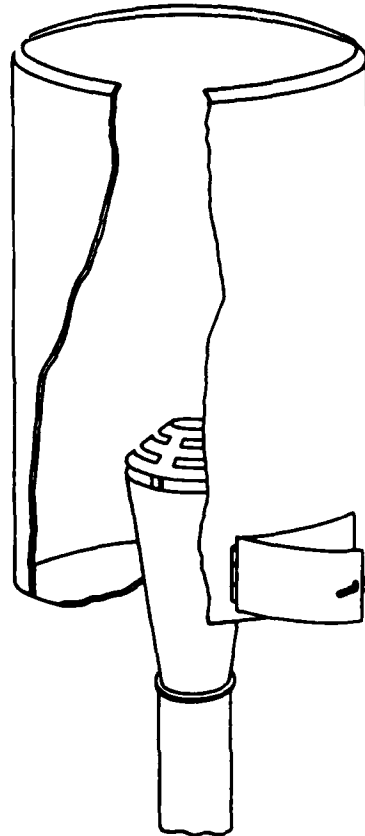


FIG. 31

the function of arresting the smut was therefore deduced to be 7ft. long if the gases diverged at the natural angle of spread of a gas stream of 5 degrees.

The quantity of soot collected was of the order of 1lb. per 600lb. of fuel burnt. This soot was too fine to slide down a shoot into a hopper but was easily removed periodically by suction through a flexible hose, as practiced by the domestic chimney sweep.

Fig. 31 showed the arrangement of arrester described.

Authors' Replies

Dr. THIRD said that he would leave Mr. Ower to deal with the points raised with regard to smuts. Before replying to the individual contributions, he said that many of them, as Mr. Burge himself had admitted, had criticized the paper for not dealing with the problem of funnel shape. The title of the paper made it quite clear that it dealt only with superstructure design in relation to the descent of funnel smoke, and that the effect of funnel shape and design was not included. Moreover, reference to this effect was made in the introductory remarks to the paper, in which it was stated that the investigation of funnel effects which was necessary to complete the research was still in progress. It was not therefore fair criticism to reproach the authors for omitting this information. They had considered holding back the present paper until the whole research had been completed, but that would have resulted probably in a delay of a year or more and certainly in a paper of almost indigestible size.

The authors were much indebted to Mr. Campbell for his co-operation in the full-scale investigations and for the account of his experience on the performance of funnels under various conditions in practice. It was quite true to say that there was no problem if the funnel were made high enough.

In his very useful contribution Mr. Burge laid great stress on the importance of studying conditions with relative winds around 20 degrees off the bow. This vital aspect of the problem had not been lost sight of by the authors; but it was more particularly a funnel problem, and was receiving close attention in the investigation on funnel design which was now in progress.

The authors had knowledge of many ships, mainly of the larger cargo carrying and tanker classes, which gave trouble in head winds. It would not be difficult to imagine trouble arising with the orthodox form having a funnel amidships and a raised poop deck, but it was rather surprising when many complaints arose with tankers. Although their funnels were only a few dozen feet from the stern, it was not uncommon for the gases to sweep down on to the decks and actually penetrate forward of the funnel, due to their not clearing the turbulent zone. Elimination of these headwind conditions was the primary concern on many such vessels.

When the relative wind moved round off the bow, the plume had a rapidly shortening length of deck to pass over, but any advantage from this could be lost when the angle reached the critical for flow round the funnel casing, which was usually around 20 degrees. This could be important, particularly for the larger passenger vessels, and was receiving attention in the investigation on funnel design, for, as Mr. Burge pointed out, the major effects in yaw were due to the funnel itself.

In the comparison between model and full-scale turbulent zones, Mr. Burge said that downwind of the funnel one might expect the path on the full-scale ship to be slightly higher than on the model, due to buoyancy arising from heated surfaces, funnel gases, etc. In so far as the latter were concerned, unless they were actually drawn down into the turbulent zone, they should have very little effect on the height of the boundary, and even when the other factors had been taken into consideration, the effect should be on the whole very slight, in the opinion of the authors.

Mr. McClimont drew attention to the importance of considering the maximum height of the turbulent zone rather than its height at the location of the funnel. On page 110 of the paper, under heading 1.1.3, it was stated that observations were made of this maximum height h , and these were the values used in the investigation. It was quite true that if the funnel was aft of the highest level of the zone, there was no need to take this level into consideration, but a study of typical ship profiles made it clear that the funnel was rarely in the position where the boundary was appreciably below the maximum. A rather special case was the tanker with midships bridge, having its funnel 250ft. or more abaft this source of turbulence. However, tests carried out in the wind tunnel since the paper was prepared indicated that the turbulence had lost most of its activity after traversing this distance in any case, and it had therefore no great influence on the smoke plume. Under these circumstances, calculations should be based on the turbulent zone originating at the after superstructure front, which was of course quite close to the funnel.

On the subject of wind speed in the tunnel, a preliminary investigation was carried out, covering a range of speeds, all of course well below the critical Reynolds number. No difference in the form of the turbulent zone was noted, and it was then decided to work at a low tunnel speed, for this resulted in a greater concentration of H₂S in the jet, with more prominent stains on the rods. The more important issue concerning the flow pattern at velocities above and below the critical Reynolds number had been dealt with fully in Part II of the paper.

The distance from the forepeak to the bridge front was kept at 2.1 times the beam—a typical value—throughout the tests, since the pattern of the turbulent zone was much the same whether the blocks were mounted on the model hull or direct upon the tunnel floor, thus proving that the presence of the hull had no great influence under head wind conditions. But it was still important to establish a level from which the effective height of superstructure had to be measured, hence the necessity to derive formulae to make allowance for sheer and forecastle.

Fig. 15 was included only as a guide to the possible effects of an intermediate step-down. When it was realized how important could be the effect of reducing the superstructure length with the front rounded in elevation (Fig. 14), a few tests were carried out to find how the multiplying factor varied with the extent of the step, particularly at a relatively small value of c , which was known to give a high turbulence boundary in the limiting condition of $a/a = 1$. It was noted that with an increase in this ratio from 0 to 1 the value of f , rose steadily to about four times its original height for a degree of rounding $r/a = 0.5$. As c was increased, the range in the value of f , decreased, since its value at the lower limit when $a/a = 0$ remained unchanged and equal to the value for the full superstructure of length c , whereas at the upper limit when $a/a = 1$, the value fell in accordance with the trend of the curves in Fig. 14 for varying superstructure length. In the limit, as the step approached the aft end of the superstructure, the value of f , became unaffected by varying a/a . Just as the factor f , for superstructure length included the allowance for rounding in elevation, so did the f , factor.

Authors' Replies

Mr. McClimont referred to the degree of accuracy claimed in making predictions of the height of the turbulence boundary. It did not seem to Dr. Third a bad result to get this order of agreement from the application to real ships of a generalized formula based on the results of comparatively few tests on simplified models, particularly in view of the ease and speed with which the calculations could be made. Moreover, as was stated under heading 2.2.2 on page 123, the change from smooth flow to strong turbulence took place not at any sharply defined line, but over a transition zone. With this in mind the authors were of the opinion that it would hardly be possible to get agreement within, say, 3 or 4 ft. even with the most accurate observations. For this and other reasons a margin should be allowed in the design of the funnel.

Dr. Third appreciated Mr. Stoot's remarks on the correlation of model tests with the performance of full-scale ships. He had no knowledge of similar wind tunnel tests carried out on superstructure models at greatly different Reynolds numbers. In the introduction to the paper, the disparity in scale and speed between model and full-scale conditions was discussed. Although reasons were there given for believing that any effects due to this cause would be small, it had been decided to include direct comparisons between model and full-scale results in order to confirm this assumption once for all and thus to establish the applicability of the model tests to full-scale conditions.

He agreed that the empirical method of estimating the height of the turbulent zone was based on the results of tests with highly simplified models. But he would remind Mr. Stoot that the method had been checked by the authors on three ships of widely different shape, both in the wind tunnel and on the full-scale, and in all cases the method gave results very close to those actually observed. Mr. Morison, in his written contribution, referred to two similar cases of agreement. It was realized from the start that the bridge front played a prominent part in creating turbulent flow conditions, hence the reason for concentrating to a large extent on the variables associated with this part of the superstructure. Fortunately, most of the other sizable obstructions on the deck of a ship, such as lifeboats, were so positioned that they had no appreciable effect on the turbulent zone, except possibly in relative winds well round on the beam, so they could be omitted from the models under test.

A very interesting point relating to the wind resistance of superstructures was raised. There was no doubt that the extent of the turbulent zone was some measure of the energy lost from this source, so that a designer could be effecting a worth while economy in this direction at the same time as he was improving the smoke conditions. However, on high speed passenger ships the designer was obliged to give careful study to another aspect of the problem—that of the wind speed over the decks themselves. If it were possible to go to the extreme by eliminating the turbulent zone entirely, the decks would become untenable. A compromise would appear to combine an overall scheme of streamlining with the judicious placing of wells and shelters.

The authors were indebted to Mr. Cromarty for the interest he had taken in the investigations leading up to the paper, and for his very willing co-operation. His account of the development of the modern profile as exemplified in Fig. 21(b) was very interesting indeed. It showed clearly that with a short funnel the gases could be made to clear the turbulent zone with careful attention to the design of the superstructure. This aspect had obviously not been considered in the case of many other modern ship profiles.

The authors were pleased to learn from Mr. Harper that he considered the division of the subject into two parts was the right way to tackle the problem.

Mr. Morison's remarks were very encouraging to the authors. He mentioned the close approximation which he found between the formulae and full-scale experience, which supported the findings of the authors in the similar comparisons they had made and reported in the paper. The influence of relatively small obstructions at the funnel top, having

as their purpose a reduction in the disturbance created by the outer casing, could be quite striking. In borderline cases a minor modification of this nature might be sufficient to carry the plume clear of the turbulent zone and show an improvement seemingly out of all proportion to the alteration itself.

Mr. Morris had commented on the difficulties in the way of applying a formula to certain large passenger liners with complex shapes. The authors believed that the method they had proposed could be used to give reasonably close predictions even for such ships; and they would like to have drawings of one or two, for which wind tunnel results were available, so that they could compare these results with those predicted by their method. It might be necessary, however, to carry out model tests to study wind conditions over the various decks from the standpoint of comfort or habitability. In that case, very little extra work would be needed to define the turbulence boundary as well.

Mr. Ower replied to the various points raised in connection with smuts. He emphasized that, as stated in the paper, the idea of an expansion in the uptake in which the smuts could fall out had not been originated by the authors but by the superintendent engineer of one of the shipping lines. All that had been done in the paper was to investigate the proposal on a theoretical basis to see whether it looked possible, and the results suggested that it did. He agreed with Mr. Campbell that a swirling action would probably be more effective; in fact, it formed the basis of certain devices in use. He was glad that Mr. Campbell had stated categorically that the best way to prevent smuts from landing on deck was to eliminate them at the source. He (Mr. Ower) had been of this opinion from the outset, but the reception he had had when he once voiced it to a marine engineer had prevented him from ever repeating it. It was encouraging to find support from a marine engineer of Mr. Campbell's standing.

The suggestion of the expansion had received both adverse and favourable comment. The only convincing way of settling a matter of this kind was to put it to the test and Mr. Ower therefore derived some satisfaction from the fact that the favourable views, namely those of Mr. Cromarty, Mr. Harper and Mr. Wynn, were founded on practical full-scale evidence that the method would work, whereas the criticism of Mr. Burge and the stronger views of Mr. McGregor were the expressions of personal opinions. Mr. Burge's criticism was confined to the belief that the heights of the expansion required would be greater than those given in Fig. 23. This might be so to some extent, but Mr. Wynn's contribution suggested that the heights would not be seriously under-estimated by the calculations. Although Mr. Wynn had not quoted any dimensions for the installations he had fitted, it appeared unlikely that he would have regarded the scheme favourably if these were impracticably large. A vertical height of 40 ft. was mentioned by Mr. Cromarty, but he had allowed a gas speed of 18 ft. per sec. in the expanded section whereas the heights suggested in the paper were based on a speed of 10 ft. per sec. Without further knowledge of speeds and dimensions, it was not possible to compare Mr. Cromarty's figures with the calculations. But it was significant that Mr. Cromarty was referring to shipboard installations, so again there could be no question of excessive sizes.

Mr. McGregor's statement in his written contribution that there was "no doubt that the enlarged section. . . would be of little use" was thus directly at variance with the experience of Mr. Cromarty, Mr. Harper and Mr. Wynn. Mr. Ower was content to rest his case on the views of these three gentlemen, which were based on established fact and not merely on prognostication. He would add only that he disputed some of Mr. McGregor's arguments and questioned the relevance of the experimental results with the orifices adduced by Mr. McGregor to support them. The conditions of these small-scale tests differed in at least one fundamental particular from those that would exist in the expanded section.

Mr. Ower could not answer Mr. McClimont's question about the origin of smuts, but he could say quite categorically

Superstructure Design in Relation to the Descent of Funnel Smoke

from his own experience that they were *not* ejected only during soot blowing.

Mr. Harper had asked about the possible effect of increasing the gas velocity after leaving the expanded section. Mr. Ower said that a relatively high velocity at the final exit from the funnel was a necessary feature of many funnel designs and added that the calculated height of the expanded section would not be affected in any way by a restriction in area following this section.

Finally, Mr. Ower said he would like to comment briefly on the controversial subject of scale effect and in particular on the questions asked by Mr. Stoot. In the first place, there still seemed to be some doubt whether the results obtained on a small model in the wind tunnel really reproduced what happened on the full-scale ship. To this he would say that the full-scale checks described in the paper should dispel such doubts in the future. Moreover, and to this Dr. Third with his great experience of model tests would agree, *ad hoc* smoke investigations had been carried out in wind tunnels for many years past on models of about the size of those used in this paper and tested at similar speeds. All the evidence was that the results deduced from such tests are borne out on the full-scale. Dr. Third confirmed that he had never known of a case where the full-scale behaviour refuted the model results. The

authors therefore had no hesitation in affirming their conviction that the air flow patterns for the wind tunnel tests and for the full-scale ships themselves are substantially the same for broad, overall effects of the kind investigated in this research.

Mr. Stoot had also asked whether tests had been carried out over a range of speeds in the wind tunnel to see whether the results at all speeds were the same. As a matter of fact they had, but if one accepted the fact that the full-scale checks that had been carried out had been done at a Reynolds number some 200 or more times that of the wind tunnel tests, one had to accept also that it was futile to carry out tests over a range of speeds in the tunnel in which the range of Reynolds number that could be covered, bearing in mind the various practical limiting factors, was probably not more than 5. Why bother about a factor of 5 when one had to extrapolate to 200 or more? Mr. Stoot also asked about the speed at which the full-scale tests were carried out. On Ship A all the tests had been made at a ship speed of about 20 knots in conditions ranging from calm to a head wind of about 20 knots. The speeds for ships B and C were rather less. All the work had been carried out so far from land that it was most unlikely that any of the effects mentioned by Mr. Burge in this context would be significant.

Superstructure Design in Relation to the Descent of Funnel Smoke

Test number	a	c	h		Superstructure form
65	0.4	1.8	0.45	$b_1=0.375$	
66	0.4	1.8	0.53	$b_1=0.50$	
67	0.4	1.8	0.58	$b_1=0.75$	
68	0.4	1.8	0.27		
69	0.4	1.8	0.18		
70	0.4	1.8	0.29		
71	0.4	1.8	0.17		
72	0.4	1.8	0.46		
73	0.4	1.8	0.48		
74	0.3	1.8	0.42	With wings	
75	0.3	1.8	0.36	Without wings	

APPENDIX B
MILITARY AIR OPERATIONS

B-1

APPENDIX B

MILITARY AIR OPERATIONS

Three air flow situations have particularly detrimental effects on helicopter and V/STOL operations. These situations are turbulence, vortex formation and the stack gas plume. The effects of these factors are discussed below.

1) Turbulence and vortices - Turbulent air flow presents a danger to pilots when the helicopter enters a turbulent region and experiences a sudden loss of lift. Most modern helicopters are neutrally or negatively stable, and are therefore fitted with automatic stabilization equipment (ASE). However, even ASE does not fully correct the problem of transient forces as the helicopter approaches a ship landing. Under such circumstances yaw maneuvers may require sudden increases in power that exceed the capabilities of the tail rotor. This situation is so critical that the amount of control available to a pilot is often considered in terms of helicopter power limitations. The critical nature of the power available for yaw maneuvers is the result of the tail rotor operating close to blade stall conditions. One can readily see that no matter how responsive a stabilization system may be, its effectiveness can only be measured in terms of the ability of a helicopter to respond to automatic control.

2) Stack Gas Plume - Often the stack plume close to a combatant ship is surrounded by turbulent flow and the plume itself is turbulent. The plume is especially dangerous because it is highly heated and has a compound detrimental effect on helicopter flight. First the hot exhaust gases decrease aerodynamic lift generated by the blades, thereby reducing both hover capability and yaw maneuverability. Secondly, the hot gases reduce the thermodynamic efficiency of the helicopter's motive gas turbine. Although the plume does not always present these dangers it can not be completely avoided in ship operations. The senior engineer of the helo class desk at NAVAIR has stated that a hot air plume with an average temperature at 140° can be "lived with" [18].

B-1

Turbulence, vortices and stack gas plumes separately or in combination present serious threats to helicopter operations from a ship but in addition many other factors which can be controlled only partially, if at all, further compound the problem. Perhaps the most serious situation the pilot faces is landing his helicopter on the deck of a ship moving in a seaway. Often the landing area is not large, cross winds are high and ship motions (primarily roll, pitch and heave) are significant. For these reasons a pilot will establish a hover immediately over the landing area so that he may assess relative motion between himself and the ship prior to touch down. This time interval, between the beginning of the hover and when the helicopter is down with the blades no longer producing significant lift, is perhaps the most critical phase of landing. Conversely, the most critical phase of take-off occurs as the helicopter lifts off the deck and rises to a height sufficient to clear the ship. While landing it is possible for the ASE to attempt to counter ships roll once the helicopter has made contact. This action can flip a helicopter over. It is therefore important for a pilot to deactivate the ASE the instant he makes contact and at the same time to manually reduce the blade pitch to a minimum.

Air operations will continually evolve as helicopters, ships and procedures are improved. Therefore the requirements for air operations can not be listed in this manual without warning the designer that these requirements will change. The only prudent instruction that can be made is by way of examples that demonstrate only the general nature of the design problems involved. When presented with a new ship class, it is the designer's responsibility to determine what effects air operations will have on the design and to combine these limitations with all of the design criteria.

SCS - The Sea Control Ship was to be designed with two locations for helicopter operations and one location for V/STOL. Model testing demonstrated the landing areas to be free from turbulence or vortex centers as long as the relative wind was from 010° clockwise to 350° (360° = 000° = head winds). However, since the plume flows with the relative wind, operations should be limited to relative wind yaw angles from 010° clockwise to 170°. Relative wind from 010° clockwise to 090° would be dangerous aft of the island while winds from 090° to 170° would be dangerous forward of the island. In this manner the safe yaw angles for various operations were determined. A study was also made to reduce turbulent wake from ship structure adjacent to areas where air operations were conducted [17].

AO177 - The "AO177 Air Flow Report" [18] contains design information about VERTREP operations. The AO has a "T-line" marked on the deck behind which the helicopter will remain during VERTREP.

During normal hovering for sling attachment to the helicopter hook, the rotor blades will be approximately 20 feet above the deck (This height includes 5 to 8 feet from deck to the hook plus an additional 12 feet to the rotor blades.) subsequent to an approach and steady hover. The blades will be 30 to 40 feet above the deck at load lift off which places the intakes 34 feet above the deck. The height of the blades will increase while under full power to 50 feet when the load will clear the ship's side. Normally the approach for VERTREP is downwind when flying empty and into the wind for loaded conditions to provide maximum lift. However, the approach can be made at any angle aft of the T-line. To allow consideration of various approach angles, the exhaust plume gas trajectory and temperatures were evaluated at several relative wind angles making the following assumptions.

1. The ship speed is 20 knots. The wind velocity will be 60 knots relative to the deck at 0° relative wind angle. This angle was chosen because it given the shortest distance of plume travel to the hovering area and therefore, the highest plume temperature.

2. The steam power plant will be operating at cruise power level.

3. Ambient temperature was assumed to be 100°F.

It was found that the center of the plume was about 90 feet above the hover point and that the temperature at the maximum hover height would be approximately ambient. Therefore the AO should present no problems for VERTREP operations.

APPENDIX C

HEAT SENSITIVITY OF TYPICAL MILITARY ANTENNAE COMPONENTS

I. INTRODUCTION

Work covered by this report was performed for NAVSEC Code 6179A.04 under Modification P00009 of Contract N00024-70-C-1127 (Consolidation and Integration of Antennas into the Sea Control Ship Hull Structure).

It is the purpose of the investigation covered by this report to determine the effects of elevated ambient temperatures on mast mounted equipments and to define if possible the maximum allowed temperature limits for the following specific items:

- o Coaxial Cable
 - RG-214, 218, 333, 1-5/8" foam dielectric
- o Waveguide
- o RADAR
 - AN/SPS-40, 52, 55
- o TACSATCOM
- o AN/SRA-17
- o AN/SRA-43
- o URD-4
- o URN-3
- o AS-571, 616, 899, 1174, 1175
- o Wire Rope (for antennas)
- o Antenna Insulators

Stack gas exit temperatures on the gas turbine-powered Sea Control Ship were expected to be much higher than those experienced on the majority of U.S. Naval ships. It is evident that, with the single-island configuration considered for the Sea Control Ship, mast and yard-mounted equipments may be subjected to increased environmental stress.

A determination of the expected ambient temperatures due to stack emissions is the subject of a separate investigation by others.

2. APPROACH

2.1 Lower Bound

The items to be considered are, in general, designed and fabricated by the lowest bidder to meet requirements of MIL-E-16400, Electronic, Interior Communication and Navigation Equipment, Naval Ship and Shore:

- Non-operating, -62 to +75°C
- Operating, -28 to +65°C

Thus, an ambient temperature of +65°C may be taken as a lower bound. Whether or not an item of equipment will withstand higher ambient temperatures depends upon a number of factors, including the design margin applied to the weakest link within the item.

2.2 Upper Bound

The upper bound for passive devices (those that dissipate no power) is obviously determined by the maximum service temperature of some critical material or component within the device.

For active devices (those that dissipate power,) the upper bound must be reduced to allow the required power dissipation to take place without exceeding the maximum service temperature of the weakest link.

As a practical matter, since both corrosion and failure rate due to thermal stress factors tend to increase exponentially with temperature, it will be necessary to operate at ambient temperatures considerably below the upper bound.

the failure rates are asymptotic. They illustrate that reduction in temperature at any range down to about 20°C is reflected by significantly lower failure rates."

The following detailed analyses of specific items shows the procedure and rationale for determining recommended maximum allowed ambient temperatures given in Table 2. In some cases, the procedure can be firmly supported by published data. Most, however, require application of judgement to incomplete data or extrapolation from similar items.

5.1 Maximum Recommended Long-Term Ambient Temperature

Values recommended for specific items in Table 2 are the lower of:

(a) The temperature required to double the predicted failure rate over the value expected at 65°C for the equipment if calculated or limiting component of that or a similar equipment or,

(b) The temperature required to quadruple the corrosion rate over that expected at 65°C.

5.2 Maximum Recommended Short-Term Ambient Temperature

Values recommended for specific items in Table 2 are the lower of:

(a) The maximum published service temperature of a limiting component of that or a similar equipment or,

(b) The temperature required to cause a 16-fold increase in corrosion rate over that expected at 65°C.

5.3 Corrosion Effects

A generality concerning rates of corrosion as a function of temperature was found quoted in several references (Corrosion Handbook, Wiley & MIL-STD-198Bp. 111) as the "rule of 10":

"Corrosion effects tend to double with each 10°C rise in temperature." It is evident that such a complex subject cannot be neatly summarized in a single sentence. It is judged, however, that application of the "rule" to this particular investigation will result in somewhat more conservative recommendations than would result from a rigorous analysis of the many materials and contaminants involved.

Accordingly, unless otherwise limited to lower values, the maximum recommended long-term ambient temperature will be that required to increase the corrosion rate by a factor of 4 over that expected at 65°C (105°C).

5.4 Individual Components

The temperature characteristics of selected components and materials are summarized in Table 1.

5.4.1 Resistors and Capacitors

Data taken directly from MIL-HDBK-217A. The figure for $\frac{1}{2}$ rating refers to resistor power rating or capacitor voltage rating. Maximum service temperature is taken as the maximum temperature for which data was given.

5.4.2 Semiconductors

Data for microwave diodes taken directly from MIL-HDBK-217A. For other semiconductors, data in MIL-HDBK-217A was found to be plotted as a function of "normalized junction temperature" given by:

$$t_n = \frac{t_a + kpq - t_s}{t_{j(max)} - t_s} \quad (1)$$

where: t_a = ambient temperature

t_s = temperature at which power rating is defined, usually 250°C.

p = power rating of the device at t_s

q = thermal resistance of the device

k = ratio of actual to rated power

$t_{j(max)}$ = maximum junction temperature, assumed to be 200°C for silicon and 85°C for germanium

Inserting these values, equation (1) becomes:

$$t_n = \frac{t_a + kpq - 25}{175} \quad \text{for silicon} \quad (2)$$

and since normalized junction temperature, $t_n = 1$ when k is unity and $t_a = t_s$, the quantity $pq = 175$ and:

$$t_n = t_a + \frac{175k - 25}{175} \quad \text{for silicon} \quad (3)$$

From equation (3), a plot of t_n against ambient temperature, t_a , was generated for several values of k . From this information and the data in MIL-HDBK-217A, curves of expected failure rate as a function of ambient temperature could be generated for desired percentages of rated power. Results are summarized in Table 1.

5.4.3 Synchro

Values were computed per section 7.8.3.2 of MIL-HDBK-217A and are summarized in Table 1.

5.4.4 Coaxial Cable (covered in paragraph 5.5)

5.4.5 Materials

Maximum service temperatures for several materials were obtained from the "Materials Selector Issue" of "Materials Engineering," Vol. 70, No. 5, Mid-October 1969, A Reinhold Publication.

5.5 Coaxial Cable

From manufacturer's data used to generate information used in NAVSHIPS 0967-177-3020 (Shipboard Antenna Systems, Installation Methods) it is determined that:

$$t = t_a + kpg$$

where: t = maximum temperature within the cable

t_a = ambient air temperature

p = power rating of the cable (usually at 40°C)

q = thermal resistance of the cable

k = derating factor = actual power/rated power

From the same sources, it is determined that maximum allowed temperatures within the cables are:

$t_{\max} = 80^{\circ}\text{C}$ for solid or foam polyethylene dielectrics

$t_{\max} = 232^{\circ}\text{C}$ for solid teflon dielectrics

$t_{\max} = 100^{\circ}\text{C}$ for air spaced teflon (Heliax, etc.)

Rearranging equation (4) and setting $t = t_{\max}$:

$$pq = (t_{\max} - t_a)/k \quad (5)$$

The quantity, pq , may be evaluated for each cable type by setting k equal to unity and inserting appropriate values for t_{\max} and t_a into equation (5). For polyethylene dielectrics:

$t_{\max} = 80^{\circ}\text{C}$

$t_a = 40^{\circ}\text{C}$, ambient temperature associated with power rating and: $pq = 40$

Then, solving equation (4) for t_a ,

$t_a = 80 - 40k$, maximum allowed ambient temperature for polyethylene dielectrics

(6)

$t_a = 232 - 192k$, maximum allowed ambient temperature for solid teflon dielectrics

(7)

$t_a = 100 - 60k$, maximum allowed ambient temperature for teflon air-spaced dielectrics

(8)

Equation (6) applies to the specific cable types to be investigated: RG-214, 218, 333 and 1-5/8-inch foam dielectric cable.

<u>Actual power</u> <u>40°C power rating</u>	<u>Maximum allowed</u> <u>ambient temperature</u> <u>°C</u>
1	40
0.5	60
0.2	72
0.1	76
0	80

These values and the values for other cable types are summarized in Table 1.

5.6 Waveguides

No information was found concerning performance of waveguide assemblies at elevated temperatures and applicable military specifications require no temperature tests for rigid assemblies. MIL-W-287C (Waveguide Assemblies, Flexible, Twistable and Non-Twistable) requires a 7-day aging test at 100°C. Most flexible waveguides appear to be covered with neoprene rubber (maximum service temperature =85°C).

For rigid waveguide assemblies, it is difficult to imagine any significant effects other than thermal expansion and corrosion that would be applicable to this investigation.

Accordingly the maximum recommended long-term ambient temperature would be that resulting in a 4-fold increase in corrosion rate over that expected at 65°C. The maximum recommended short-term ambient temperature would be that showing a 16-fold increase. However, the limiting factor would seem to be the neoprene O-rings used to gasket each flange joint. Accordingly, values of 85 and 100°C are recommended in Table 2.

For flexible waveguides the corresponding recommended values are 85°C and 100°C reflecting the maximum published service temperature and heat aging test for the neoprene cover.

5.7 RADAR, TACSATCOM, AS-571, 616, 899, 1174, 1175, URD-4 URN-3

After examining the items in Table 1 it would appear that synchros are the limiting component, for rotating devices in general. Long and short-term values of 80 and 85°C are therefore recommended. Particular care should be taken to insure that lubricants are compatible with these temperatures.

5.8 AN/SRA-17

A parts list for the Radio Frequency Tuner was assembled from the Antenna Group Technical Manual (Navships 93205) and a reliability prediction made for several ambient temperatures per MIL-HDBK-217A, Section 5. Maximum service temperatures for each component were also noted. Maximum service temperature was limited to 120°C by R202 (operating at 20% of rated power) and to 125°C by a number of resistors, capacitors, and relays.

Failure rates were computed for each electronic component at 20, 40, 65, 80, 100, and 140°C. Values for the unit were:

Ambient °C	Failure rate per 10 ⁶ hrs
20	2.5
40	3.0
65	3.8
80	4.9
100	11.2

Failure rates are summarized in Table 1. Recommended maximum ambient temperatures given in Table 2 were determined by taking the minimums from the following tabulation:

Source of Data	Long-term °C	Short-term °C
Temperature to double unit failure rate	65°C	
Limiting component service temperature		120
Corrosion	85	105
Neoprene gaskets	85	100
Recommended maximums	85	100

5.9 AN/SRA-43

The TN-438/SRA-43 RF Tuner was analyzed in the same manner as used in 5.8. Maximum service temperature was limited to 85°C by the synchro contained within the unit,

as well as several mica capacitors. It is interesting to note that the plexiglass dessicant window alone would limit maximum temperatures to 95°C. Failure rates were computed for each electronic component at 20, 65, 80, and 140°C.

Ambient °C	Failure Rate per 10 ⁶ hrs
20	1.5
65	2.9
80	7.8

Failure rates are summarized in Table 1. Recommended maximum ambient temperatures given in Table 2 were determined by taking minimums from the following tabulations:

Source of Data	Long-Term °C	Short-Term °C
Temperature to double 65°C failure rate	78	
Limiting component service temperature		85
Corrosion	85	105
Neoprene gaskets & O-rings	85	100
Recommended maximums	78	85

5.10 Wire Rope for Antennas

Vinyl covered wire rope per FED-SPEC-LP-390 has a polyethylene jacket which has a maximum service temperature of 80°C. Wire rope for antennas in general has a polypropylene core (MIL-24261) exhibiting a maximum service temperature of 120°C. Recommended maximum ambient temperatures given in Table 2 were determined by taking minimum from the following tabulations:

<u>Source</u>	<u>Long-Term</u>	<u>Short-Term</u>
VINYL COVERED		
Jacket		80
Core		120
Corrosion	85	105
Recommended maximums	80	80
UNJACKETED		
Core		120
Corrosion	85	105
Recommended Maximums	85	105

5.11 Antenna Insulators

The maximum allowed temperature for fiberglass insulators is determined by the quality of the resin used to fabricate them. However, performance will in general be limited by associated neoprene gaskets and recommended maximum temperatures listed in Table 2 are accordingly 85 and 100°C. Ceramic bowl insulators will also be temperature limited by gaskets and the same values given for fiberglass insulators are recommended. It is judged that strain insulators with metallic inserts will be limited by corrosion, and recommended values of 85 and 105°C are given in Table 2.

TABLE 1
COMPONENT TEMPERATURE CHARACTERISTICS

<u>ITEM</u>	<u>to double 20°C failure rate</u>	<u>to double 65°C failure rate</u>	<u>maximum service temperature</u>
<u>RESISTOR</u>			
Composition, 50% rating	55	75	100
10% rating	80	80	125
Power, fixed film, 50% rating	125	0	125
10% rating	-	-	200
<u>CAPACITOR</u>			
Mica, Char P, 50% rating	80	125	150
10% rating	80	125	150
Ceramic, Char C, 50% rating	45	85	150
10% rating	90	95	150
<u>SEMICONDUCTORS</u>			
Diodes, Germanium	-	-	85
Diodes, Silicon power, 50% rating	55	-	115
10% rating	55	95	180
Diodes & NPN transistor, (silicon) 50% rating	65	-	115
10% rating	40	115	180
Diodes, microwave, 50% rating (detector & mixer) 20% rating	-	-	115
20% rating	150	-	150
<u>SYNCHRO, 31TX6b</u>	55	80	85
<u>AN/SRA-17 ANTENNA TUNER</u>	80	95	120
<u>AN/SRA-43 ANTENNA TUNER</u>	65	78	85
<u>COAXIAL CABLE</u>			
Polyethylene, 100% rating			40
solid or foam 50% rating			60
20% rating			72
10% rating			76
0% rating			80
Teflon, solid diel., 100% rating			40
50% rating			136
Teflon, air-spaced diel. 100% rating			40
50% rating			70
20% rating			88
0% rating			100

TABLE 2

Maximum Recommended Ambient Temperature, (°C)

<u>ITEM</u>	<u>Long-term</u>	<u>Short-term (Less than 10 min/hr)</u>
Coaxial Cable, RG-214, 218, 333, and 1-5/8" foam filled		
100% power rating	40	40
50% power rating	60	60
20% power rating	72	72
10% power rating	76	76
0% power rating	80	80
Waveguides, rigid & flexible	85	100
RADAR, TACSATCOM, AS-571, 616, 899, 1174, 1175, URD-4, URN-3	80	85
AN/SRA-17	85	100
AN/SRA-43	78	85
Wire rope, vinyl covered unjacketed	80 85	80 105
Antenna Insulators, fiberglass	85	100
Ceramic bowl	85	100
Ceramic strain	85	105

Important Note: None of the above items is required by specification to exceed the requirements of MIL-E-16400 (65°C operating, 75°C non-operating). Increased ambient temperatures will severely reduce service life and will demand increased maintenance.

C

C

C

APPENDIX D
BIBLIOGRAPHY

APPENDIX D

BIBLIOGRAPHY

GENERAL STACK DESIGN REFERENCES

Acker, H.C., "Stack Design to Avoid Smoke Nuisance," SNAME Transactions, Vol. 60, 1952.

Berg, Karl-Arne, "Shape of Superstructure, Funnel Heights and Downwash of Funnel Gases," European Shipbuilding, No. 4, 1957.

Nolan, Robert W., "Design of Stacks to Minimize Smoke Nuisance," SNAME Transactions, Vol. 54, 1946.

Ower, E., and A.D. Third, "Superstructure Design in Relation to the Decent of Funnel Smoke," Transactions, Institute of Marine Engineers (London), Vol. 1, 1959.

Sherlock, R.H., and E.A. Stalker, "A Study of Flow Phenomena in the Wake of Smokestacks," Engineering Research Bulletin No. 29, Department of Engineering Research, University of Michigan, Ann Arbor, March 1941.

Third, A.D., and E. Ower, "Funnel Design and the Smoke Plume," Transactions, Institute of Marine Engineers (London), Vol. 72, 1962.

Thornton, C.P., "Ship Smoke Stacks: A Review of Aerodynamic Factors and Wind Tunnel Methods," DME/NAE Quarterly Bulletin, 1962(4).

THEORETICAL PLUME BEHAVIOR REFERENCES AND MODEL TEST SERIES OF A PLUME IN A CROSSWIND

Charwat, Andrew F., Summary Report: Exhaust Stack Studies, P.O. #9159, Letter to Mr. Henry Hunter, Litton Ship Systems, July 10, 1971.

Charwat, Andrew F., Summary Report: Stack Ejector Study, P.O. M.C. 9159, letter to Mr. Henry Hunter, Litton Ship Systems, July 28, 1971.

Fay, James, Marcel Escudier and David Hault, "A Correlation of Field Observations of Plume Rise," Air Pollution Control Association Journal, Vol. 20, pp. 391-7, June 1970.

Gordier, Robert L., "Studies on Fluid Jets Discharging Normally into Moving Liquid," St. Anthony Falls Hydraulic Lab., Minneapolis, Minnesota, August 1959.

Hault, David D., James A. Fay, and Larry J. Forney, "A Theory of Plume Rise Compared With Field Observations," Fluid Mechanics Lab., Department of Mechanical Engineering, MIT, March 1963.

Jordinson, R., "Flow in a Jet Directed Normal to the Wind," Ministry of Supply, Aeronautical Research Council, Reports and Memoranda, London, 1958.

Keffer, J.F., and W.D. Bates, "The Round Turbulent Jet in a Crosswind," Journal of Fluid Mechanics, Vol. 15, pp 481-96, 1963.

NSRDC, "Wind Tunnel Investigations of Smokestack Annulus Parameters," August 1967.

Schlichting, Dr. Hermann, "Boundary Layer Theory," Sixth Edition, pp. 681-707, McGraw-Hill Book Company, 1968.

Weil, Jeffrey C., "Model Experiments of High Stack Plumes," MIT Master's Thesis, August 1968.

FULL SCALE TESTS

Exhaust Plume Temperature Survey, DD 963, Propulsion Gas Turbine Module, Test Report, General Electric, Aircraft Engine Group, Document No. PF-1-100, Lynn, Mass/Cincinnati, Ohio, September 1972.

Funnel Gas Plume Trail, HMS DEVONSHIRE, 15 October 1971, DG Ships 112/601 Report (British), November 8, 1971.

"Gas Turbine Funnel Plume Temperature Trials," AMEE Technical Report No. 27/72 (British), Project No. 2103, September 1972.

SHIP MODEL TESTS

Ficken, N.I., and H.F. Lo, "Study of Stack-Gas Flow on LSD 28 and LSD 32-Class Ships From Tests with Model 4552 in the Circulating Water Channel," NSRDC Report 1335, July 1970.

Hampton, G.A., "Stack Gas Investigations for a Sea Control Ship (SCS) Represented by Model 5299-2, and 5299-4," NSRDC, November 1973.

STACK GAS INVESTIGATIONS FOR VARIOUS SHIPS

D'Arcy, Ron., "Plume Flow/Temperature Analysis for DD 963 AEGIS," J.J. McMullen, Hyattsville, Maryland

Frazier, T. and G. Baham, "AO177 Class Air Flow and Stack Gas Dispersion Report," George Sharp, Inc., June 1974.

NAVSEC, Code 6110, "Patrol Frigate Gas Turbine Exhaust Stack Plume Temperatures and Temperature Distribution, (FOUO)" September 1972,

NAVSEC, Code 6136, "Sea Control Ship, Air Flow and Stack Gas Dispersion Prediction," Hyattsville, Md. January 1973.

NAVSEC, Code 6136, Memo: Patrol Frigate-Exhaust Plume Studies, Hyattsville, Maryland December 1973

Pollitt, G., D.N. McCallum and T.C. Harrington, "Sea Control Ship (SCS) Stack Gas Air Flow Report (Confidential), NAVSEC Code 6136, Hyattsville, Md. February 1974.

Stoner, W., "Estimated Probabilities of Mast Overtemperature Due to the Gas Turbine Exhaust Plumes," Office Correspondence to D.A. Rains, October 1971.

DG/AEGIS Air Flow/ Stack Gas Study - George Sharp Inc., June 1974.

MISCELLANEOUS

Johnston, J.B.B., "The Operation of Helicopters from Small Ships," Royal Aircraft Establishment, Bedford, England, AGARD Conference Proceedings, 1973.

Pollitt, P., and D. McCallum, "Mean Stack Gas Velocity Ratios and Probabilities of Relative Wind Direction for Known Ship Speed Characteristics," Sec. 6136 August 1974.

Sea Control Ship Plume Temperature; Effects on Mast Mounted Electronic Equipment and Cabling, Memo: NAVSEC 6179 to NAVSEC 6110.05.

"Effects of Elevated Ambient Temperatures on Mast Mounted Equipment for Sea Control Ship (SCS)," NAVSEC Code 6179A.04, Letter Report 827-15-1, 28 July 1972.